RESTRICTED

COPY No. 1
RM No. E8J28b

NACA

RESEARCH MEMORANDUM

ALTITUDE-WIND-TUNNEL INVESTIGATION OF WESTINGHOUSE 19B-2, 19B-8, AND 19XB-1 JET-PROPULSION ENGINES

III - PERFORMANCE AND WINDMILLING DRAG CHARACTERISTICS

By William A. Fleming and Robert O. Dietz, Jr.

Lewis Flight Propulsion Laboratory
Cleveland, Ohio

NATIONAL ADVISORY COMMITTEE FOR AERONAUTICS

WASHINGTON

November 26, 1948

NB

RESTRICTED

NATIONAL ADVISORY COMMITTEE FOR AERONAUTICS

RESEARCH MEMORANDUM

ALTITUDE-WIND-TUNNEL INVESTIGATION OF WESTINGHOUSE 19B-2, 19B-8, AND 19XB-1 JET-PROPULSION ENGINES

III - PERFORMANCE AND WINDMILLING DRAG CHARACTERISTICS

By William A. Fleming and Robert O. Dietz, Jr.

SUMMARY

The performance characteristics of the 19B-8 and 19XB-1 turbojet engines and the windmilling drag characteristics of the 19B-8 engine were determined in the NACA Cleveland altitude wind tunnel. The 19B engine is one of the earliest experimental Westinghouse axial-flow engines. The 19XB-1 engine is an experimental prototype of the Westinghouse 19XB series, having a rated thrust of 1400 pounds. Improvements in performance and operational characteristics have resulted in the 19XB-2B engine with a rated thrust of 1600 pounds. The investigations were conducted on the 19B-8 engine at simulated altitudes from 5000 to 25,000 feet with various free-stream ram-pressure ratios and on the 19XB-1 engine at simulated altitudes from 5000 to 30,000 feet with approximately static free-stream conditions.

Data for these two engines are presented to show the effect of altitude, free-stream ram-pressure ratio, and tail-pipe-nozzle area on engine performance. A 21-percent reduction in tail-pipe-nozzle area of the 19B-8 engine increased the jet thrust 43 percent, the net thrust 72 percent, and the fuel consumption 64 percent. An increase in free-stream ram-pressure ratio raised the jet thrust and the air flow and lowered the net thrust throughout the entire range of engine speeds for the 19B-8 engine. At similar operating conditions, the corrected jet thrust and corrected air flow were approximately the same for both engines, and the corrected specific fuel consumption based on jet thrust was lower for the 19XB-1 engine than for the 19B-8 engine. The thrust and air-flow data obtained with both engines at various altitudes for a given free-stream ram-pressure ratio were generalized to standard sea-level atmospheric conditions. The performance parameters involving fuel consumption generalized only at high engine speeds at simulated altitudes as high as 15,000 feet. The windmilling drag of the 19B-8 engine increased rapidly as the airspeed was increased.

INTRODUCTION

Investigations were conducted in the NACA Cleveland altitude wind tunnel during October and November, 1944, to determine the performance and operational characteristics of the 19B-2, 19B-8, and 19XB-1 turbojet engines. Operational characteristics of all three engines are presented in reference 1 and the performance characteristics of the turbine in the 19B-8 engine are presented in reference 2. Performance characteristics of the 19B-8 and 19XB-1 turbojet engines over a range of simulated flight conditions are presented herein. Data for the 19B-2 engine are omitted because it is an earlier production model of the 19B-8 engine.

The effects of altitude, free-stream ram-pressure ratio, and tail-pipe-nozzle area on engine performance are shown. The performance data are generalized to show the applicability of methods used to determine performance at any altitude from runs at a given altitude. Windmilling drag characteristics of the 19B-8 engine are also presented.

Results are shown for the 19B-8 engine at simulated altitudes from 5000 to 25,000 feet at free-stream ram-pressure ratios up to 1.155 and for the 19XB-1 engine at simulated altitudes from 5000 to 30,000 feet at free-stream ram-pressure ratios below 1.01.

DESCRIPTION OF ENGINES

19B-8 engine. - The 19B-8 turbojet engine has a static sea-level rating of 1365 pounds of thrust at an engine speed of 17,500 rpm. At this rating the engine has an air flow of 28 pounds per second and a fuel consumption of approximately 1800 pounds per hour. The over-all length of the engine is $104\frac{1}{2}$ inches with the adjustable tail cone extended; the maximum diameter is $20\frac{3}{4}$ inches and the total weight is 825 pounds. The maximum diameter does not include the accessory group mounted on the front bearing support at the compressor inlet.

This engine has a six-stage axial-flow compressor, an annular-type combustion chamber, and a single-stage turbine. Fuel is injected downstream into the combustion chamber through 24 nozzles mounted circumferentially in the manifold at the forward end of the combustion chamber. The gases leaving the turbine pass through a

tail pipe equipped with a movable inner cone, which has a total axial travel of 5 inches. When the inner cone is moved from the "in," or forward, position to the "4-inches-out" position, the tail-pipe-nozzle area is decreased from 135 to 106 square inches. The change in area is nearly linear with respect to the travel of the tail cone.

In order to cool the oil for lubricating the engine bearings and accessory drive, a cylindrical oil cooler 2 feet long with an inside diameter of 14 inches is attached to the front of the engine. The inner wall of the cylinder provides the heat-exchanger surface for the oil.

19XB-1 engine. - The 19XB-1 turbojet engine is a modification of the 19B-8 engine that contains a ten-stage axial-flow compressor and has the same over-all engine dimensions. The tail pipe has a fixed inner cone and the tail-pipe-nozzle area is 103 square inches. The 19XB-1 engine has a sea-level rating of approximately 1400 pounds static thrust at a rated engine speed of 16,500 rpm. At this rating the air flow is 29 pounds per second and the fuel consumption is approximately 1600 pounds per hour.

INSTALLATION AND PROCEDURE

Each engine was installed in a nacelle mounted under a stub wing that extended from one side of the 20-foot-diameter test section of the wind tunnel. (See fig. 1.) The engine air was admitted at the front of the nacelle, and a small duct beneath the leading edge of the wing admitted air to cool the outer wall of the combustion chamber and the tail pipe. For the runs at approximately static conditions, when the free-stream ram-pressure ratio was below 1.01, the part of the cowling enclosing the tail pipe and the rear of the combustion chamber was removed because the cooling-air flow through the cowling was inadequate.

Survey rakes were installed at several stations in the engine (fig. 2) in order to obtain temperature and pressure measurements from which the component and over-all performance of the engine could be determined. The methods used to calculate performance parameters are presented in the appendix.

Throughout the part of the investigation discussed, a 6-mesh screen of 0.032-inch-diameter steel wire was attached to the front flange of the oil cooler to protect the compressor from flying objects in the tunnel.

The 19B-8 engine was operated at simulated altitudes from 5000 to 25,000 feet with free-stream ram-pressure ratios up to 1.155; and the 19XB-1 engine, from 5000 to 30,000 feet at approximately static free-stream conditions. The tunnel temperature was held at approximately NACA standard values for each flight condition. At each simulated flight condition, the engine was run over the full range of operable engine speeds. The fuel specified for these engines, 62-octane unleaded gasoline, was used.

During the investigation, the combustion chambers were modified several times (see reference 1) in an attempt to increase the operating range of the engines at high altitudes. Because none of the modifications made any significant improvement in the operating range of the engine, all the data presented are for the engines with the standard combustion chambers as received from the manufacturer.

SYMBOLS

The following symbols are used in this paper:

A	cross-sectional area, square feet
B	thrust-scale reading, pounds
C_D	installation drag coefficient
c_p	specific heat of gas at constant pressure, Btu per pound $^{\circ}R$
D'	windmilling drag, pounds
F_j	jet thrust, pounds
F_n	net thrust, pounds
f/a	fuel-air ratio
g	acceleration of gravity, 32.2 feet per second per second
J	mechanical equivalent of heat, 778 foot-pounds per Btu
m	mass flow, slugs per second
N	engine speed, rpm

P	total pressure, pounds per square foot absolute
p	static pressure, pounds per square foot absolute
R	gas constant, 53.4 foot-pounds per pound $^{\circ}R$
S	wing area, square feet
T	total temperature, $^{\circ}R$
T_i	indicated temperature, $^{\circ}R$
t	static temperature, $^{\circ}R$
thp	net thrust horsepower
V	velocity, feet per second
V'	velocity, miles per hour
W_a	air flow, pounds per second
W_f	fuel consumption, pounds per hour
W_f/F_j	specific fuel consumption based on jet thrust, pounds per hour pound thrust
W_f/F_n	specific fuel consumption based on net thrust, pounds per hour pound thrust
W_f/thp	specific fuel consumption based on net thrust horsepower, pounds per hour per thrust horsepower
γ	ratio of specific heats for gases
δ	ratio of absolute tunnel static pressure to absolute static pressure of NACA standard atmospheric conditions at sea level, $p_0/2116$
θ	ratio of absolute tunnel static temperature to absolute static temperature of NACA standard atmospheric conditions at sea level, $t_0/519$
ρ	mass density, slugs per cubic foot

Subscripts:

a	air
f	fuel
g	gas
j	station at which static pressure in jet reaches ambient static pressure
0	ambient free stream
1	cowl inlet
2	compressor inlet
5	turbine outlet

The following performance parameters generalized to NACA standard atmospheric conditions at sea level were used:

D_w/δ	corrected windmilling drag, pounds
F_j/δ	corrected jet thrust, pounds
F_n/δ	corrected net thrust, pounds
$(f/a)/\theta$	corrected fuel-air ratio
$N/\sqrt{\theta}$	corrected engine speed, rpm
$V'_0/\sqrt{\theta}$	corrected true airspeed, miles per hour
$W_a\sqrt{\theta}/\delta$	corrected air flow, pounds per second
$W_f/(\delta\sqrt{\theta})$	corrected fuel consumption, pounds per hour
$W_f/(F_j\sqrt{\theta})$	corrected specific fuel consumption based on jet thrust, pounds per hour per pound thrust
$W_f/(F_n\sqrt{\theta})$	corrected specific fuel consumption based on net thrust, pounds per hour per pound thrust
W_f/thp	corrected specific fuel consumption based on net thrust horsepower, pounds per hour per thrust horsepower

PERFORMANCE CHARACTERISTICS

Effect of Inlet Screen

The screen installed at the cowl inlet for the wind-tunnel investigation caused a total-pressure loss between the free stream and the compressor inlet that varied with the corrected engine speed. The ram-pressure ratios used in this report are based on measurements of free-stream total pressure instead of compressor-inlet total pressure. Because the tunnel-test section airspeed was used to calculate net thrust and net thrust horsepower, the engine-performance characteristics involving these parameters were slightly affected. The relation between corrected engine speed and the ratio of compressor-inlet total pressure to free-stream total pressure is shown in figure 3. The curve shown in this figure was determined from data obtained throughout the entire range of flight conditions investigated. The compressor-inlet ram-pressure ratio at any engine speed may be obtained for the data presented by multiplying the free-stream ram-pressure ratio by the value of P_2/P_0 obtained from figure 3 for the corresponding corrected engine speed.

Effect of Altitude

19B-8 engine. - The 19B-8 engine performance at simulated altitudes of 5000, 15,000 and 25,000 feet, a free-stream ram-pressure ratio of 1.013, and with a tail-pipe-nozzle area of 135 square inches, is shown in figure 4. Because of the high minimum speed of the engine at altitudes above 17,000 feet (reference 1), no data could be shown for an engine speed below 15,500 rpm at an altitude of 25,000 feet. The variations in jet thrust, net thrust, fuel consumption, air flow, and specific fuel consumption based on net thrust with increasing altitude are shown in figures 4(a) and 4(e), respectively.

Above an engine speed of 13,000 rpm the fuel-air ratios at simulated altitudes of 5000 and 15,000 feet were the same (fig. 4(f)). At an altitude of 25,000 feet, however, the fuel-air ratio throughout the entire operable range of the engine was higher than at 5000 and 15,000 feet. The high fuel-air ratio obtained at 25,000 feet was probably related to the reduction in combustion efficiency. A low combustion efficiency at a simulated altitude of 25,000 feet was indicated by the narrow operating range of the engine as limited by combustion blow-out. At engine speeds below

13,000 rpm, the increase in fuel-air ratio at an altitude of 15,000 feet above that at 5000 feet was also caused by the reduction in combustion efficiency that accompanied an increase in altitude.

19XB-1 engine. - The 19XB-1 engine performance at approximately static conditions (free-stream ram-pressure ratio less than 1.01) and simulated altitudes of 5000 to 30,000 feet is shown in figure 5. Maximum engine speed was limited by high tail-pipe temperatures and above an altitude of 15,000 feet the minimum engine speed began to increase. The reduction in jet thrust, fuel consumption, and air flow that resulted from an increase in altitude, is shown in figures 5(a) to 5(c), respectively. No net-thrust curve is presented inasmuch as these data were obtained at approximately static conditions where the jet and net thrusts are equal. Variation of specific fuel consumption based on jet thrust with altitude and engine speed is shown in figure 5(d). For high engine speeds, the specific fuel consumption was slightly higher at altitudes of 25,000 and 30,000 feet than at the lower altitudes. The effect of altitude on the relation between engine speed and fuel-air ratio is shown in figure 5(e).

Effect of Ram-Pressure Ratio

The effect of varying the free-stream ram-pressure ratio from 1.012 to 1.155 throughout the operable speed range of the 19B-8 engine with a tail-pipe-nozzle area of 106 square inches at an altitude of 15,000 feet is presented in figure 6. The maximum engine speed obtainable with the tail cone 4 inches out (tail-pipe-nozzle area, 106 sq in.) was limited to about 16,500 rpm by high tail-pipe temperatures. Increasing the ram-pressure ratio raised the jet thrust (fig. 6(a)) and the air flow (fig. 6(c)) and lowered the net thrust (fig. 6(b)) throughout the entire range of engine speeds. At all engine speeds below 16,500 rpm the fuel consumption was lowered as the ram-pressure ratio was increased (fig. 6(d)).

At low engine speeds, the specific fuel consumption based on net thrust increased as the ram-pressure ratio was raised from 1.012 to 1.155 (fig. 6(e)). Above a speed of 14,000 rpm, however, the specific fuel consumption increased only for a change in ram-pressure ratio from 1.012 to 1.122. The specific fuel consumption based on net thrust horsepower decreased with increasing ram-pressure ratio throughout the entire range of engine speeds (fig. 6(f)). At an engine speed of 16,500 rpm, the specific fuel

consumption based on net thrust increased from 1.51 at a ram-pressure ratio of 1.012 to 1.62 at a ram-pressure ratio of 1.155 (fig. 6(e)) and the specific fuel consumption based on net thrust horsepower decreased from 5.25 to 1.85 for a corresponding increase in ram-pressure ratio (fig. 6(f)). The relation between specific fuel consumption based on net thrust and net thrust is shown in figure 6(g).

The fuel-air ratio (fig. 6(h)) was reduced throughout the entire range of engine operation as the ram-pressure ratio was increased.

Effect of Tail-Pipe-Nozzle Area on Performance

The effect of a 21-percent reduction in tail-pipe-nozzle area (from 135 to 106 sq in.), which was obtained by moving the tail cone from the in position to the 4-inches-out position, on the performance of the 19B-8 engine at a free-stream ram-pressure ratio of 1.131 and at a simulated altitude of 10,000 feet, is shown in figure 7. With a tail-pipe-nozzle area of 106 square inches, the maximum engine speed was limited to 16,500 rpm by the turbine-inlet temperature (1500° F). The reduction in tail-pipe-nozzle area increased the jet thrust (fig. 7(a)), net thrust (fig. 7(b)), and fuel consumption (fig. 7(c)) and lowered the air flow (fig. 7(d)) throughout the range of engine speeds. At an engine speed of 16,500 rpm, the reduction in nozzle area increased the jet thrust 43 percent (fig. 7(a)), the net thrust 72 percent (fig. 7(b)), and the fuel consumption 64 percent (fig. 7(c)).

Throughout the range of engine speeds, the specific fuel consumption based on net thrust (fig. 7(e)) and the specific fuel consumption based on net thrust horsepower (fig. 7(f)) were lower with a tail-pipe-nozzle area of 106 square inches than with an area of 135 square inches. At an engine speed of 16,500 rpm, the specific fuel consumption based on net thrust was approximately 6 percent higher with a tail-pipe-nozzle area of 135 square inches than with an area of 106 square inches. Changing the tail-pipe-nozzle area had no effect on the relation between the specific fuel consumption based on net thrust and the net thrust (fig. 7(g)).

The reduction in tail-pipe-nozzle area increased the back pressure on the turbine and as a result the engine required a higher turbine-inlet temperature, that is, a higher fuel-air ratio to maintain a given engine speed. The increase in fuel-air ratio resulting from a reduction in tail-pipe-nozzle area is shown in figure 7(h).

GENERALIZED PERFORMANCE

The concept of flow similarity and the application of dimensional analysis to the performance of turbojet engines has led to the development of the pressure and temperature reduction factors δ and θ with which data obtained at several altitudes may be generalized. Data thus far presented that were obtained at various altitudes and free-stream ram-pressure ratios are generalized to NACA standard conditions at sea level in order to test the applicability of the factors δ and θ to the performance of the 19B-8 and 19XB-1 turbojet engines.

Application of the factors δ and θ give the following generalized performance variables: corrected engine speed, $N/\sqrt{\theta}$; corrected jet thrust, F_j/δ; corrected net thrust, F_n/δ; corrected air flow, $(W_a\sqrt{\theta})/\delta$, corrected fuel consumption, $W_f/(\delta\sqrt{\theta})$; corrected specific fuel consumption based on jet thrust, $W_f/(F_j\sqrt{\theta})$; corrected specific fuel consumption based on net thrust, $W_f/(F_n\sqrt{\theta})$; corrected specific fuel consumption based on net thrust horsepower, W_f/thp; and corrected fuel-air ratio, $(f/a)/\theta$.

The generalized performance variables that contain fuel consumption exclude the effects of variations in combustion efficiency, which is a component of the factor of thermal expansion of the working fluid included in the dimensional analysis. This exclusion admittedly lessens the possibilities of successfully generalizing the data in cases where the combustion efficiency changes.

The effect of altitude on the generalized performance of the 19B-8 and 19XB-1 engines is shown in figures 8 and 9, respectively. The corrected jet thrust (figs. 8(a) and 9(a)), the corrected net thrust (fig. 8(b)), and the corrected air flow (figs. 8(c) and 9(b)) generalized to a single curve for each engine. The parameters involving fuel consumption, that is, corrected fuel consumption (figs. 8(d) and 9(c)), corrected specific fuel consumption (figs. 8(e), 9(d), and 9(e)), and corrected fuel-air ratio (figs. 8(g) and 9(f)), generalized only in the upper range of engine speeds for simulated altitudes as high as 15,000 feet.

Performance data obtained at various ram-pressure ratios did not generalize to a single curve inasmuch as the factors δ and θ are not meant to correct for the changes in cycle efficiency that accompany variations in ram-pressure ratios. The effect of ram-pressure ratio on the generalized performance of the 19B-8 engine

is shown in figure 10. The performance parameters involving corrected jet thrust (fig. 10(a)), corrected net thrust (fig. 10(b)), corrected air flow (fig. 10(c)), corrected fuel consumption (fig. 10(d)), corrected specific fuel consumption based on net thrust (figs. 10(e) and 10(f)), specific fuel consumption based on net thrust horsepower (fig. 10(g)), and corrected fuel-air ratio (fig. 10(h)) produced a family of curves for various free-stream ram-pressure ratios.

In the use of generalized performance curves, the effect of ram-pressure ratio on engine performance at various altitudes can be determined only by use of the entire family of curves. It is impossible to predict the performance parameters involving fuel consumption at low engine speeds or at high altitudes because the effects of varying combustion efficiency are excluded from the factors used in this report.

A comparison of generalized performance data of the 19B-8 and 19XB-1 engines at a corrected engine speed of 17,000 rpm is presented in the following table:

	Engine	
	19B-8	19XB-1
Tail-pipe-nozzle area, sq in.	106	103
Corrected engine speed, $N/\sqrt{\theta}$, rpm	17,000	17,000
Corrected jet thrust, F_j/δ, lb	1370	1375
Corrected air flow, $W_a\sqrt{\theta}/\delta$, lb/sec	27.0	26.5
Corrected fuel consumption, $W_f/\delta\sqrt{\theta}$, lb/hr	1965	1825
Corrected specific fuel consumption based on jet thrust, $W_f/(F_j\sqrt{\theta})$, lb/(hr)(lb thrust)	1.435	1.328
Corrected fuel-air ratio, $(f/a)/\theta$	0.0202	0.0192

Data presented in this table were obtained from figure 9 for the 19XB-1 engine at static conditions and from figure 10 for the 19B-8 engine at a free-stream ram-pressure ratio of 1.012. At static conditions, the ejector effect of the jet produced a velocity in the tunnel test section at a maximum engine speed equivalent to a free-stream ram-pressure ratio of approximately 1.012. For the conditions given in the table, the compressor-inlet ram-pressure ratio for both engines was 0.938. Generalized data are used because the inlet-air temperatures were different for the two engines.

The corrected jet thrust and the corrected air flow of both engines at a corrected engine speed of 17,000 rpm were approximately the same. The corrected specific fuel consumption based on jet thrust was lower for the 19XB-1 engine than for the 19B-8 engine.

WINDMILLING DRAG

The magnitude of the windmilling drag obtained when an engine is inoperative and is allowed to windmill during flight is equal to the change of momentum of the air as it passes through the engine. A limited amount of windmilling drag data was obtained for the 19B-8 engine at simulated altitudes from 5000 to 30,000 feet and tunnel-test-section airspeeds from 176 to 373 miles per hour with the screen installed at the cowl inlet. Generalized values of windmilling drag (fig. 11(a)) show that the windmilling drag increased rapidly as the corrected true airspeed was increased. A single curve was drawn through the generalized values obtained at various altitudes. The relation between the ratio of windmilling drag to the maximum net thrust obtainable with a tail-pipe-nozzle area of 135 square inches and the tunnel-test-section true airspeed is shown in figure 11(b). These data show that at any altitude the windmilling drag of the engine at an airspeed of 200 miles per hour was 2.5 percent of the maximum net thrust obtainable at this airspeed and that at an airspeed of 375 miles per hour the windmilling drag was 11 percent of the maximum net thrust obtainable at this airspeed. The generalized values of air flow obtained with the engine windmilling (fig. 11(c)) fell on a single curve for all altitudes investigated.

SUMMARY OF RESULTS

From an investigation in the Cleveland altitude wind tunnel of the performance characteristics of the 19B-8 and 19XB-1 turbojet engines and the windmilling drag characteristics of the 19B-8 engine, the following results were obtained:

1. A reduction in tail-pipe-nozzle area of the 19B-8 engine from 135 to 106 square inches at a simulated altitude of 10,000 feet and a free-stream ram-pressure ratio of 1.131 gave an increase in jet thrust, net thrust, and fuel consumption with a reduction in air flow and specific fuel consumption based on net thrust throughout the entire range of engine speeds. This reduction in tail-pipe-nozzle area at an engine speed of 16,500 rpm raised the jet thrust 43 percent, the net thrust 72 percent, and the fuel consumption 64 percent.

2. With a tail-pipe-nozzle area of 106 square inches on the 19B-8 engine, an increase in free-stream ram-pressure ratio from 1.012 to 1.155 at a simulated altitude of 15,000 feet raised the jet thrust and air flow and lowered the net thrust throughout the entire range of engine speeds. The fuel consumption was lowered at all engine speeds below 16,500 rpm.

3. At similar operating conditions, the corrected jet thrust and the corrected air flow were approximately the same for both engines and the corrected specific fuel consumption based on jet thrust was lower for the 19XB-1 engine than for the 19B-8 engine.

4. With the use of generalizing pressure and temperature factors jet-thrust, net-thrust, and air-flow data obtained from both the 19B-8 and 19XB-1 engines at a given ram-pressure ratio and tail-pipe-nozzle area, and at any altitude could be used to estimate the performance of the engines at any other altitude. The performance parameters involving fuel consumption generalized only at high engine speeds at simulated altitudes up to 15,000 feet. Above this altitude these parameters did not generalize at any engine speed.

5. The windmilling drag of the 19B-8 engine while it was inoperative amounted to 2.5 percent of the maximum net thrust of the engine at an airspeed of 200 miles per hour, and 11 percent of the maximum net thrust of the engine at an airspeed of 375 miles per hour.

Lewis Flight Propulsion Laboratory,
National Advisory Committee for Aeronautics,
Cleveland, Ohio.

APPENDIX - METHODS OF CALCULATION

Temperature. - A sample thermocouple of the type used was calibrated cold up to a Mach number of 0.8. This calibration showed the thermocouple measured the static temperature plus approximately 85 percent of the adiabatic temperature rise due to the impact of the air on the thermocouple. Static temperature may be determined from indicated temperature by applying this factor to the adiabatic relation between temperature and pressure:

$$t = \frac{T_i}{1 + 0.85\left[\left(\frac{P}{p}\right)^{\frac{\gamma-1}{\gamma}} - 1\right]}$$

and the total temperature is

$$T = \frac{T_i\left(\frac{P}{p}\right)^{\frac{\gamma-1}{\gamma}}}{1 + 0.85\left[\left(\frac{P}{p}\right)^{\frac{\gamma-1}{\gamma}} - 1\right]}$$

In order to determine the static temperature of the jet, the assumption was made that no loss occurred in total temperature or total pressure between station 5 in the tail pipe and station j in the jet. When this assumption is made, the static temperature in the jet is

$$t_j = \frac{T_5}{\left(\frac{P_5}{p_0}\right)^{\frac{\gamma_j-1}{\gamma_j}}}$$

The tunnel-test-section static temperature was determined from the indicated temperature measured in the large section of the tunnel just ahead of the test section. Because the velocity in the large section of the tunnel was very low, the indicated temperature measured in the large section is equal to the test-section total temperature. The static temperature in the test section then is

$$t_0 = \frac{T_0}{\left(\frac{P_0}{p_0}\right)^{\frac{\gamma_0-1}{\gamma_0}}}$$

Tunnel-test-section velocity. - The tunnel-test-section velocity was obtained from

$$V_0 = \sqrt{2J\ g\ c_p\ t_0 \left[\left(\frac{P_0}{p_0}\right)^{\frac{\gamma_0-1}{\gamma_0}} - 1\right]}$$

Air flow. - The air flow through the engine was determined from pressure and temperature measurements obtained with four survey rakes at the cowl inlet (station 1, fig. 1). The equation used to calculate the air flow is

$$W_a = \rho_1 A_1 V_1 g = \frac{p_1 A_1}{R} \sqrt{\frac{2J\ g\ c_p}{t_1} \left[\left(\frac{P_1}{p_1}\right)^{\frac{\gamma_1-1}{\gamma_1}} - 1\right]}$$

Thrust and windmilling drag. - Two methods were used to calculate the jet thrust. For the tests at approximately static conditions when the tunnel-test-section velocity was low, the thrust was measured directly on the balance scales. The external drag of the nacelle and the initial momentum of the inlet air were added to the scale thrust reading, which gave the following equation for jet thrust:

$$F_j = B + 1/2\ \rho_0 V_0^2\ C_D\ S + m_a\ V_0 \qquad (1)$$

Inasmuch as the scale-thrust term B of equation (1) was the major part of the total thrust and could be measured within ±2 pounds, the jet thrust could be determined accurately at low test-section velocities. Although variations in the drag coefficient accompanying a change in inlet-velocity ratios could not be determined, an error of as much as 50 percent in the drag coefficient would result in less than a 1-percent error in thrust at test-section airspeeds below 100 feet per second.

For test-section airspeeds of 100 miles per hour or more, the jet thrust was determined by using the mass air flow measured at the cowl inlet, the fuel consumption, and the jet velocity at the vena contracta in the following equation:

$$F_j = (m_a + m_f)\, V \qquad (2)$$

Calculating the jet thrust with these two methods for the static tests gave a calibration factor that could be applied to equation (2). The value of the calibration factor, which is the ratio of measured scale thrust to calculated tail-pipe thrust, was found to be 1.015. By expansion of equation (2) and application of this factor to it, the following expression used to calculate the jet thrust for all of the tests except the static tests was obtained:

$$F_j = 1.015\, m_g \sqrt{2J\, g\, c_{p,j}\, t_j \left[\left(\frac{p_5}{p_0} \right)^{\frac{\gamma_j - 1}{\gamma_j}} - 1 \right]}$$

The net thrust was then determined by subtracting the free-stream momentum of the inlet air for the jet thrust:

$$F_n = F_j - m_a V_0$$

The net thrust horsepower was determined from the net thrust and the true airspeed by the expression

$$thp = \frac{F_n V_0}{550}$$

The windmilling drag of the engine was determined from the product of the mass air flow and the change in velocity of the air that passes through the engine by use of the equation

$$D_w = m_a (V_0 - V_j)$$

REFERENCES

1. Fleming, William A.: Altitude-Wind-Tunnel Investigation of Westinghouse 19B-2, 19B-8, and 19XB-1 Jet-Propulsion Engines. I - Operational Characteristics. NACA RM No. E8J28, 1948.

2. Krebs, Richard P., and Suozzi, Frank L.: Altitude-Wind-Tunnel Investigation of Westinghouse 19B-2, 19B-8, and 19XB-1 Jet-Propulsion Engines. II - Analysis of Turbine Performance of 19B-8 Engine. NACA RM No. E8J28a, 1948.

Page intentionally left blank

Page intentionally left blank

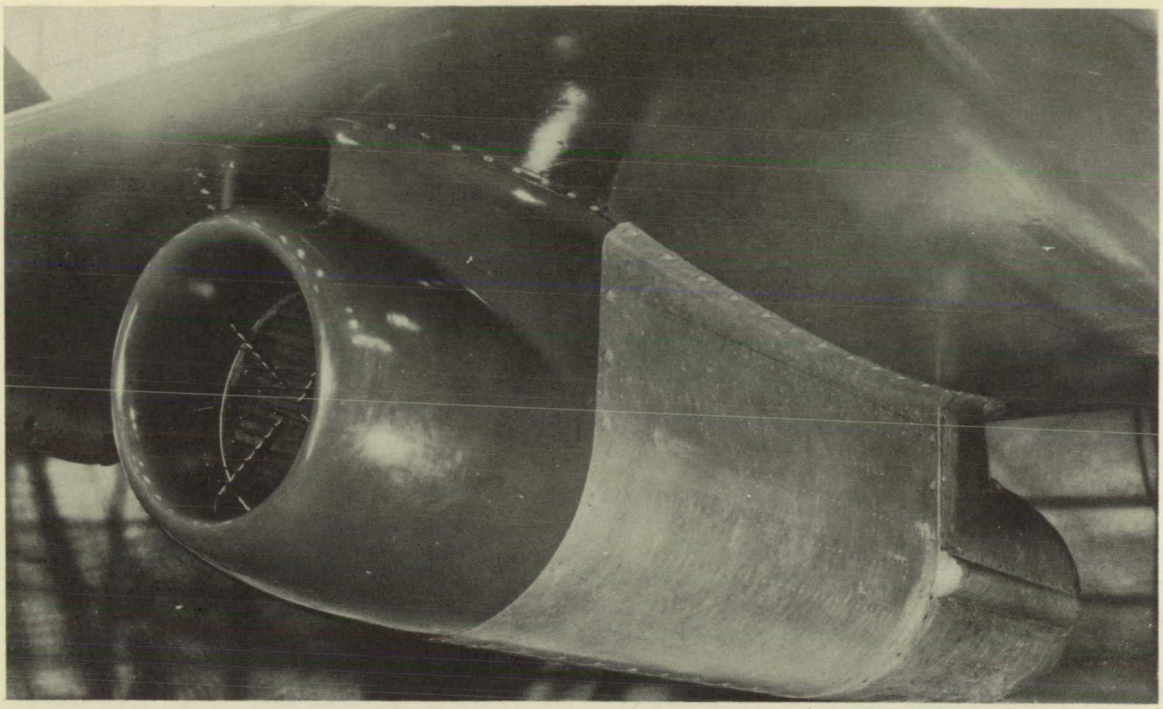

(a) With cowling.

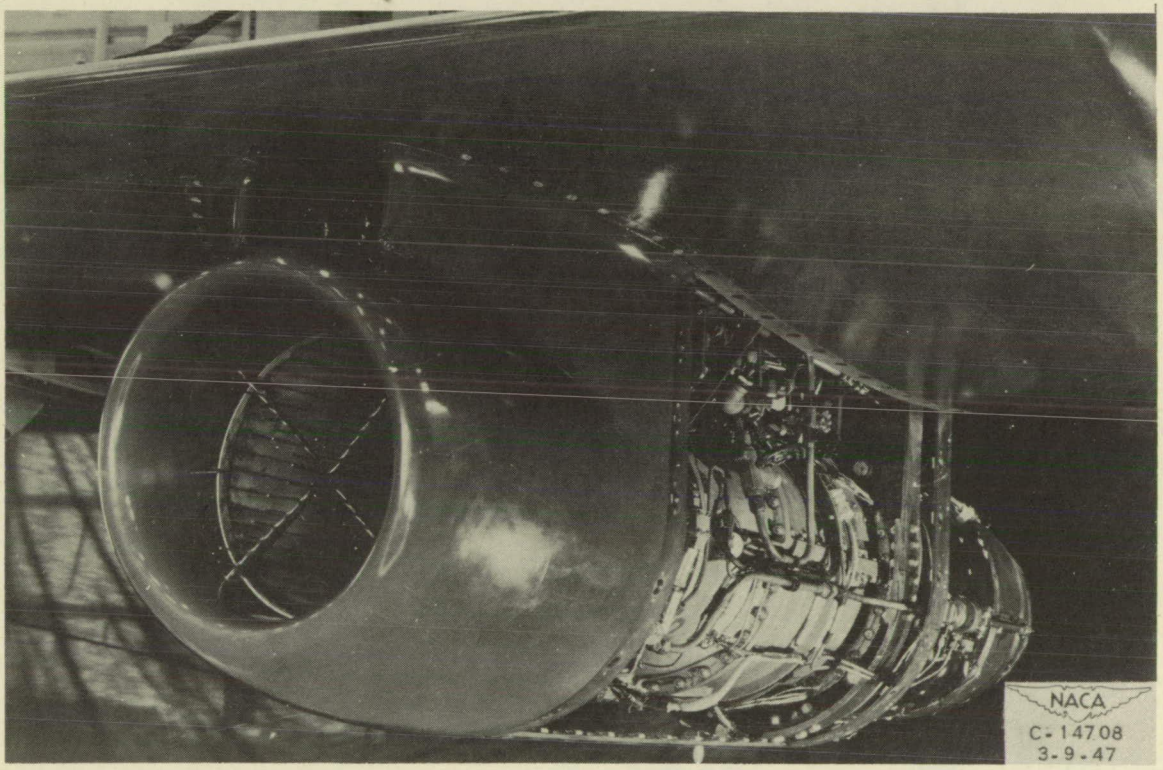

(b) Without cowling

Figure 1. - Installation of 19B turbojet engine in underslung nacelle for investigation in altitude wind tunnel.

Page intentionally left blank

Page intentionally left blank

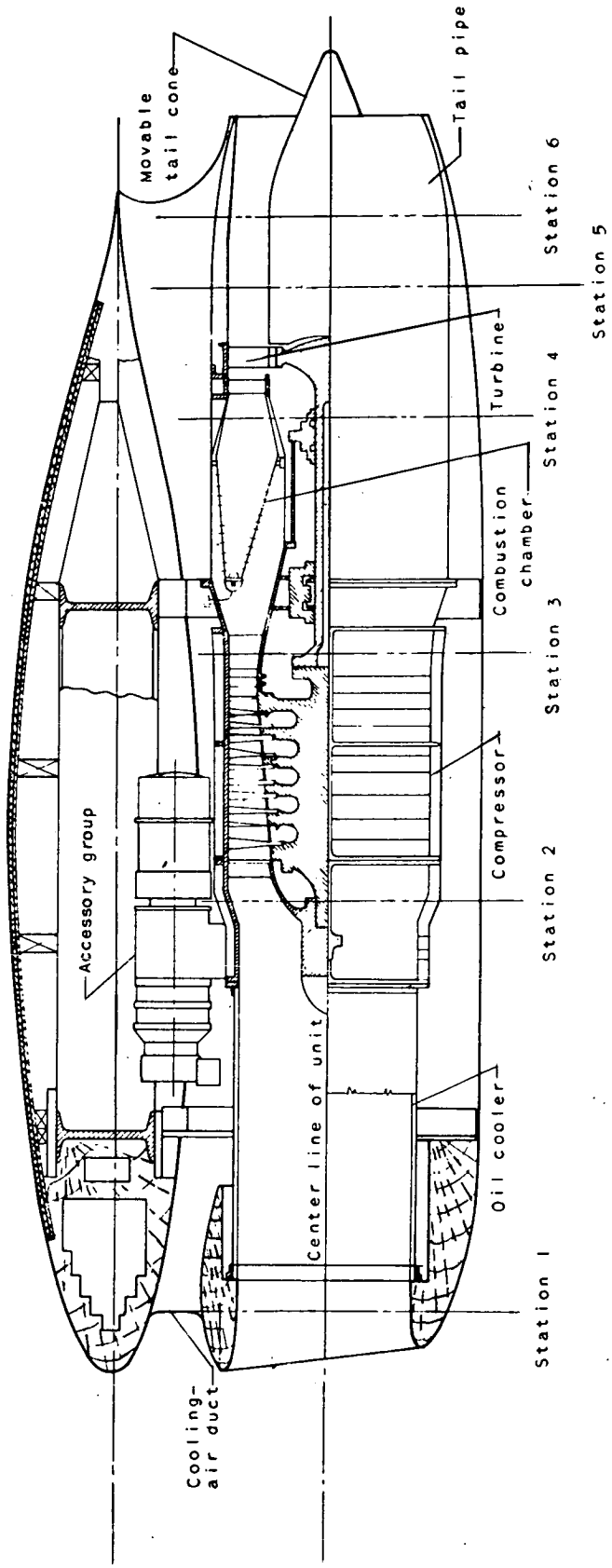

Figure 2. - Longitudinal section of I98 turbojet-engine installation showing measuring stations.

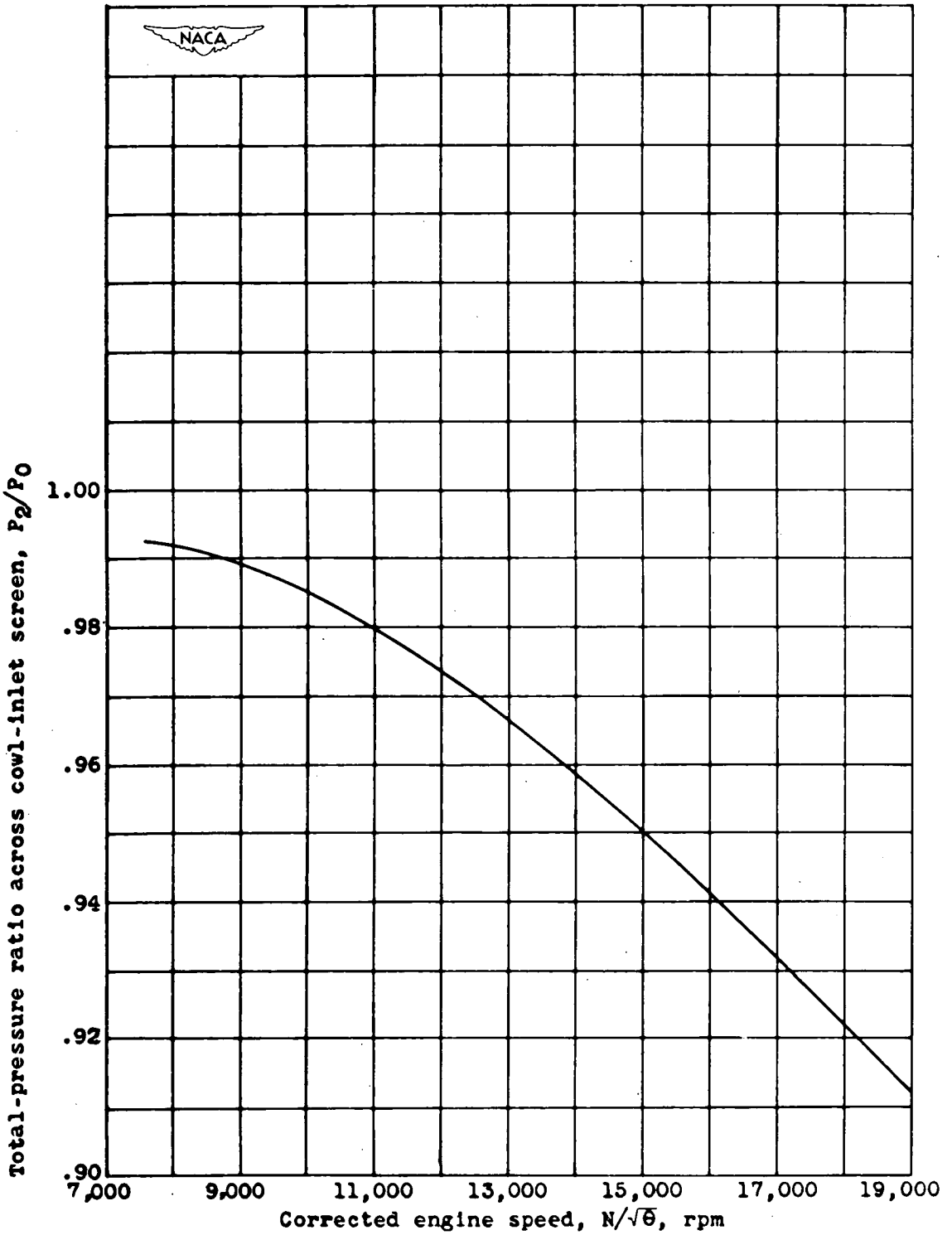

Figure 3.- Relation between total-pressure ratio across cowl-inlet screen and corrected engine speed for range of simulated altitudes and flight speeds.

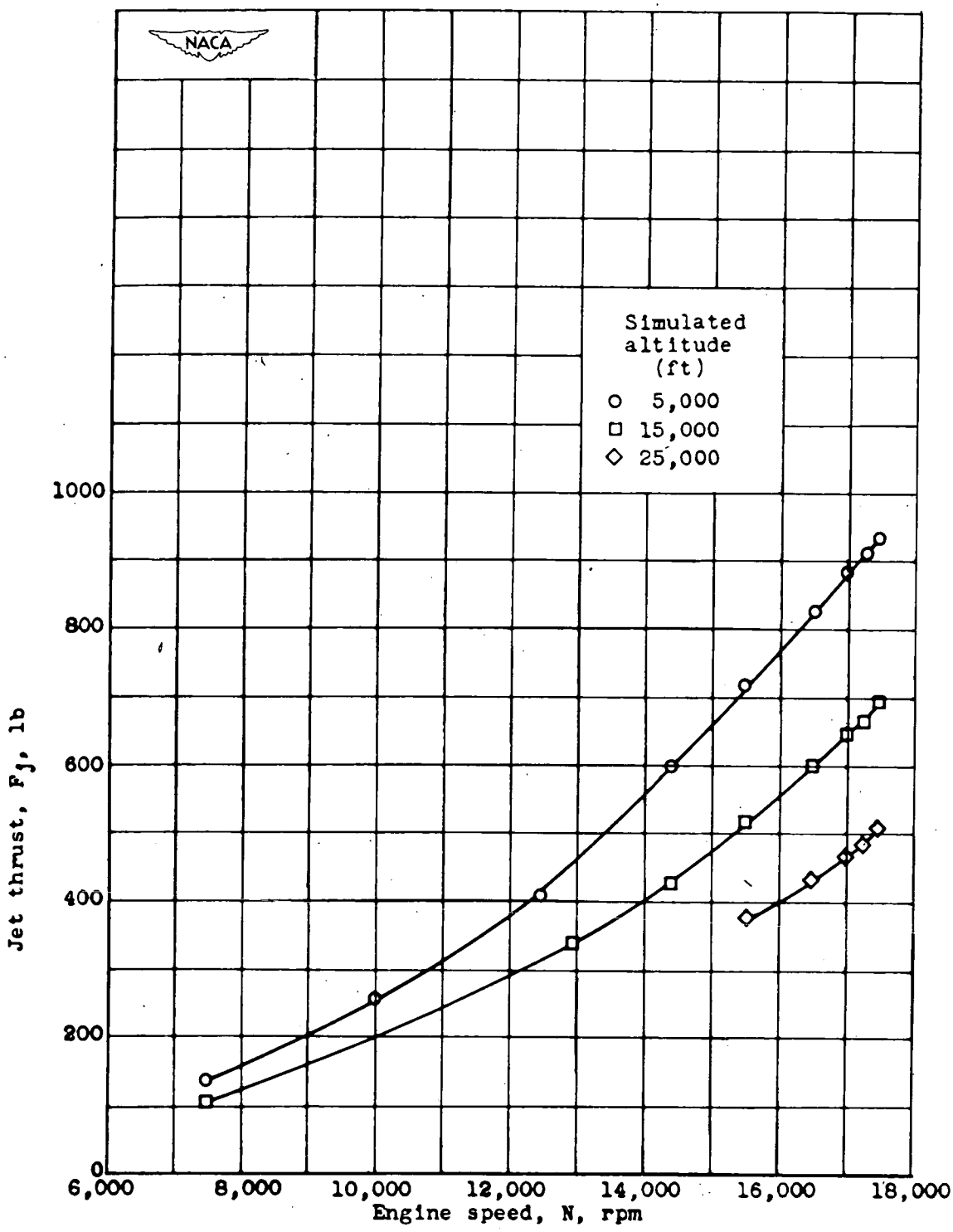

(a) Relation between jet thrust and engine speed.

Figure 4.- Effect of altitude on performance characteristics of 19B-8 turbojet engine. Tail-pipe-nozzle area, 135 square inches; free-stream ram-pressure ratio, 1.013.

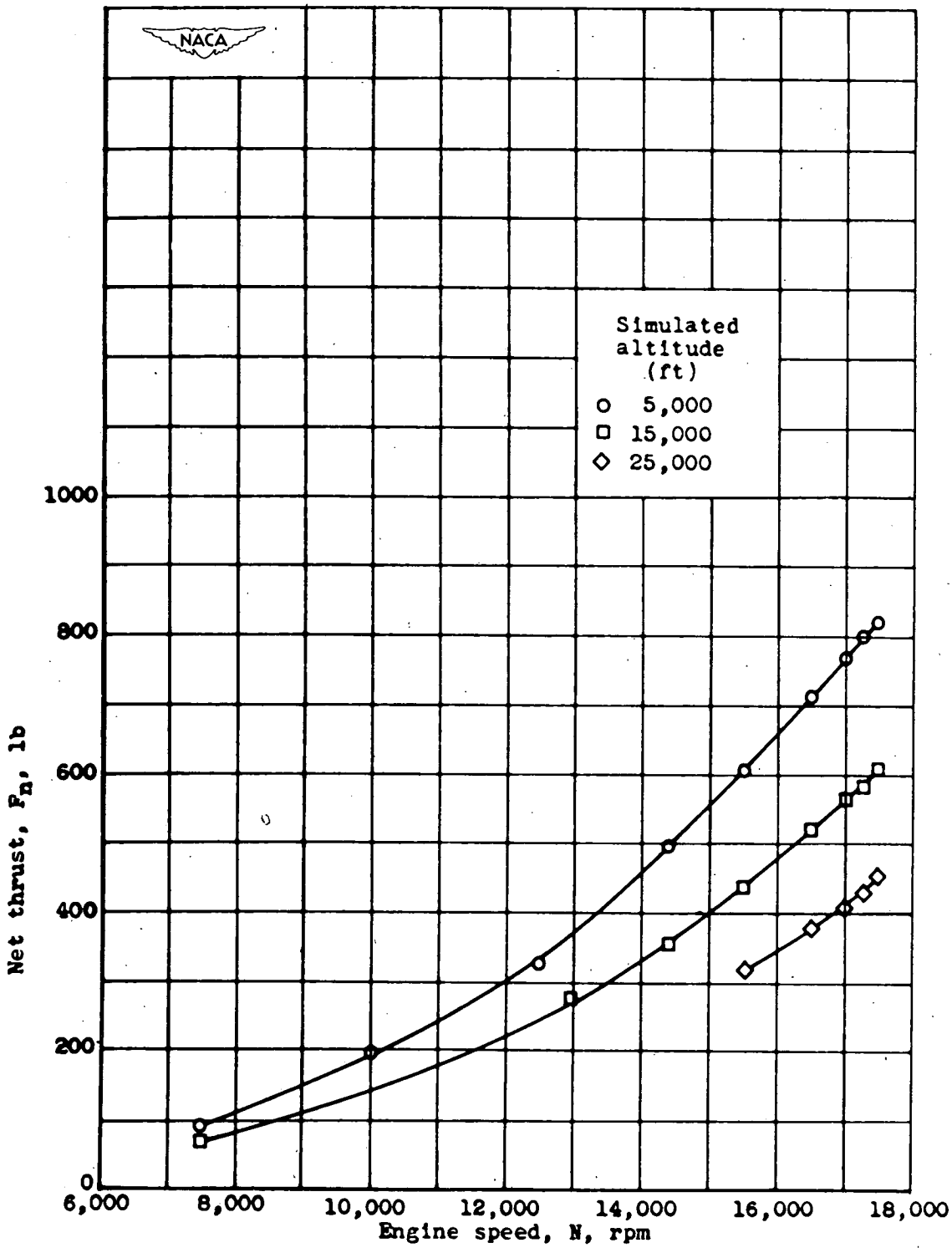

(b) Relation between net thrust and engine speed.

Figure 4.- Continued. Effect of altitude on performance characteristics of 19B-8 turbojet engine. Tail-pipe-nozzle area, 135 square inches; free-stream ram-pressure ratio, 1.013.

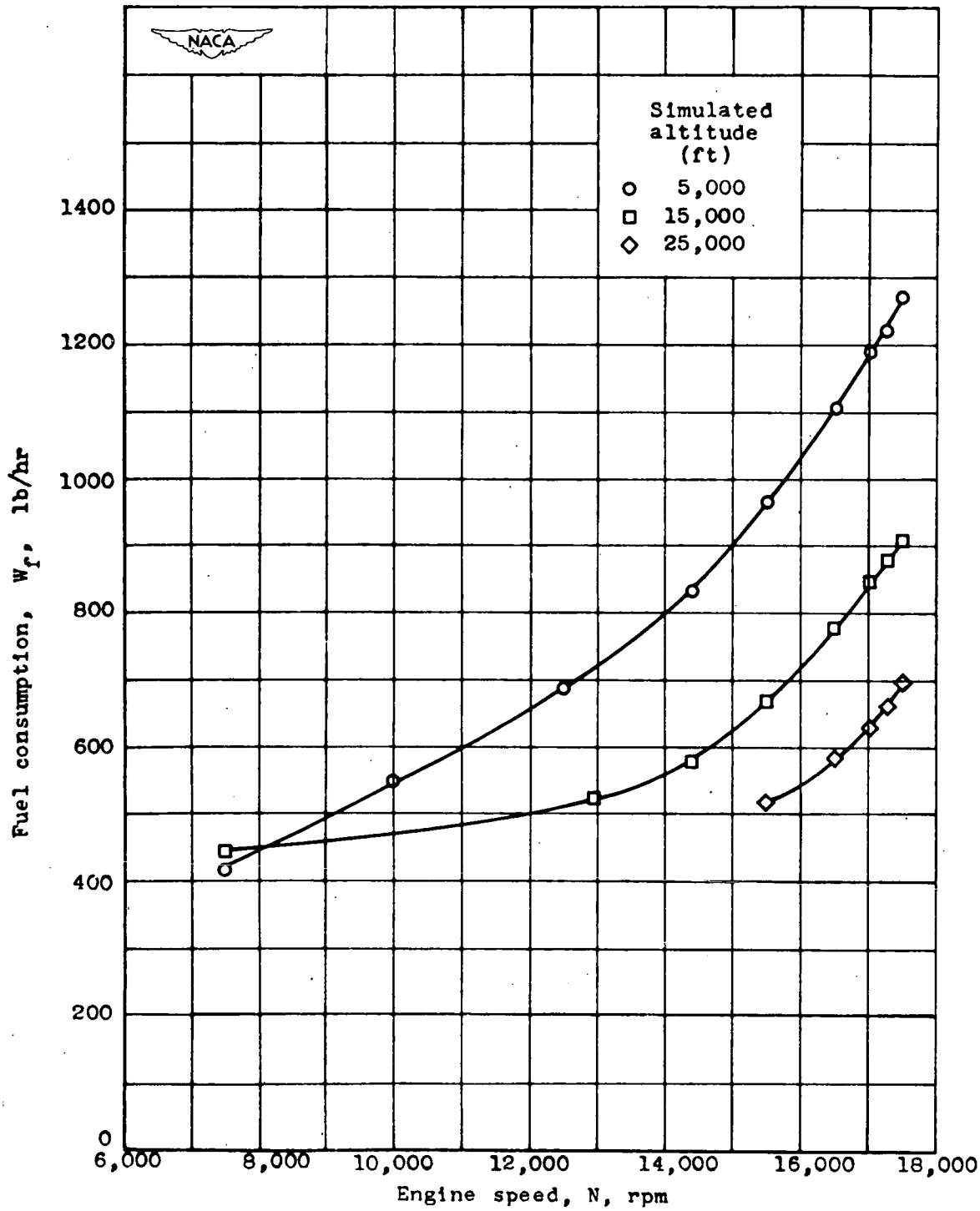

(c) Relation between fuel consumption and engine speed.

Figure 4.- Continued. Effect of altitude on performance characteristics of 19B-8 turbojet engine. Tail-pipe-nozzle area, 135 square inches; free-stream ram-pressure ratio, 1.013.

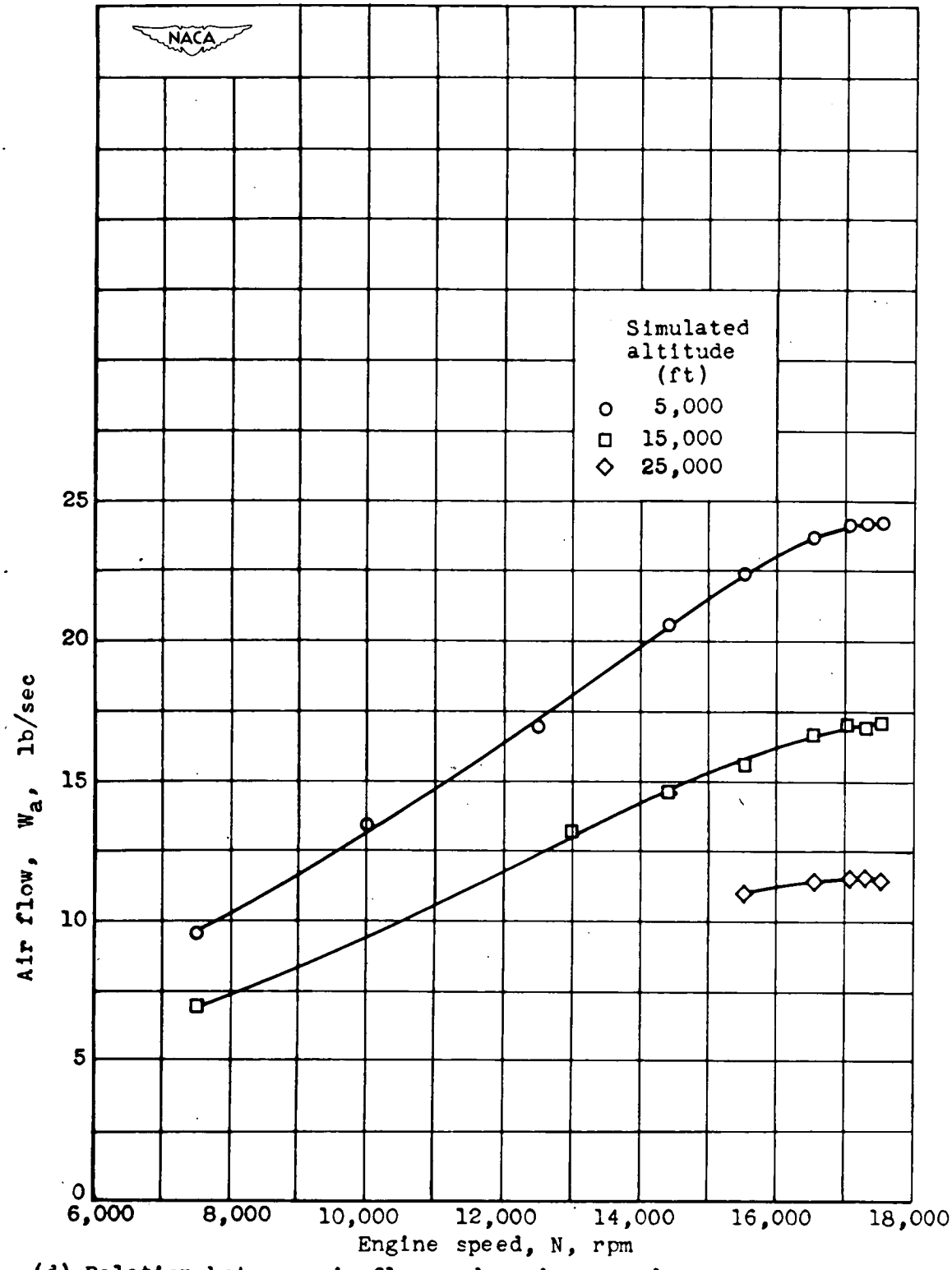

(d) Relation between air flow and engine speed.

Figure 4.- Continued. Effect of altitude on performance characteristics of 19B-8 turbojet engine. Tail-pipe-nozzle area, 135 square inches; free-stream ram-pressure ratio, 1.013.

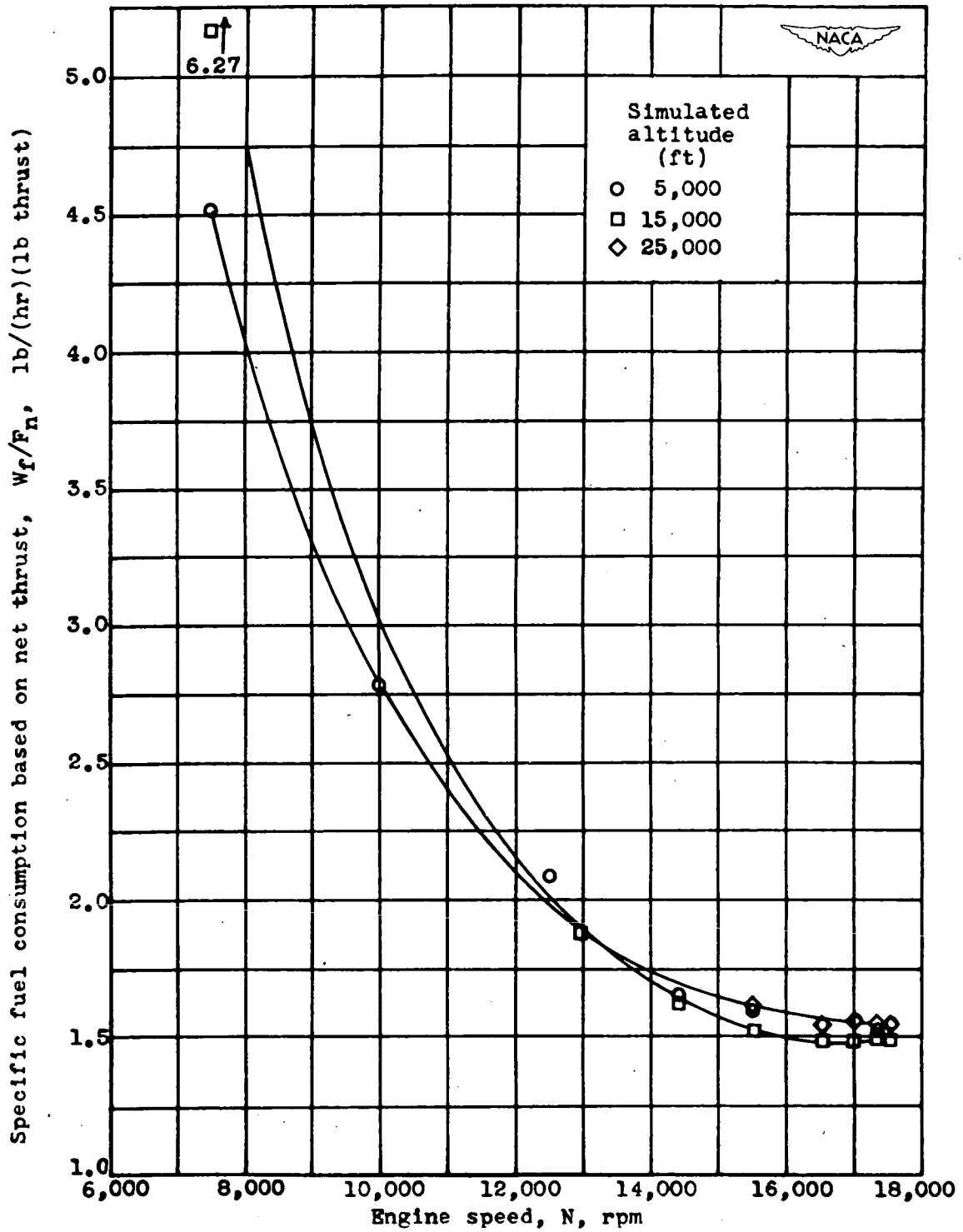

(e) Relation between specific fuel consumption based on net thrust and engine speed.

Figure 4.- Continued. Effect of altitude on performance characteristics of 19B-8 turbojet engine. Tail-pipe-nozzle area, 135 square inches; free-stream ram-pressure ratio, 1.013.

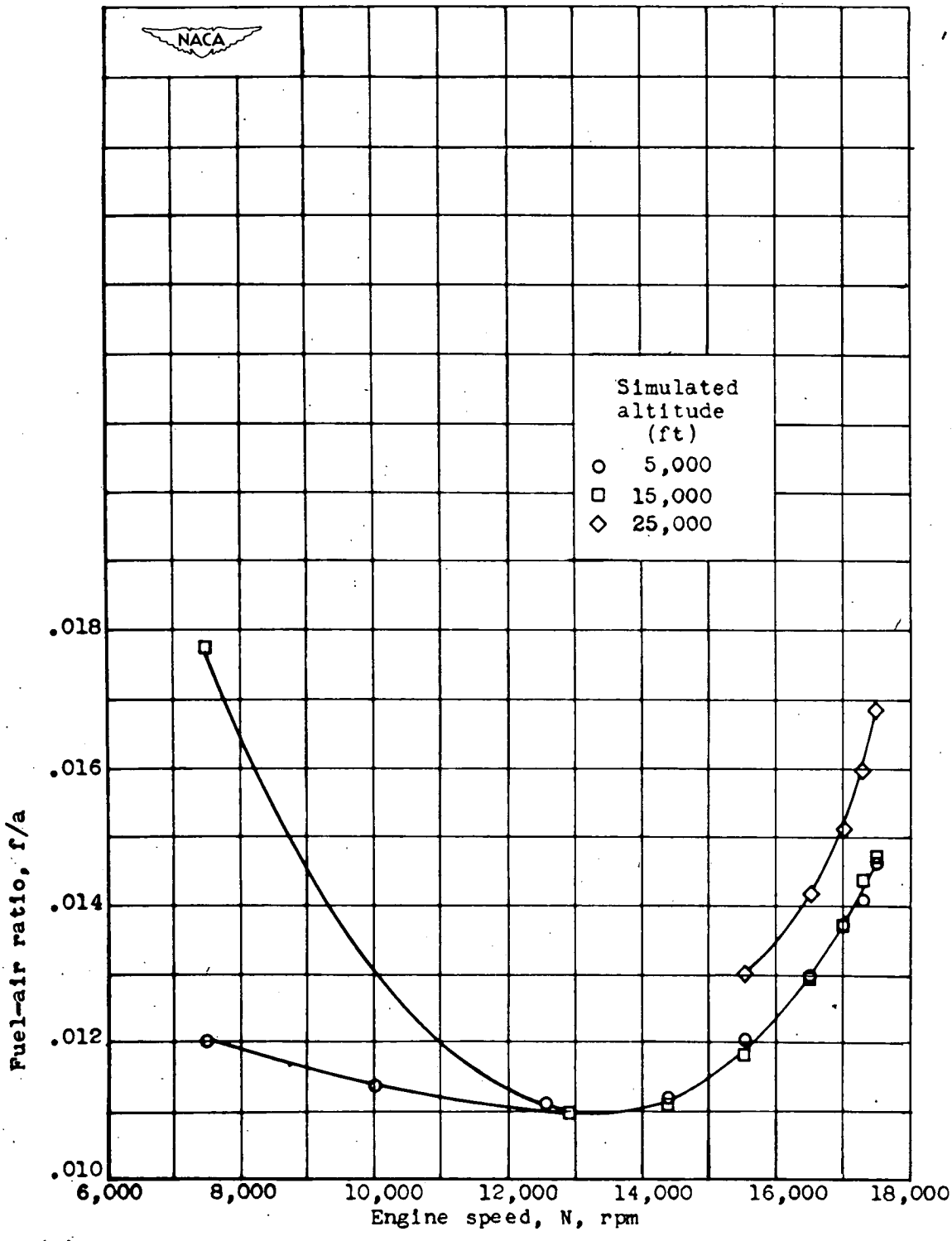

(f) Relation between fuel-air ratio and engine speed.

Figure 4.- Concluded. Effect of altitude on performance characteristics of 19B-8 turbojet engine. Tail-pipe-nozzle area, 135 square inches; free-stream ram-pressure ratio, 1.013.

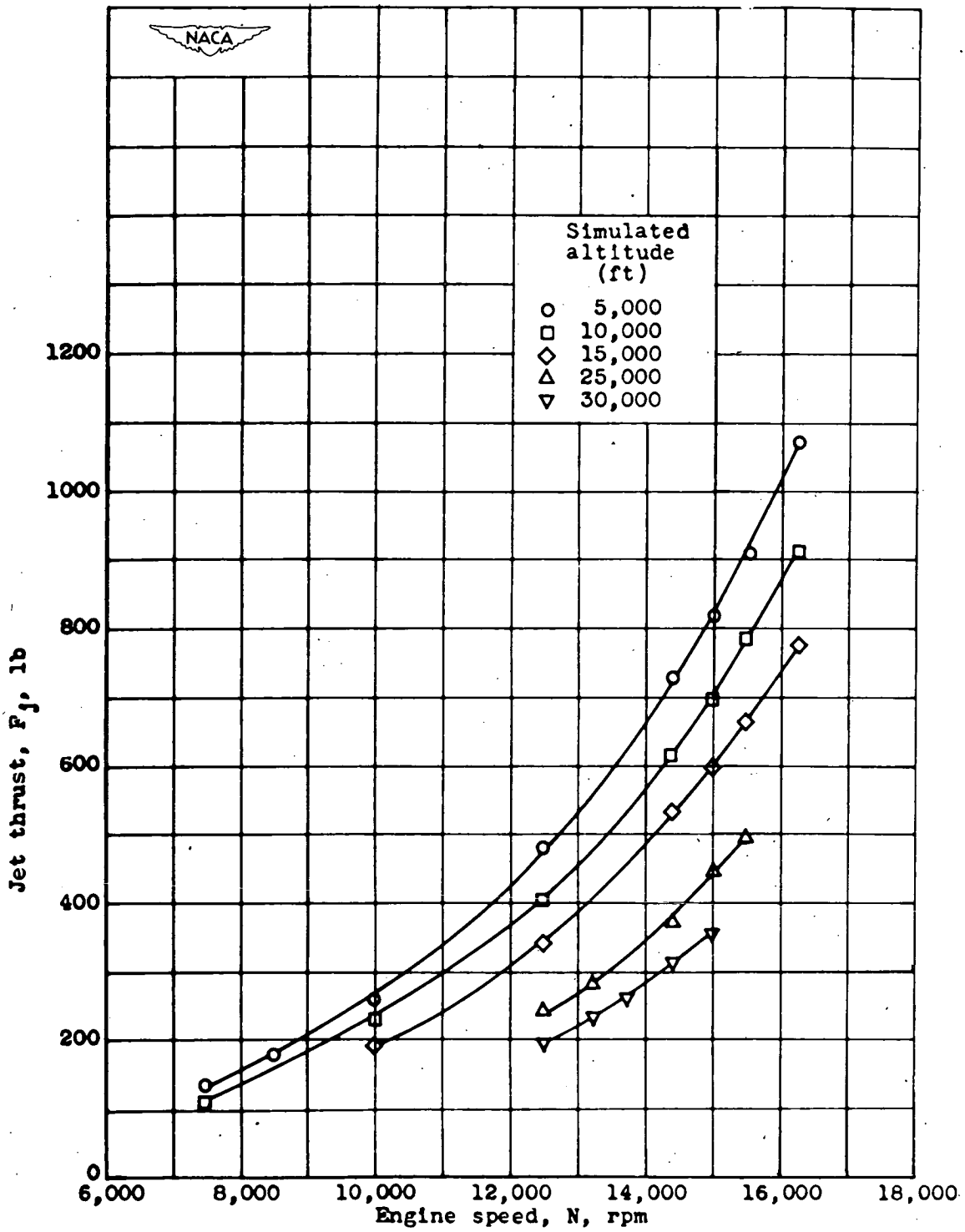

(a) Relation between jet thrust and engine speed.

Figure 5.- Effect of altitude on performance characteristics of 19XB-1 turbojet engine. Approximately static conditions.

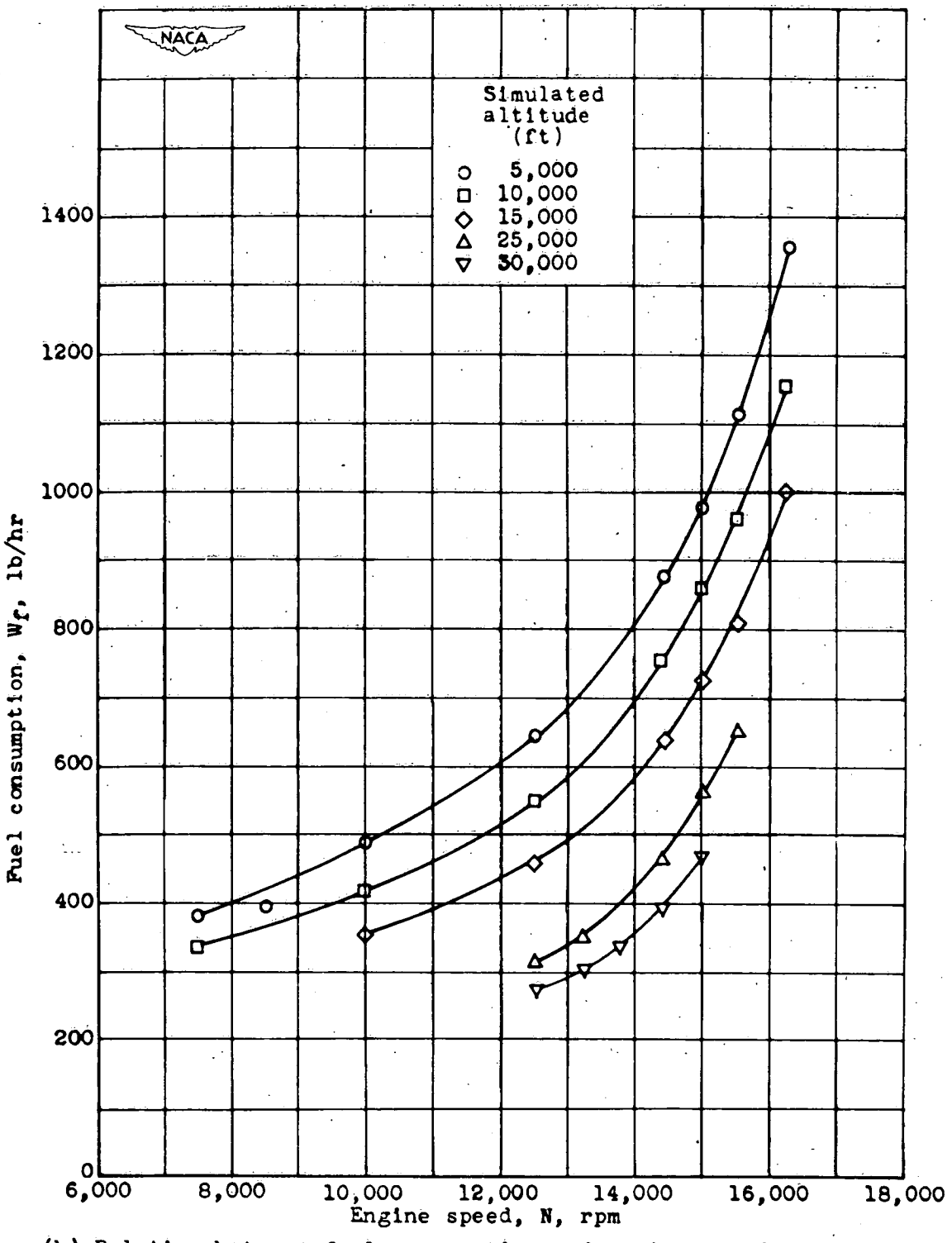

(b) Relation between fuel consumption and engine speed.

Figure 5.- Continued. Effect of altitude on performance characteristics of 19XB-1 turbojet engine. Approximately static conditions.

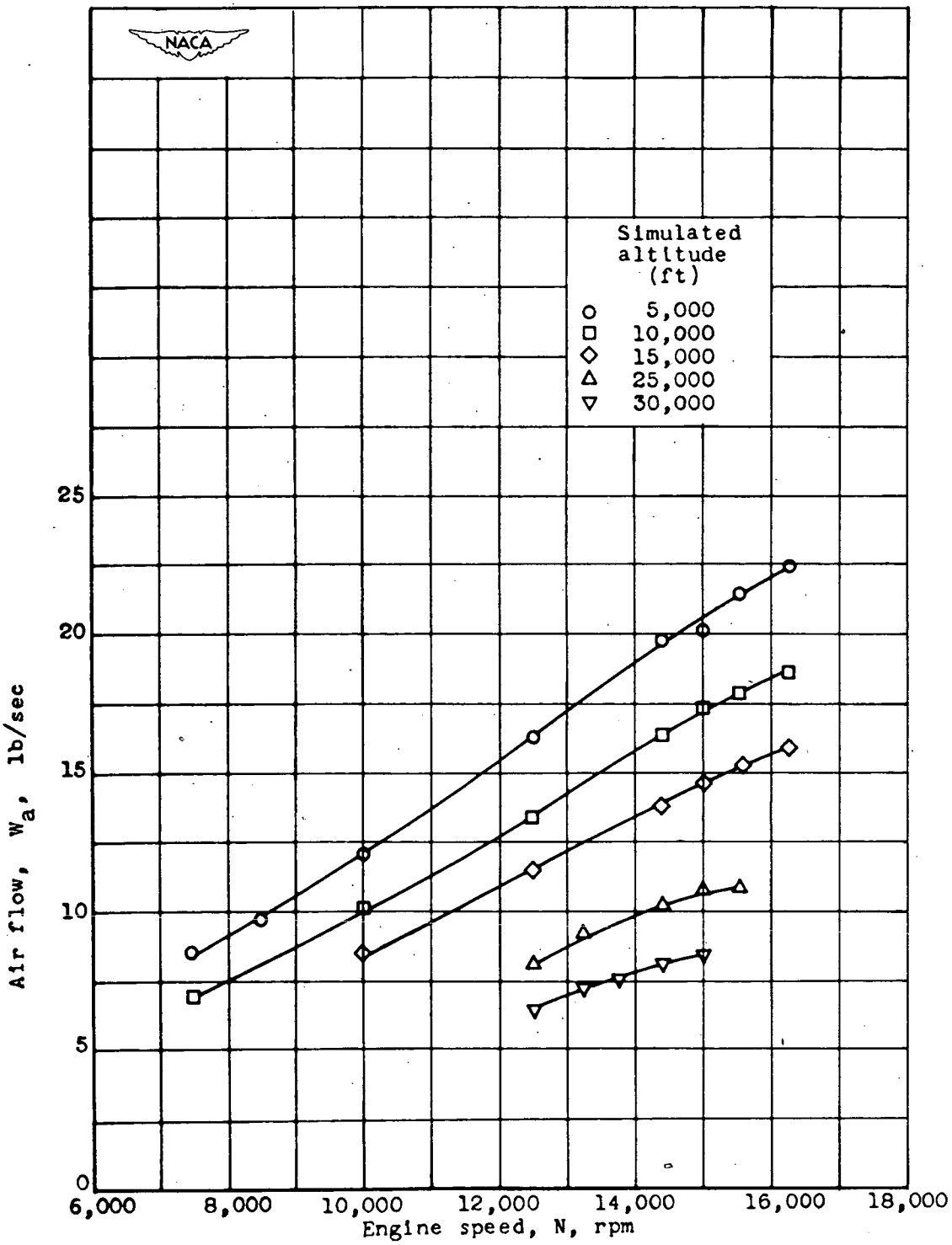

(c) Relation between air flow and engine speed.

Figure 5.- Continued. Effect of altitude on performance characteristics of 19XB-1 turbojet engine. Approximately static conditions.

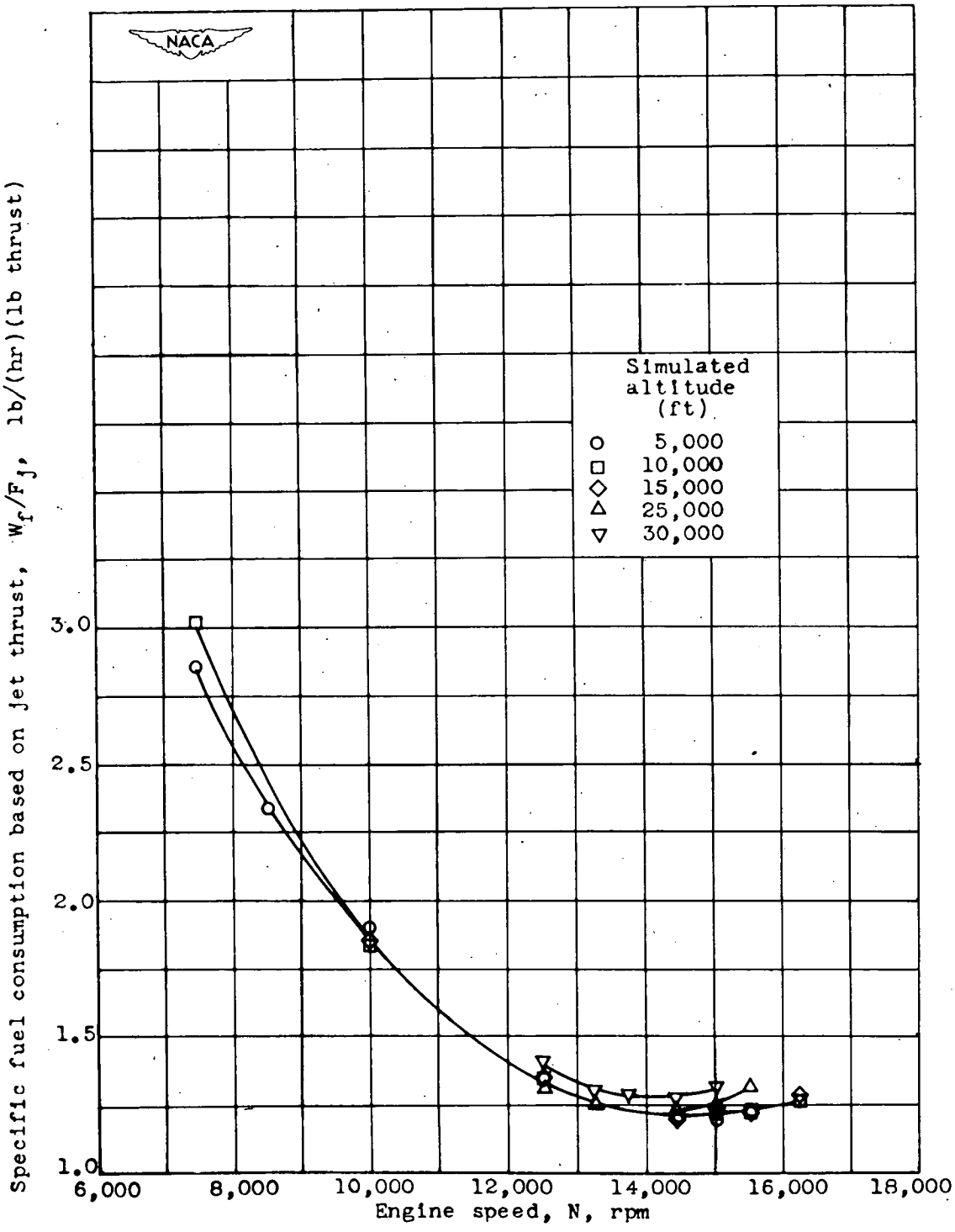

(d) Relation between specific fuel consumption based on jet thrust and engine speed.

Figure 5.- Continued. Effect of altitude on performance characteristics of 19XB-1 turbojet engine. Approximately static conditions.

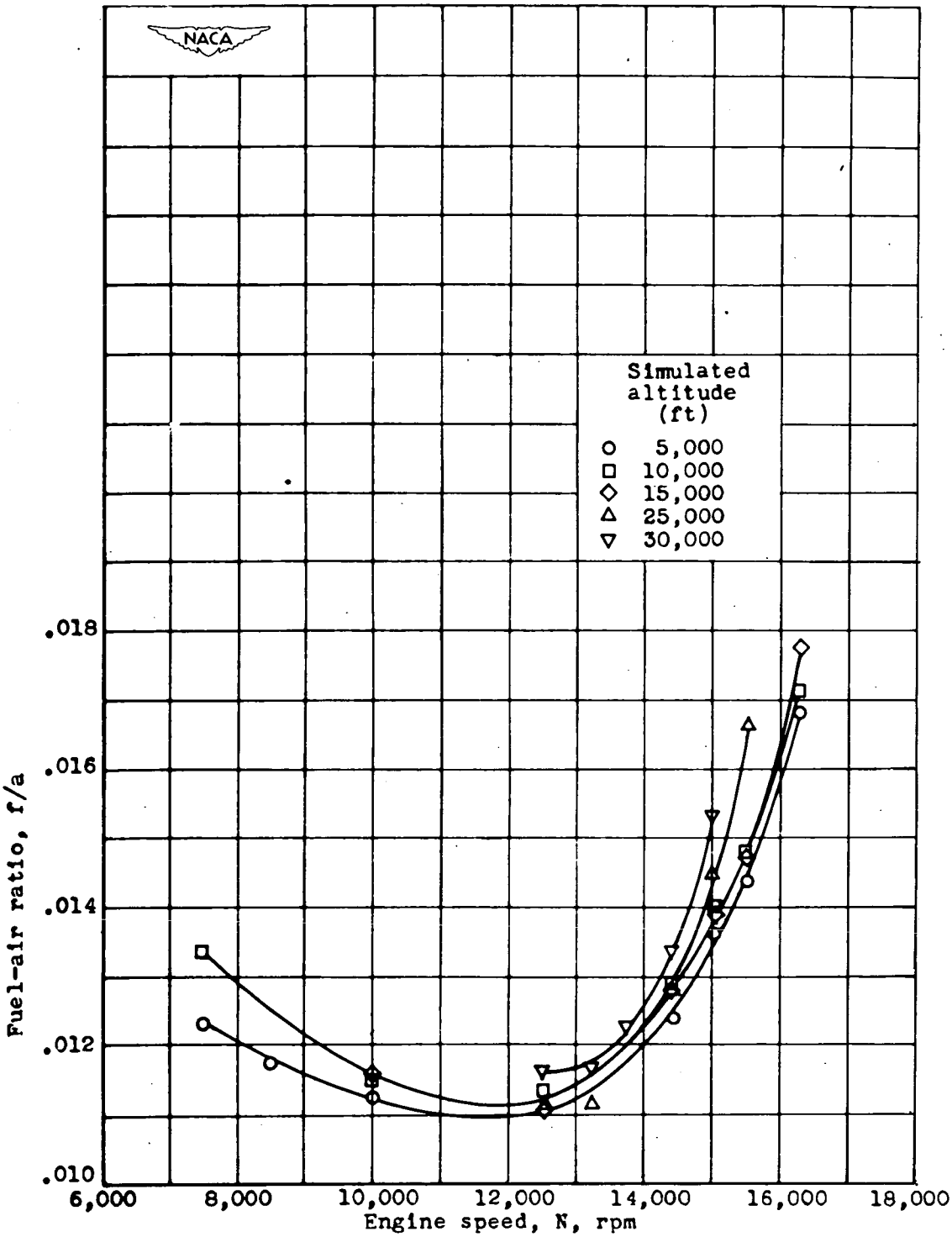

(e) Relation between fuel-air ratio and engine speed.

Figure 5.- Concluded. Effect of altitude on performance characteristics of 19XB-1 turbojet engine. Approximately static conditions.

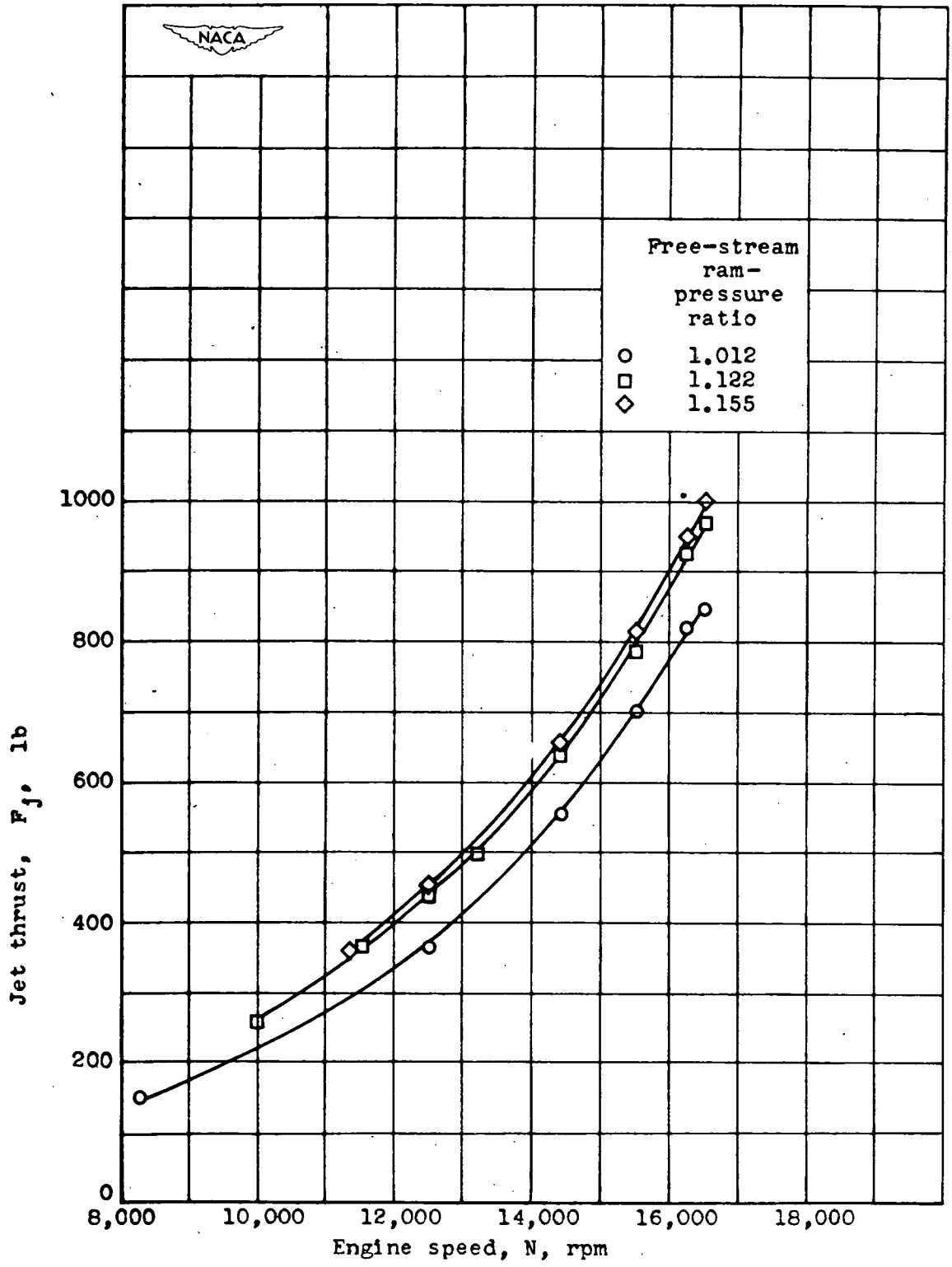

(a) Relation between jet thrust and engine speed.

Figure 6.- Effect of free-stream ram-pressure ratio on performance characteristics of 19B-8 turbojet engine. Tailpipe-nozzle area, 106 square inches; simulated altitude, 15,000 feet.

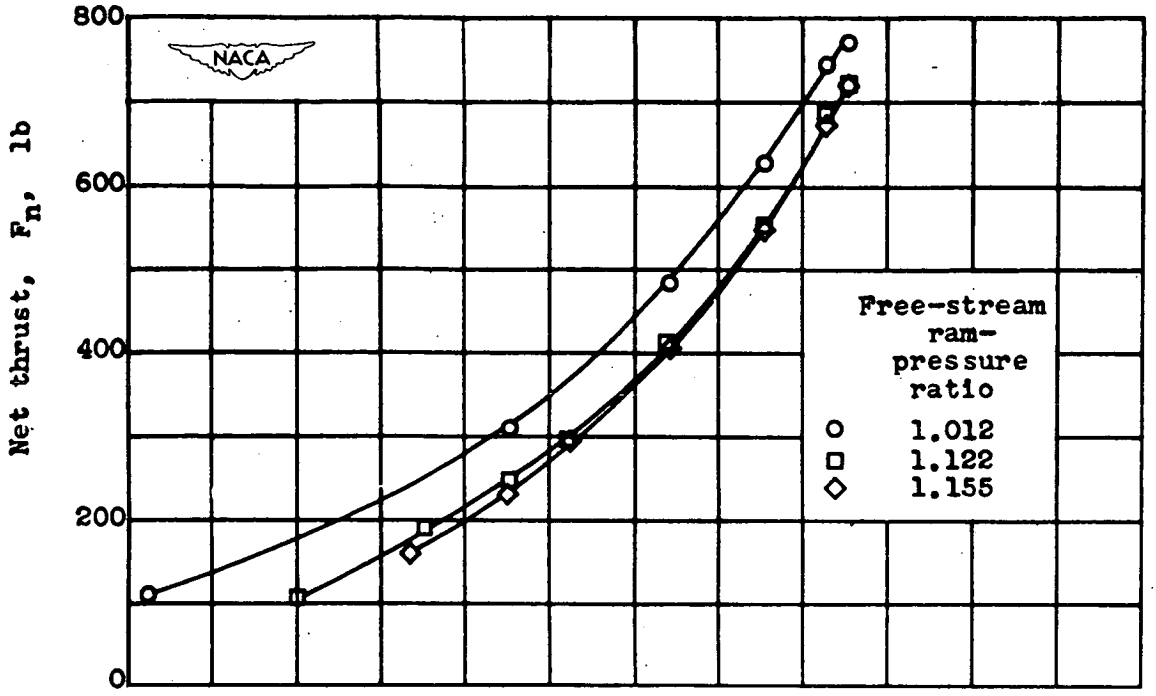

(b) Relation between net thrust and engine speed.

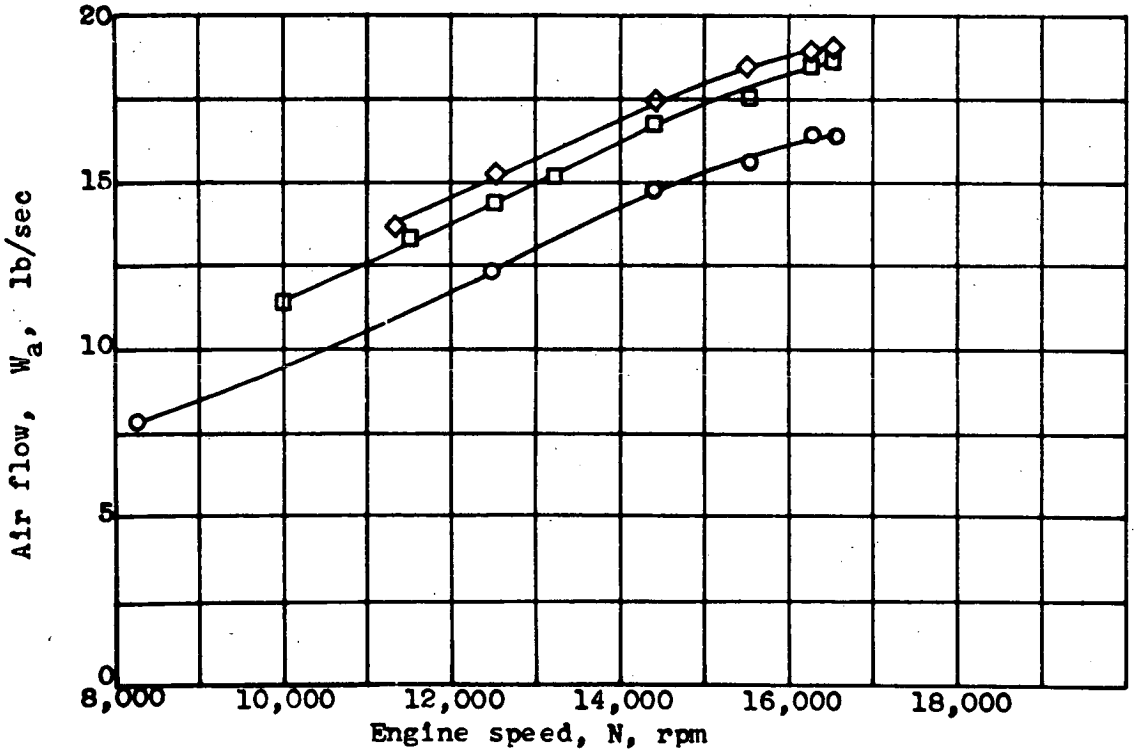

(c) Relation between air flow and engine speed.

Figure 6.- Continued. Effect of free-stream ram-pressure ratio on performance characteristics of 19B-8 turbojet engine. Tail-pipe-nozzle area, 106 square inches; simulated altitude, 15,000 feet.

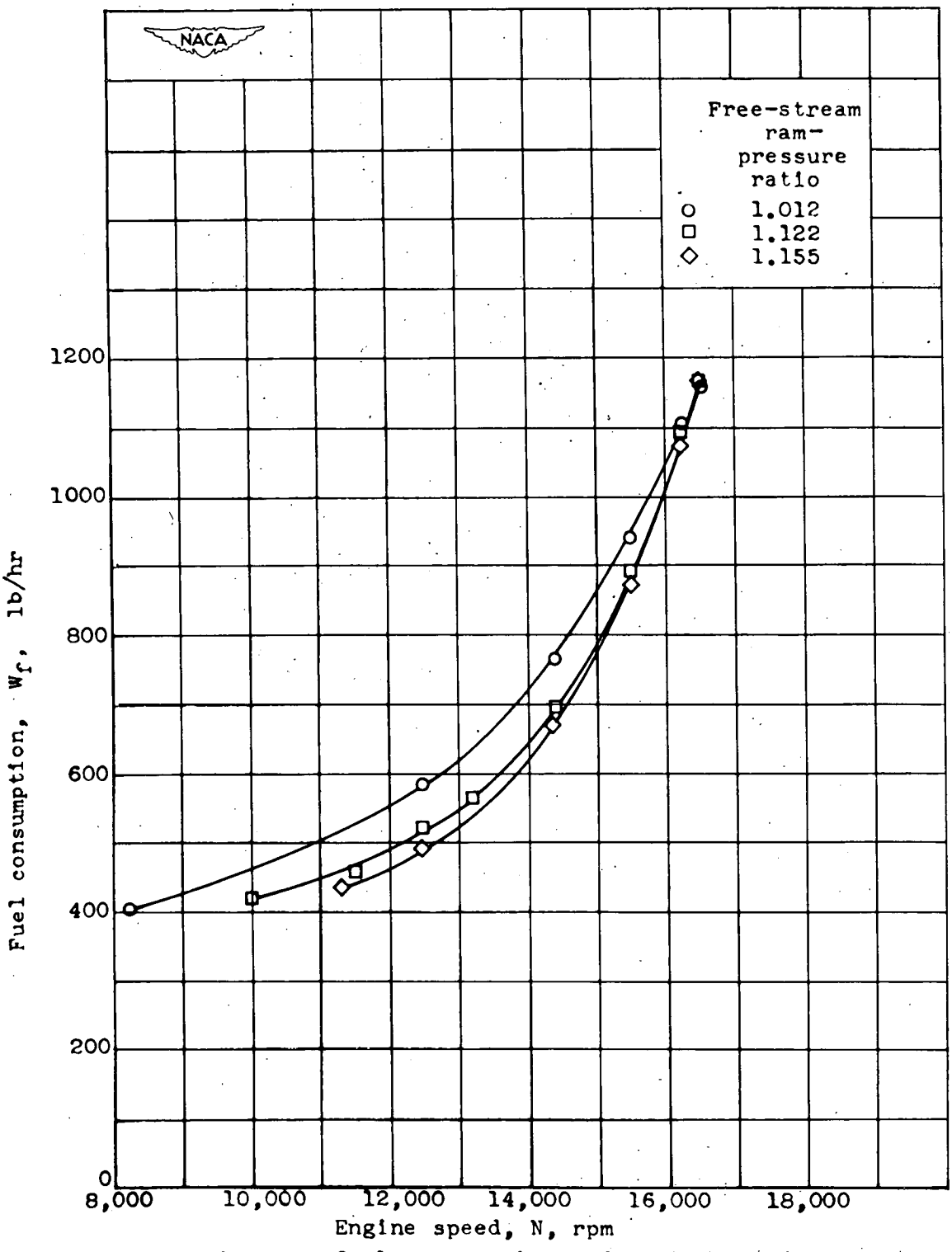

(d) Relation between fuel consumption and engine speed.

Figure 6.- Continued. Effect of free-stream ram-pressure ratio on performance characteristics of 19B-8 turbojet engine. Tail-pipe-nozzle area, 106 square inches; simulated altitude, 15,000 feet.

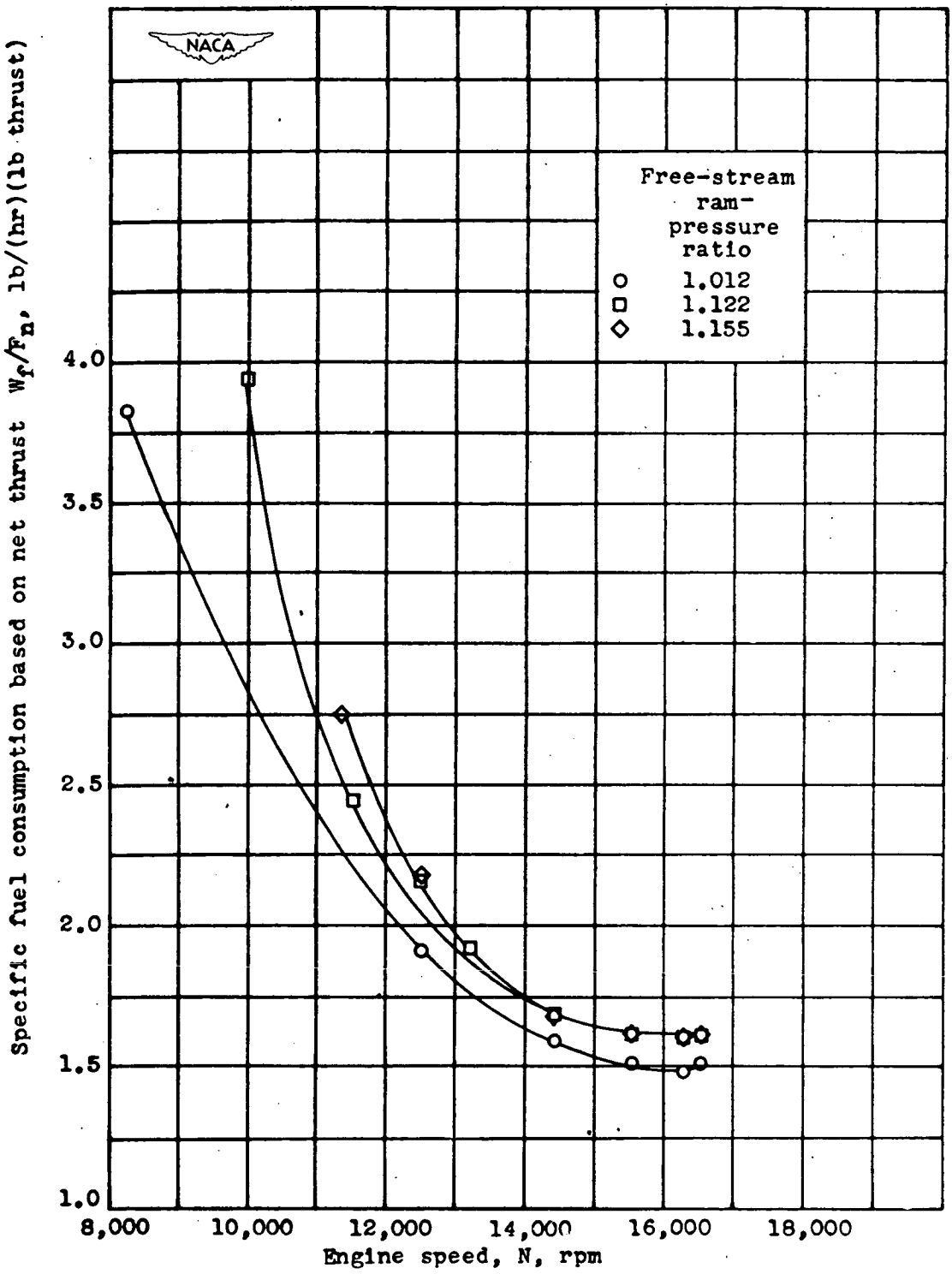

(e) Relation between specific fuel consumption based on net thrust and engine speed.

Figure 6.- Continued. Effect of free-stream ram-pressure ratio on performance characteristics of 19B-8 turbojet engine. Tail-pipe-nozzle area, 106 square inches; simulated altitude, 15,000 feet.

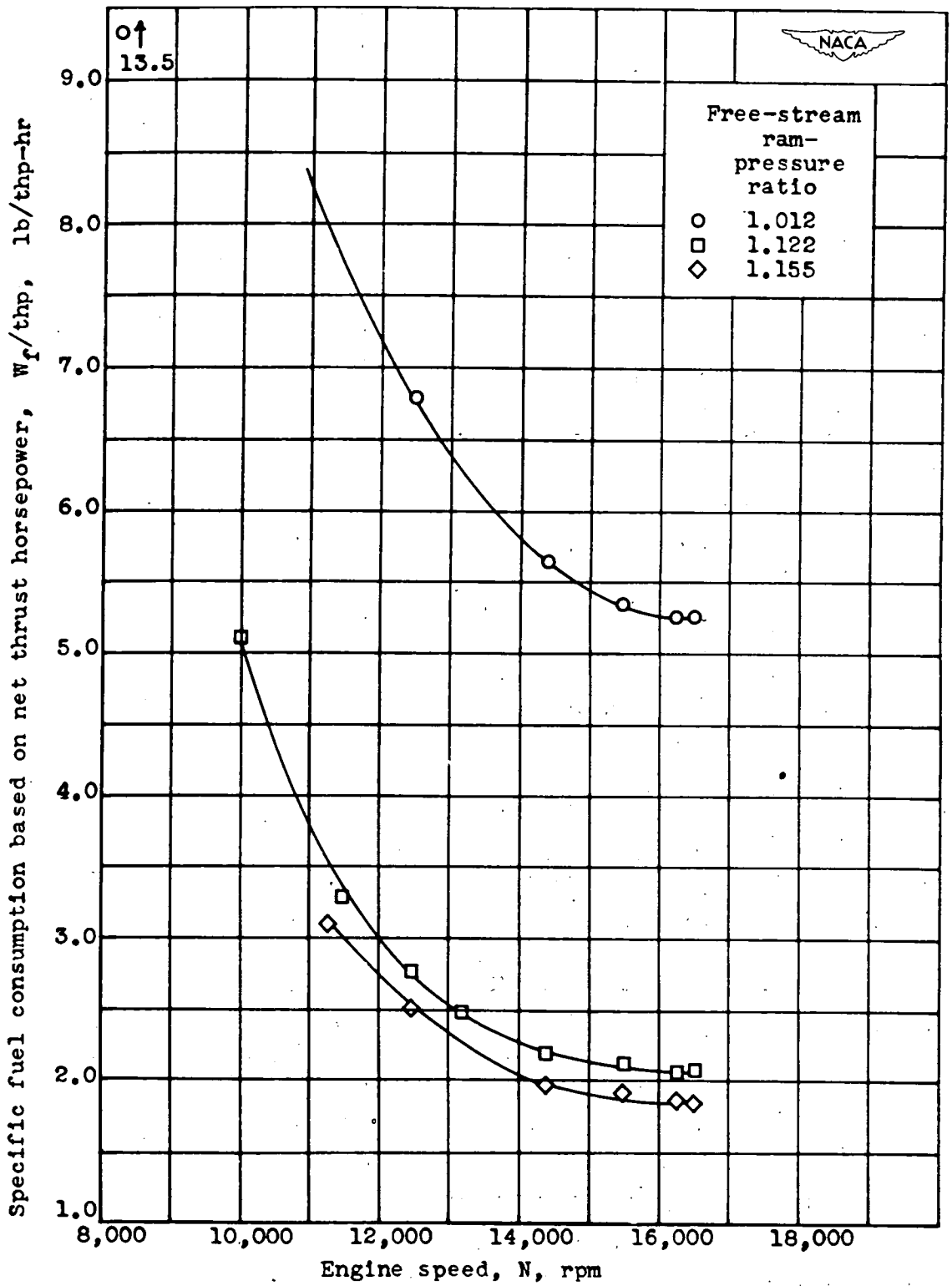

(f) Relation between specific fuel consumption based on net thrust horsepower and engine speed.

Figure 6.- Continued. Effect of free-stream ram-pressure ratio on performance characteristics of 19B-8 turbojet engine. Tail-pipe-nozzle area, 106 square inches; simulated altitude, 15,000 feet.

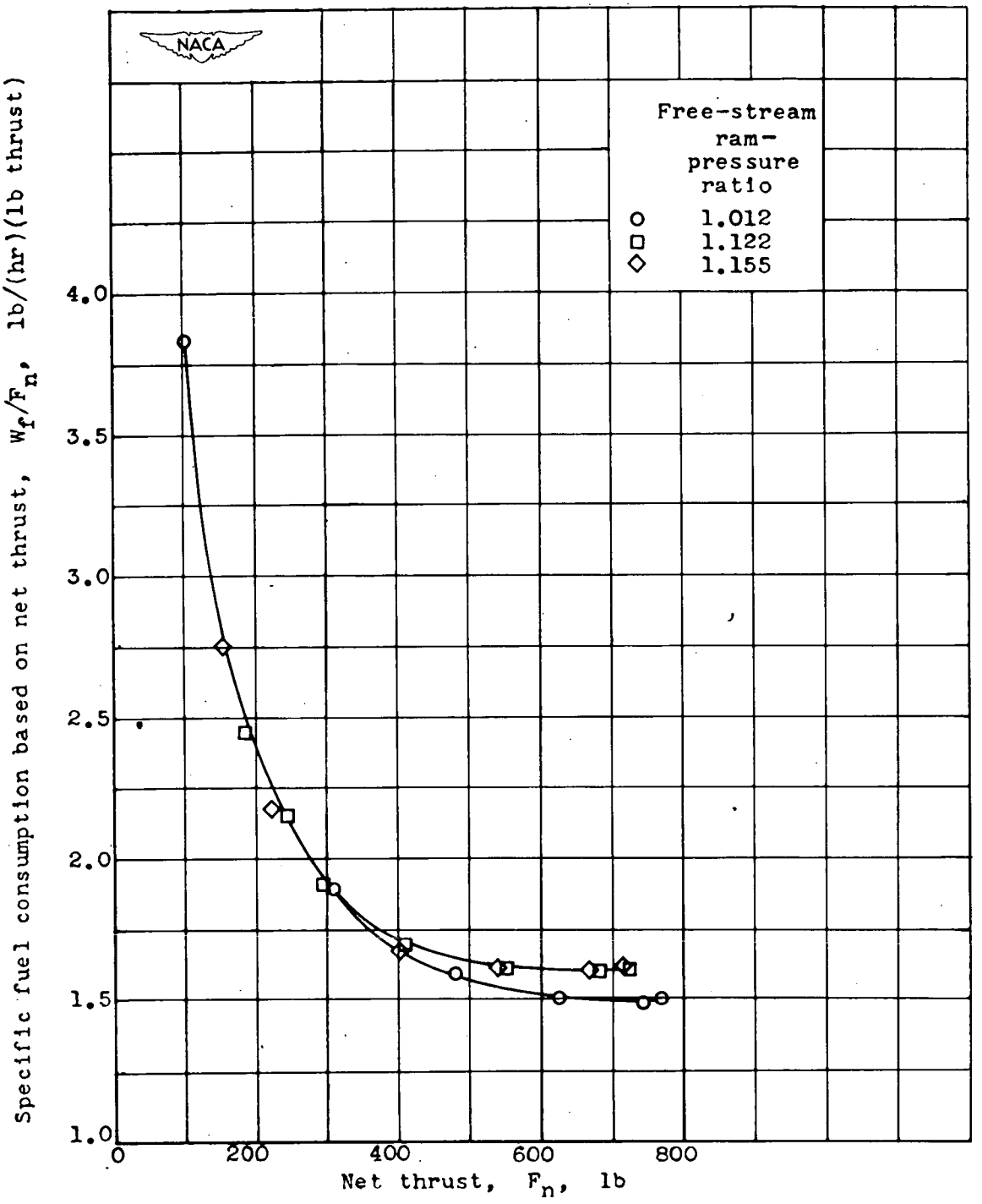

(g) Relation between specific fuel consumption based on net thrust and net thrust.

Figure 6.- Continued. Effect of free-stream ram-pressure ratio on performance characteristics of 19B-8 turbojet engine. Tail-pipe-nozzle area, 106 square inches; simulated altitude, 15,000 feet.

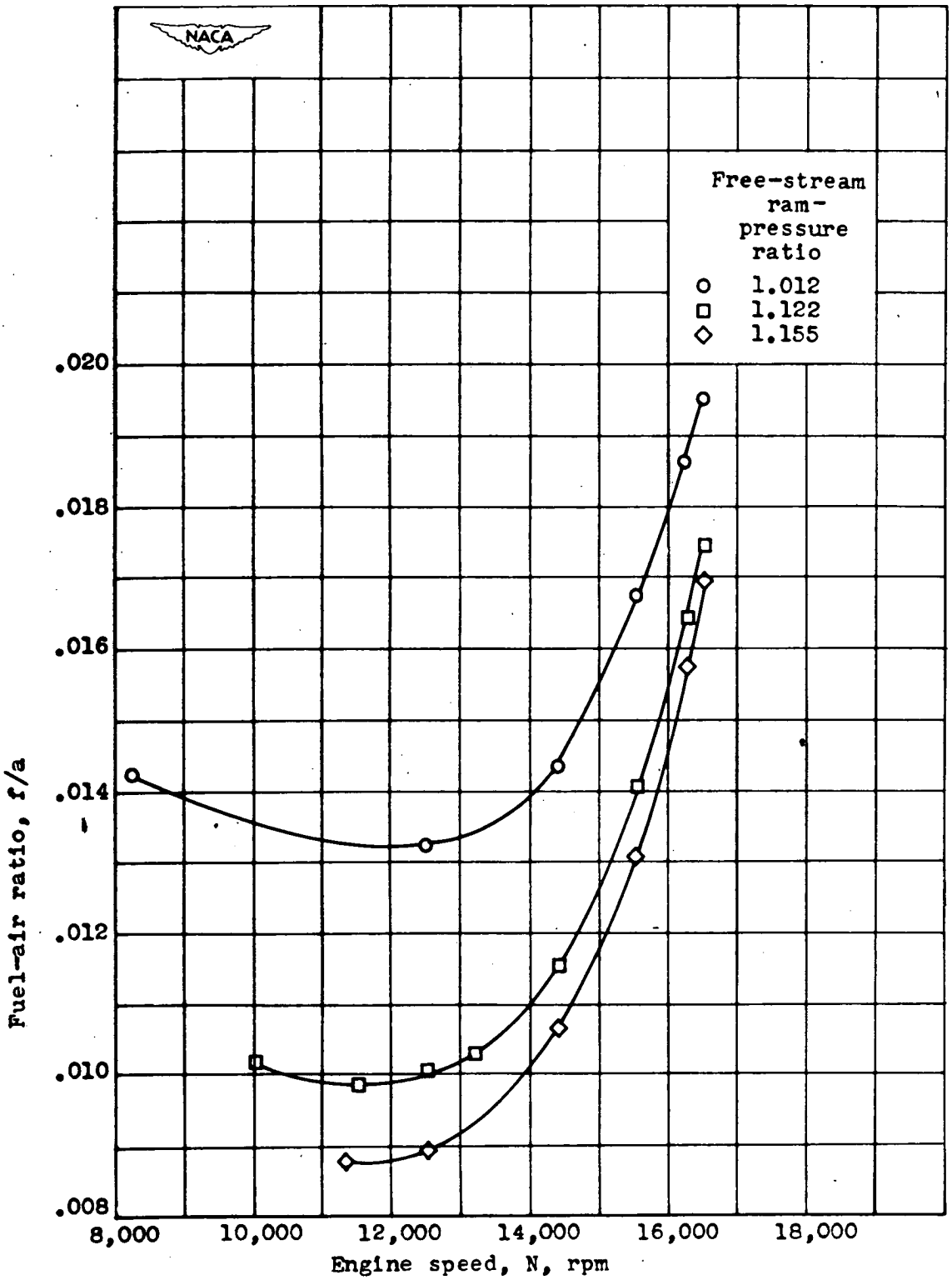

(h) Relation between fuel-air ratio and engine speed.

Figure 6.- Concluded. Effect of free-stream ram-pressure ratio on performance characteristics of 19B-8 turbojet engine. Tail-pipe-nozzle area, 106 square inches; simulated altitude, 15,000 feet.

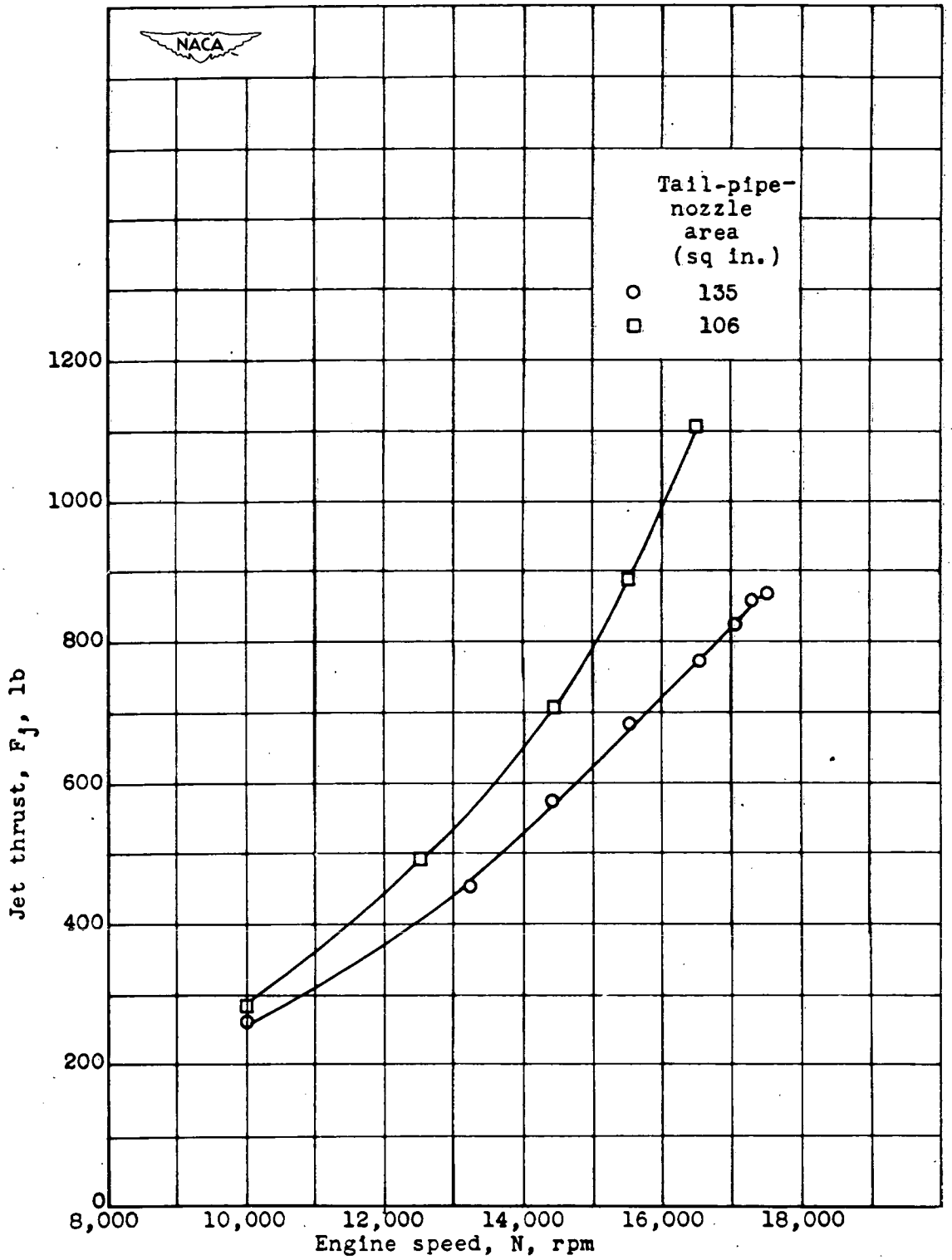

(a) Relation between jet thrust and engine speed.

Figure 7.- Effect of tail-pipe-nozzle area on performance characteristics of 19B-8 turbojet engine. Free-stream ram-pressure ratio, 1.131; simulated altitude, 10,000 feet.

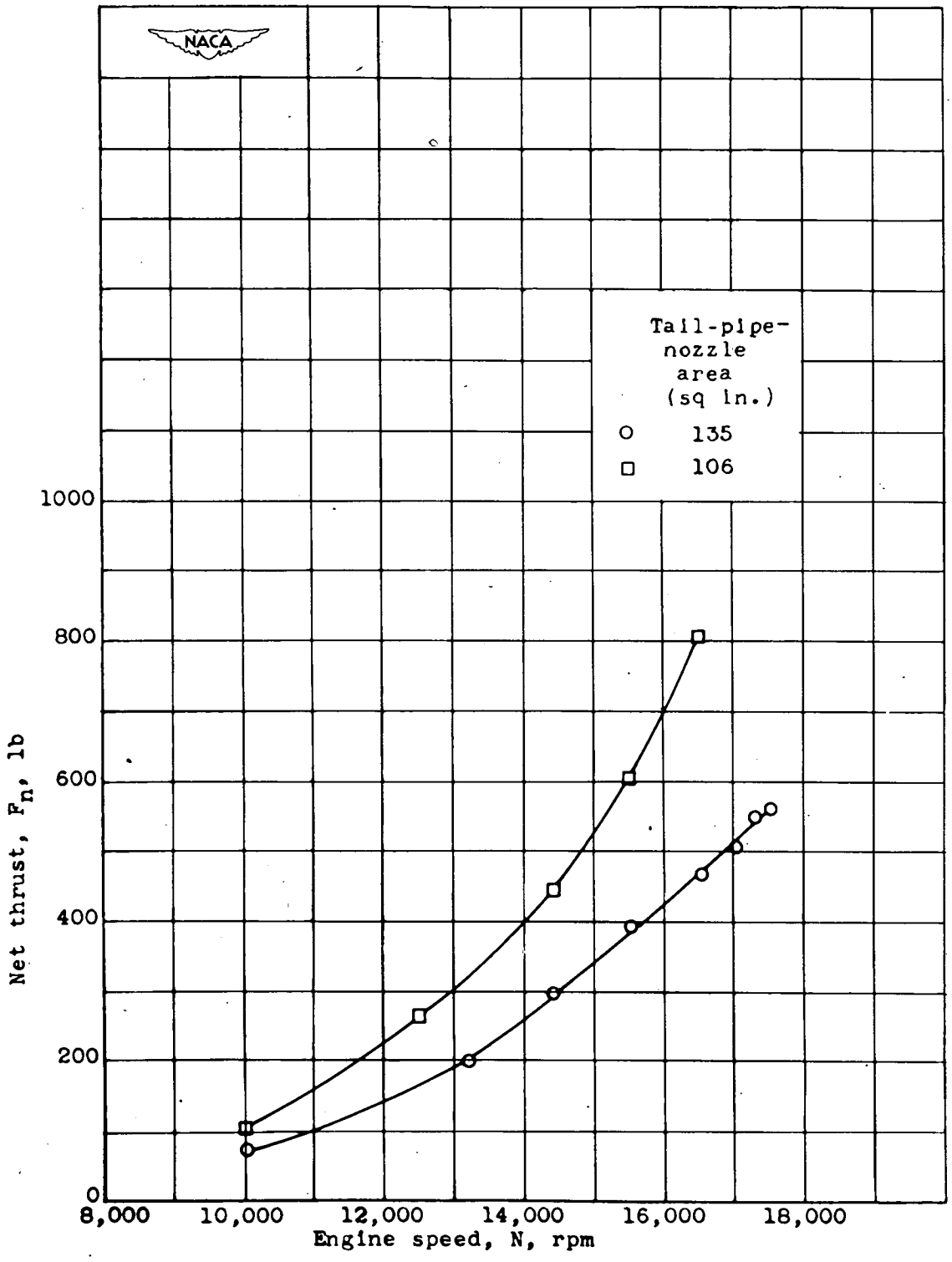

(b) Relation between net thrust and engine speed.

Figure 7.- Continued. Effect of tail-pipe-nozzle area on performance characteristics of 19B-8 turbojet engine. Free-stream ram-pressure ratio, 1.131; simulated altitude, 10,000 feet.

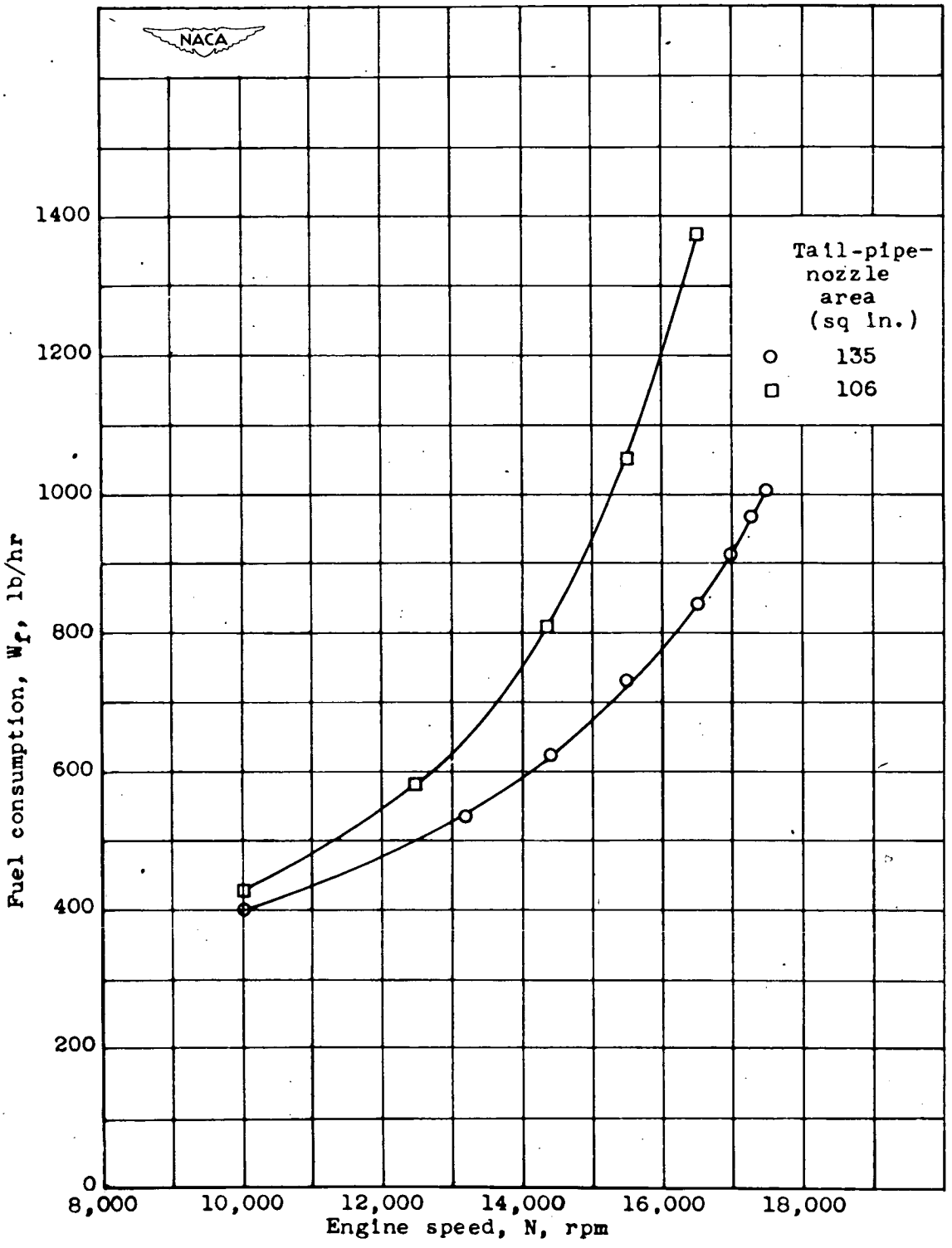

(c) Relation between fuel consumption and engine speed.

Figure 7.- Continued. Effect of tail-pipe-nozzle area on performance characteristics of 19B-8 turbojet engine. Free-stream ram-pressure ratio, 1.131; simulated altitude, 10,000 feet.

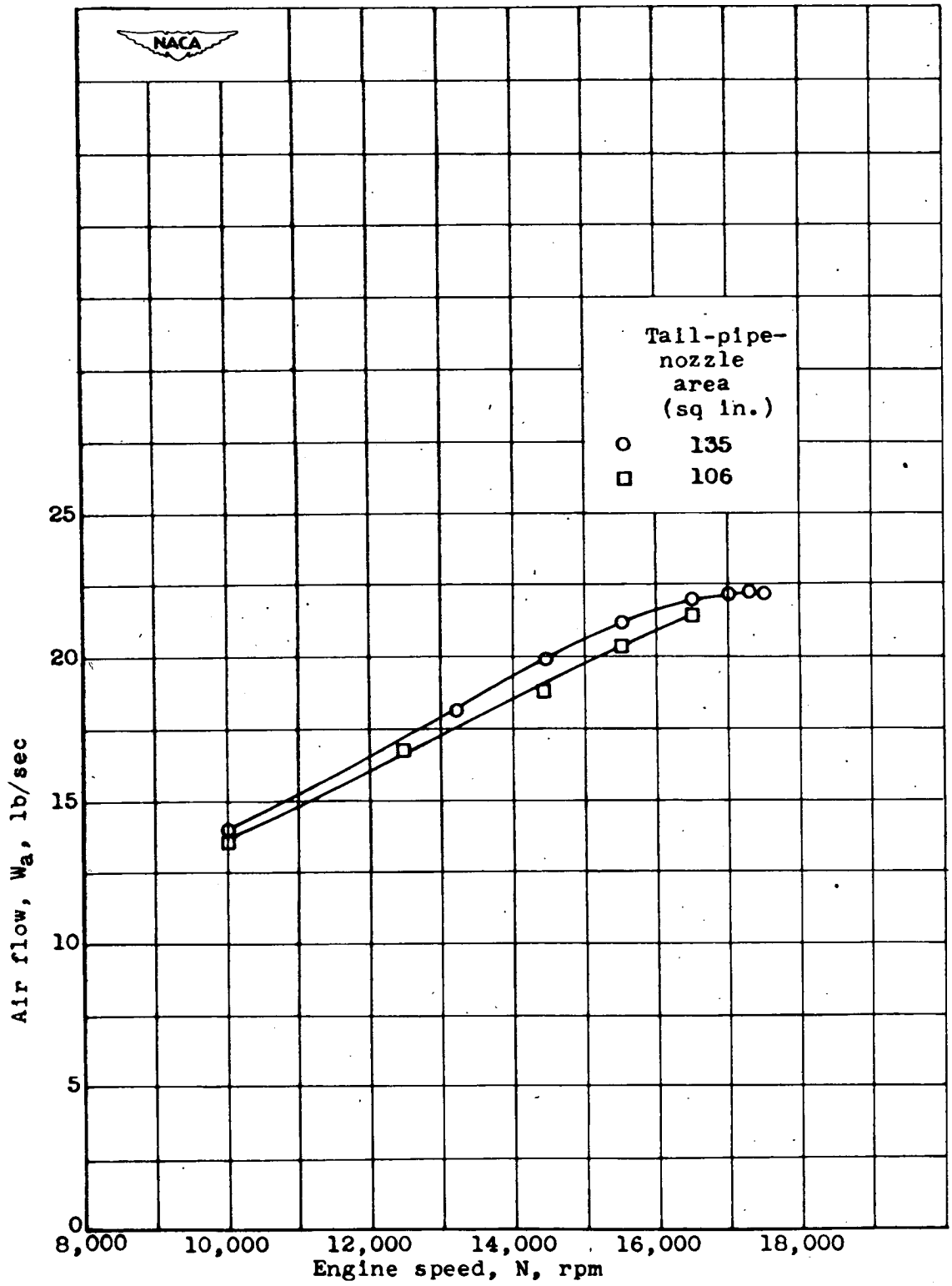

(d) Relation between air flow and engine speed.

Figure 7.- Continued. Effect of tail-pipe-nozzle area on performance characteristics of 19B-8 turbojet engine. Free-stream ram-pressure ratio, 1.131; simulated altitude, 10,000 feet.

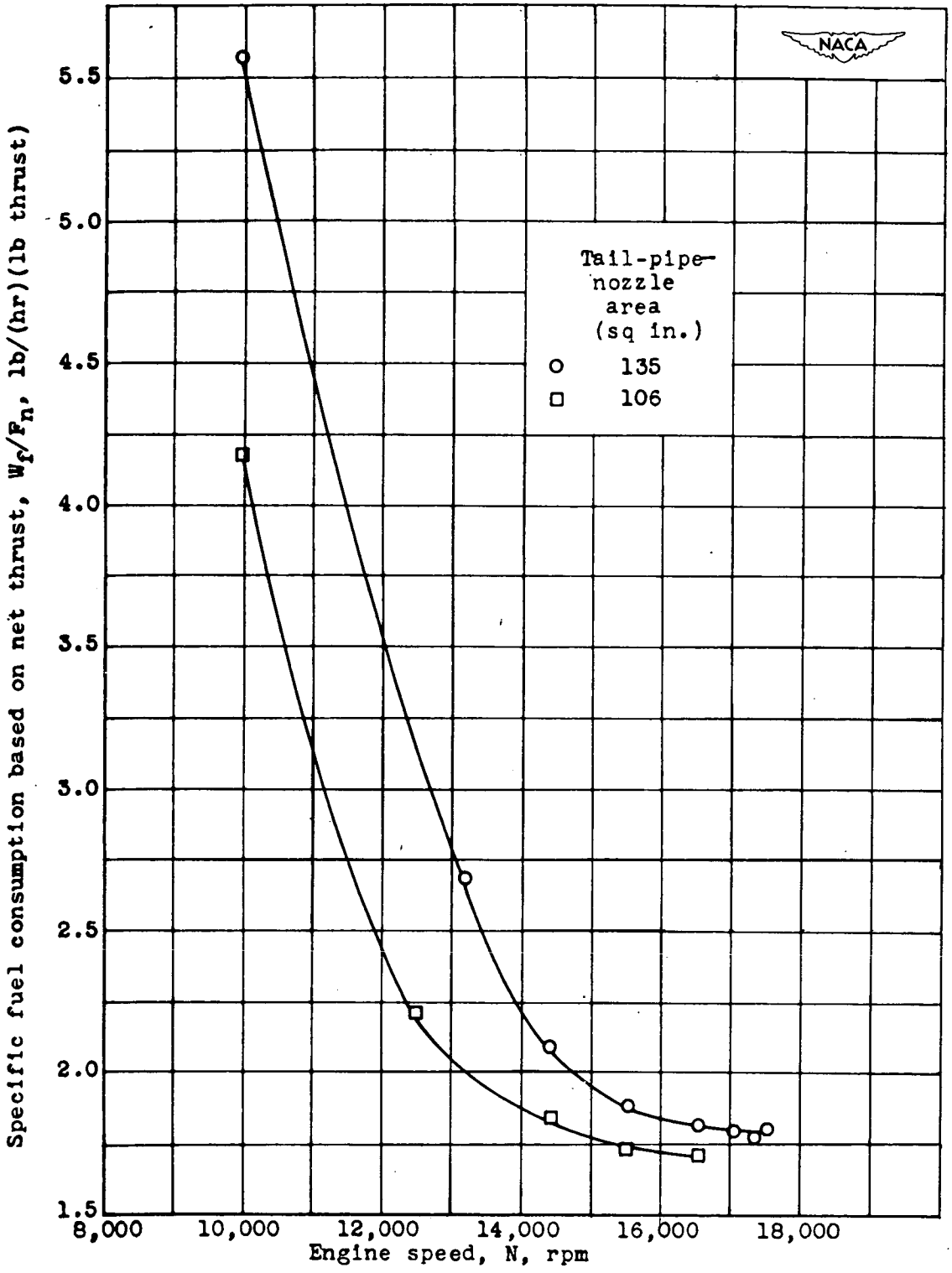

(e) Relation between specific fuel consumption based on net thrust and engine speed.

Figure 7.- Continued. Effect of tail-pipe-nozzle area on performance characteristics of 19B-8 turbojet engine. Free-stream ram-pressure ratio, 1.131; simulated altitude, 10,000 feet.

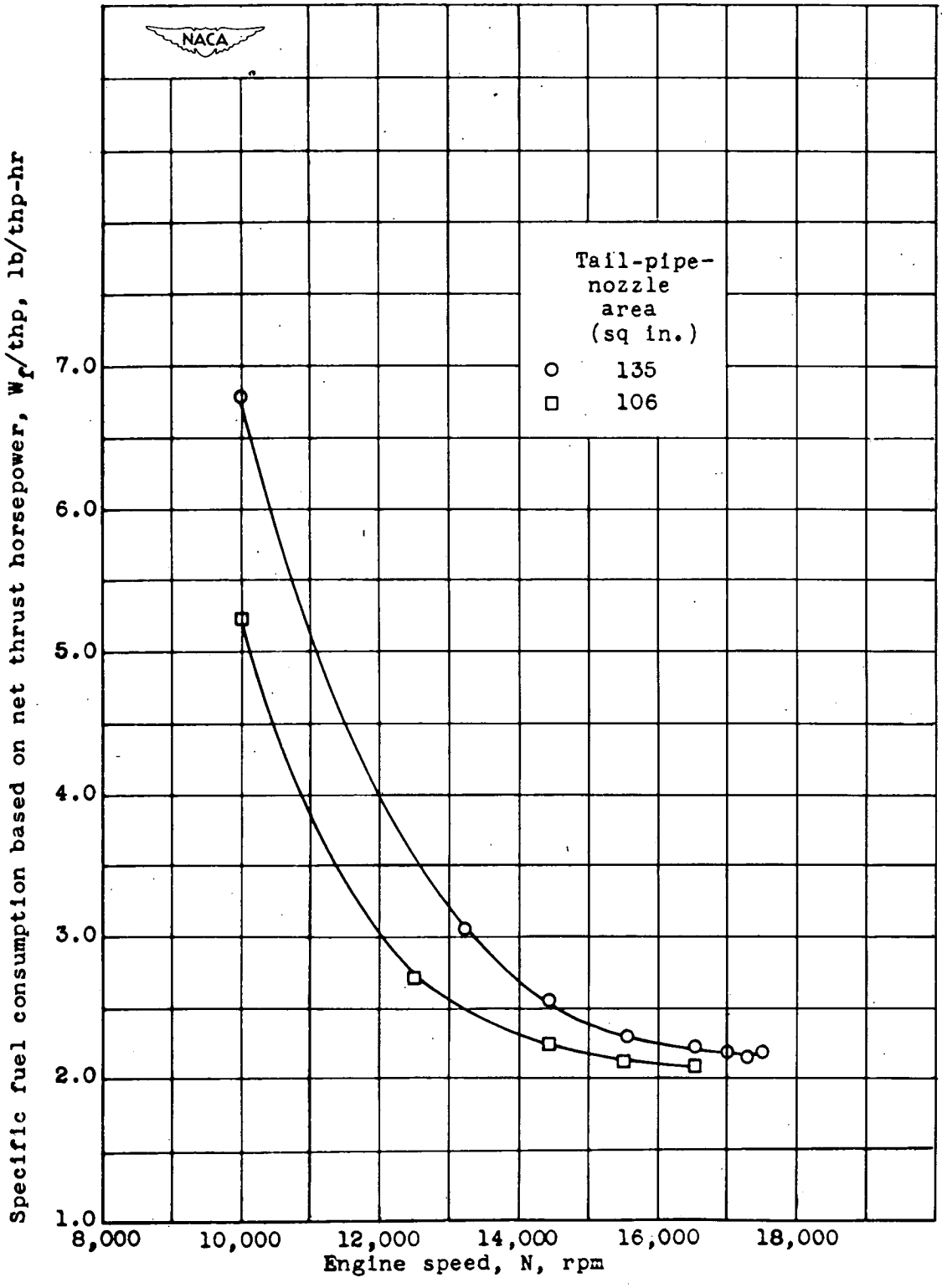

(f) Relation between specific fuel consumption based on net thrust horsepower and engine speed.

Figure 7.- Continued. Effect of tail-pipe-nozzle area on performance characteristics of 19B-8 turbojet engine. Free-stream ram-pressure ratio, 1.131; simulated altitude, 10,000 feet.

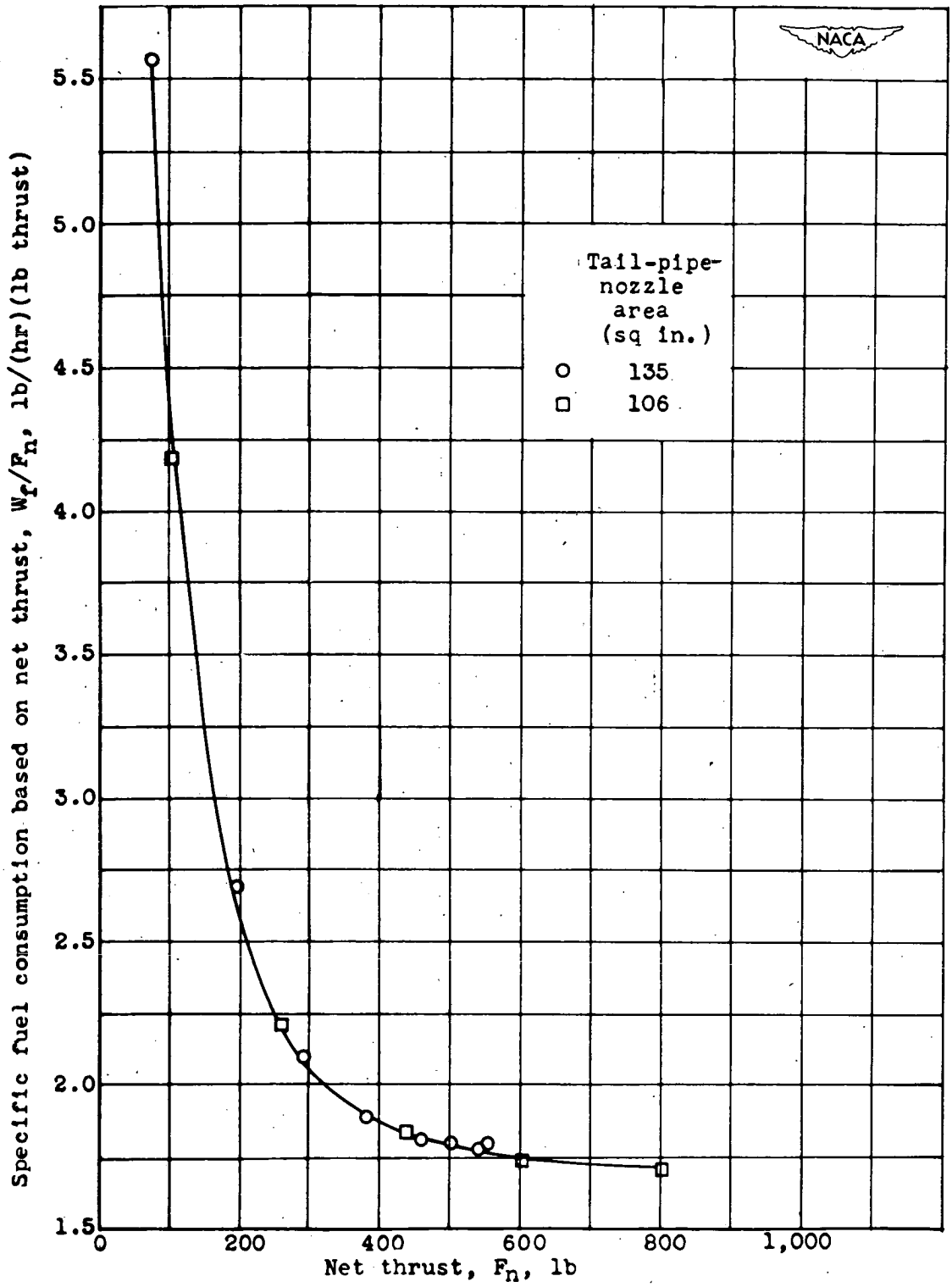

(g) Relation between specific fuel consumption based on net thrust and net thrust.

Figure 7.- Continued. Effect of tail-pipe-nozzle area on performance characteristics of 19B-8 turbojet engine. Free-stream ram-pressure ratio, 1.131; simulated altitude, 10,000 feet.

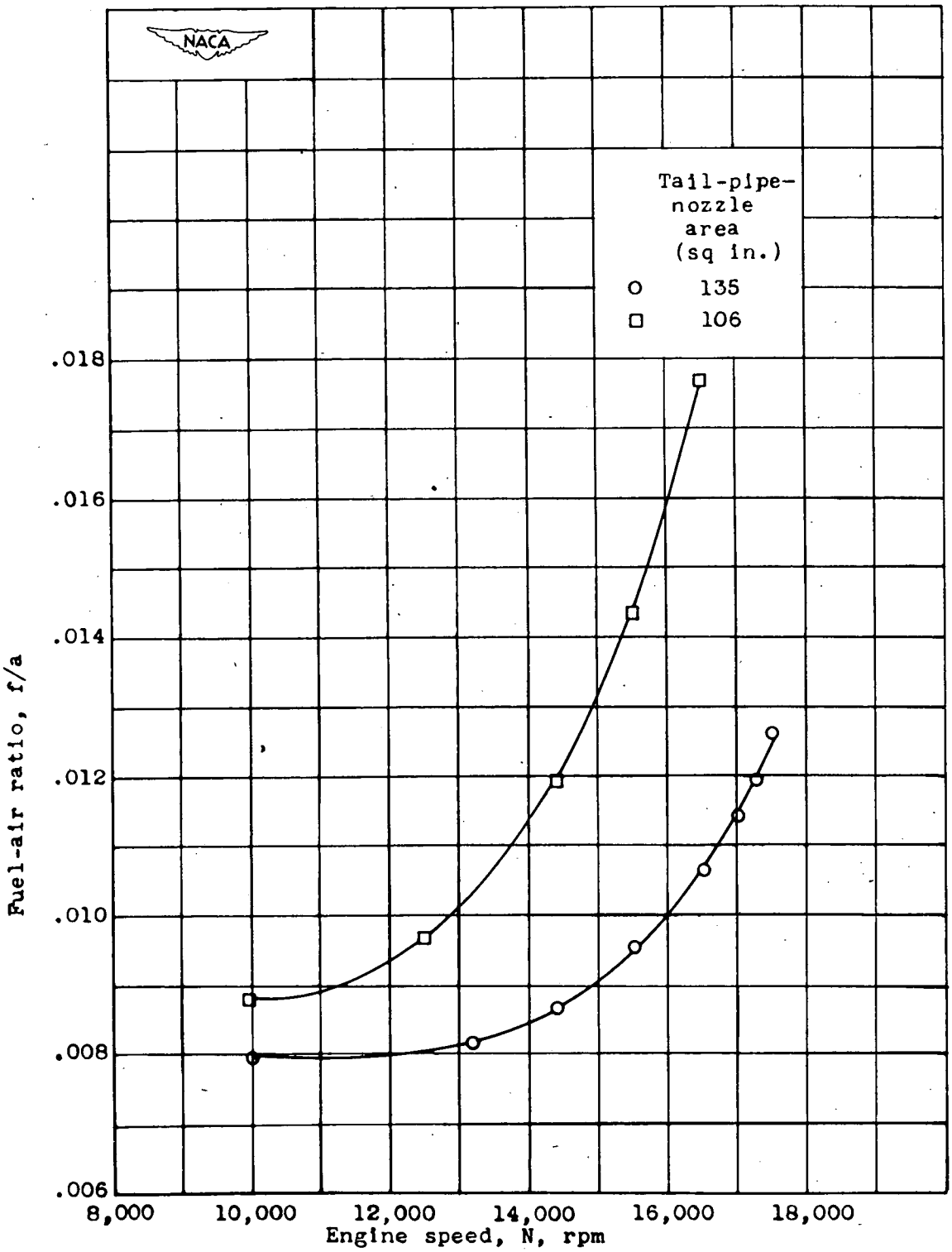

(h) Relation between fuel-air ratio and engine speed.

Figure 7.- Concluded. Effect of tail-pipe-nozzle area on performance characteristics of 19B-8 turbojet engine. Free-stream ram-pressure ratio, 1.131; simulated altitude, 10,000 feet.

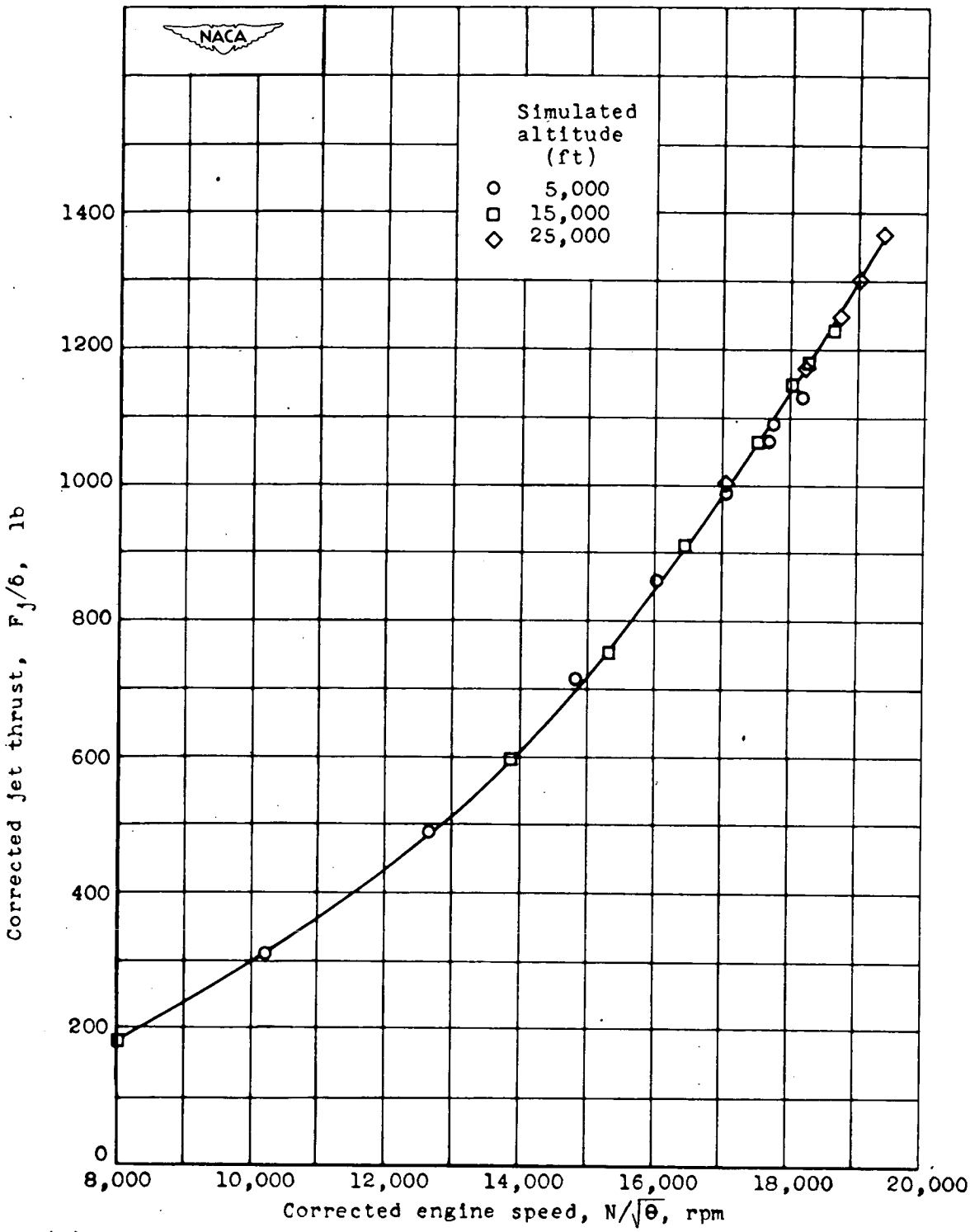

(a) Relation between corrected jet thrust and corrected engine speed.

Figure 8.- Effect of altitude on generalized performance characteristics of 19B-8 turbojet engine. Free-stream ram-pressure ratio, 1.013. Tail-pipe-nozzle area, 135 square inches. Performance parameters corrected to NACA standard atmospheric conditions at sea level.

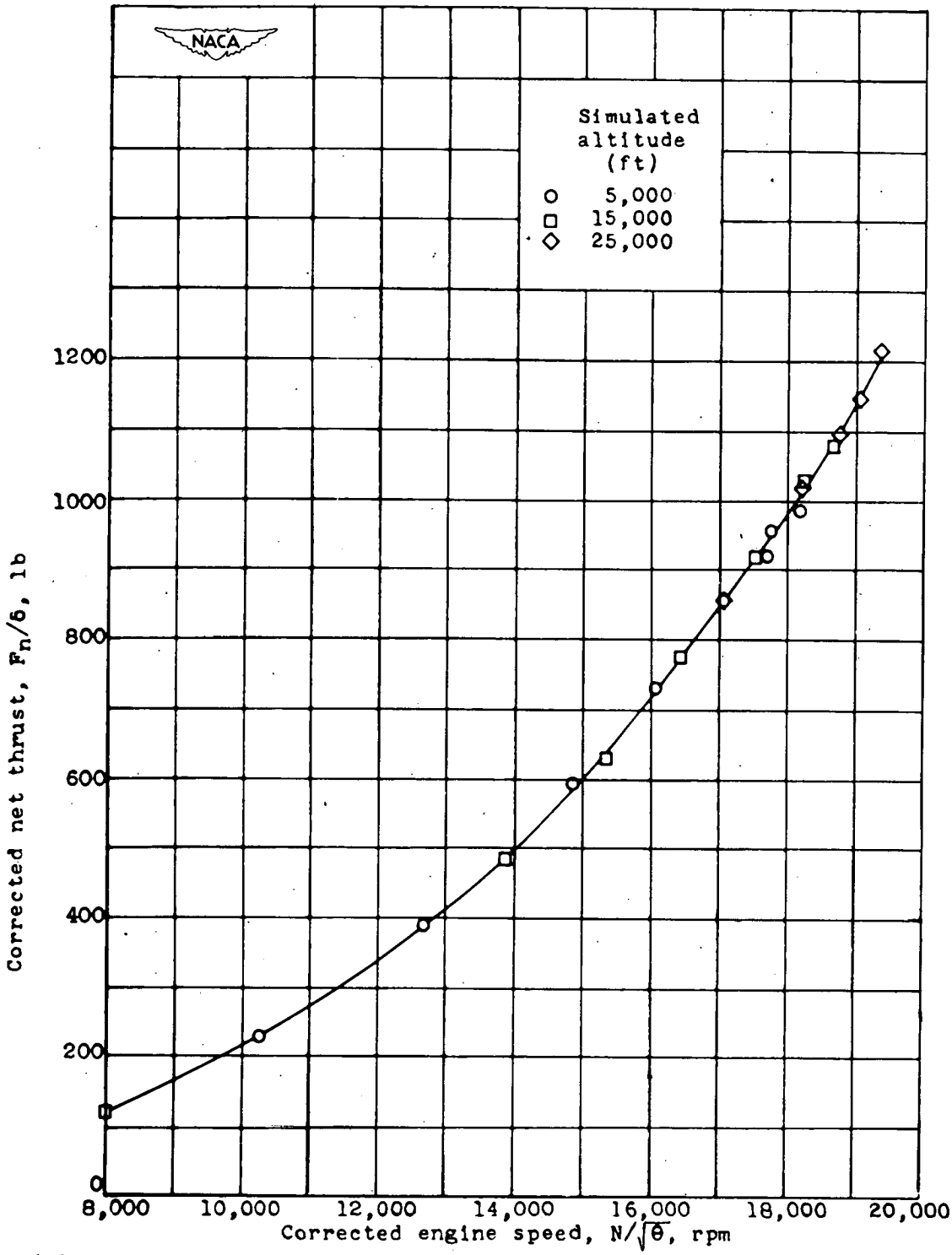

(b) Relation between corrected net thrust and corrected engine speed.

Figure 8.- Continued. Effect of altitude on generalized performance characteristics of 19B-8 turbojet engine. Free-stream ram-pressure ratio, 1.013. Tail-pipe-nozzle area, 135 square inches. Performance parameters corrected to NACA standard atmospheric conditions at sea level.

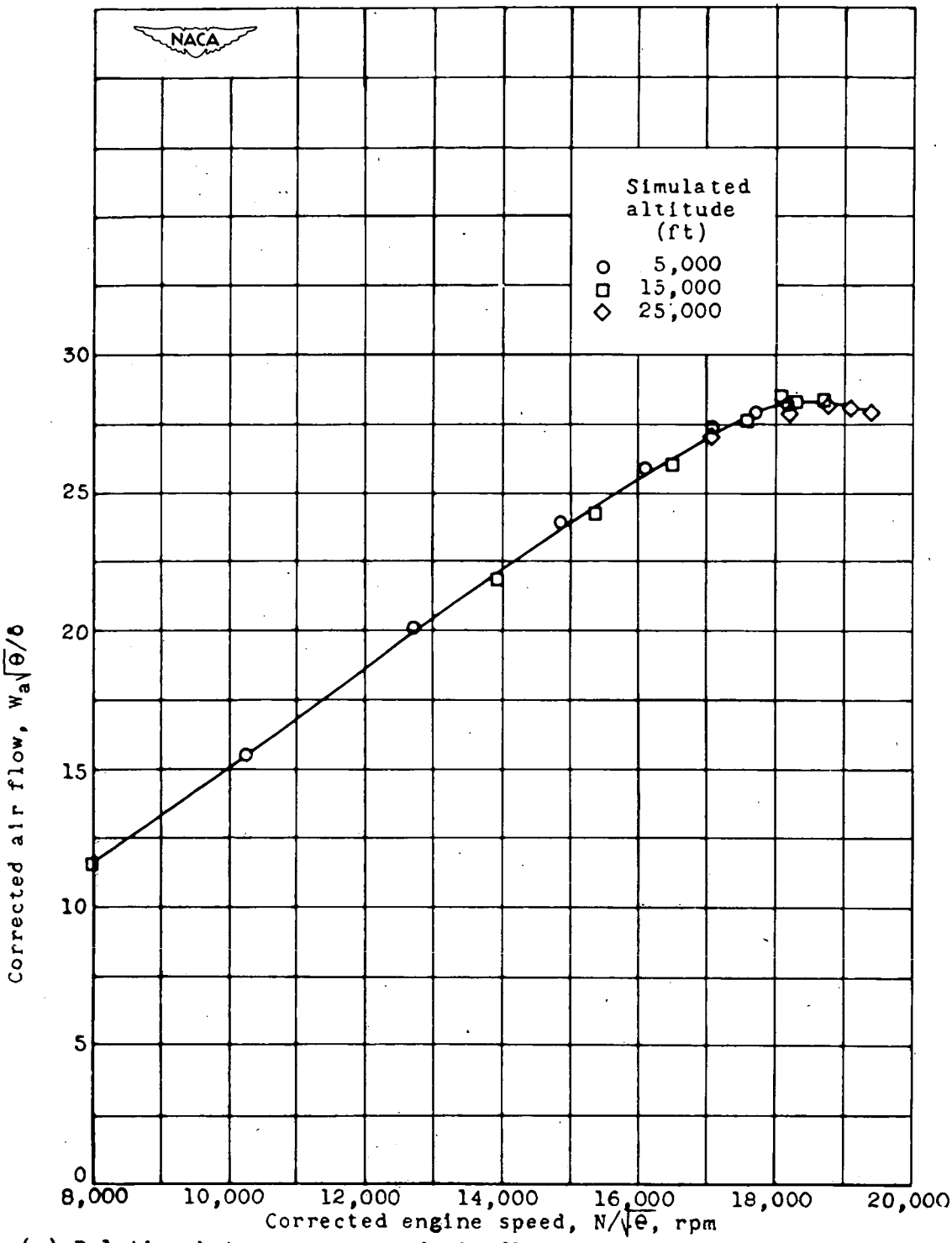

(c) Relation between corrected air flow and corrected engine speed.

Figure 8.- Continued. Effect of altitude on generalized performance characteristics of 19B-8 turbojet engine. Free-stream ram-pressure ratio, 1.013. Tail-pipe-nozzle area, 135 square inches. Performance parameters corrected to NACA standard atmospheric conditions at sea level.

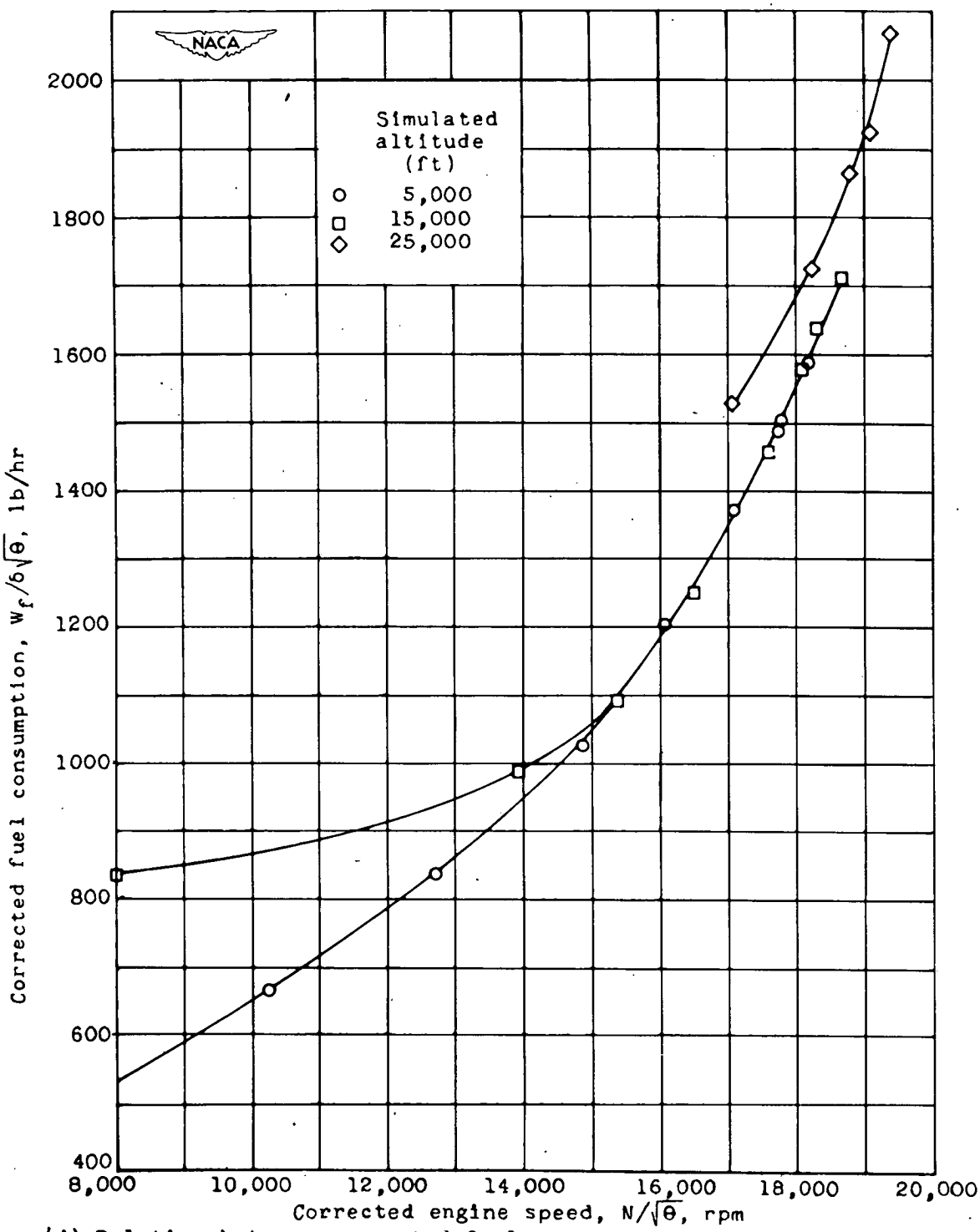

(d) Relation between corrected fuel consumption and corrected engine speed.

Figure 8.- Continued. Effect of altitude on generalized performance characteristics of 19B-8 turbojet engine. Free-stream ram-pressure ratio, 1.013. Tail-pipe-nozzle area, 135 square inches. Performance parameters corrected to NACA standard atmospheric conditions at sea level.

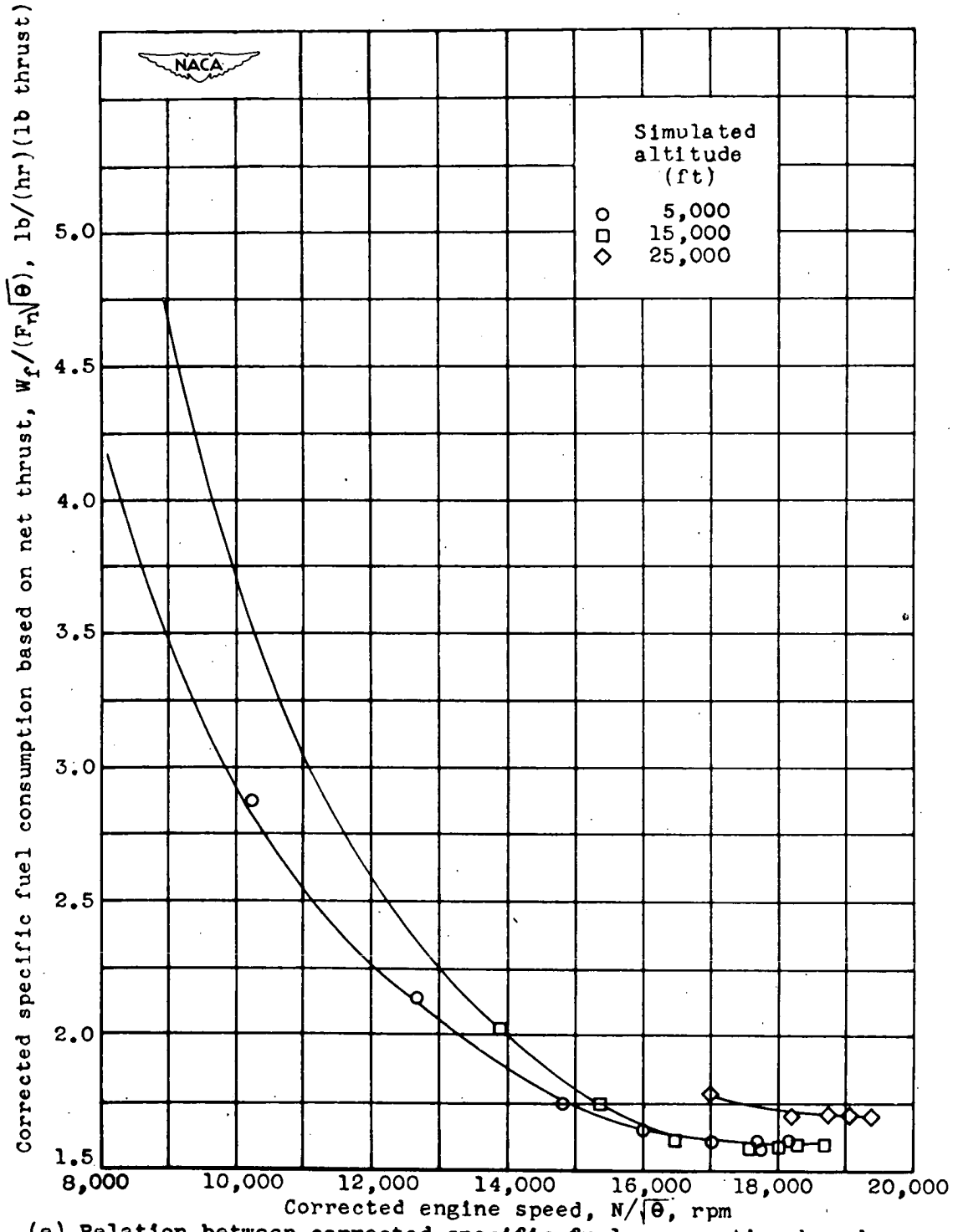

(e) Relation between corrected specific fuel consumption based on net thrust and corrected engine speed.

Figure 8.- Continued. Effect of altitude on generalized performance characteristics of 19B-8 turbojet engine. Free-stream ram-pressure ratio, 1.013. Tail-pipe-nozzle area, 135 square inches. Performance parameters corrected to NACA standard atmospheric conditions at sea level.

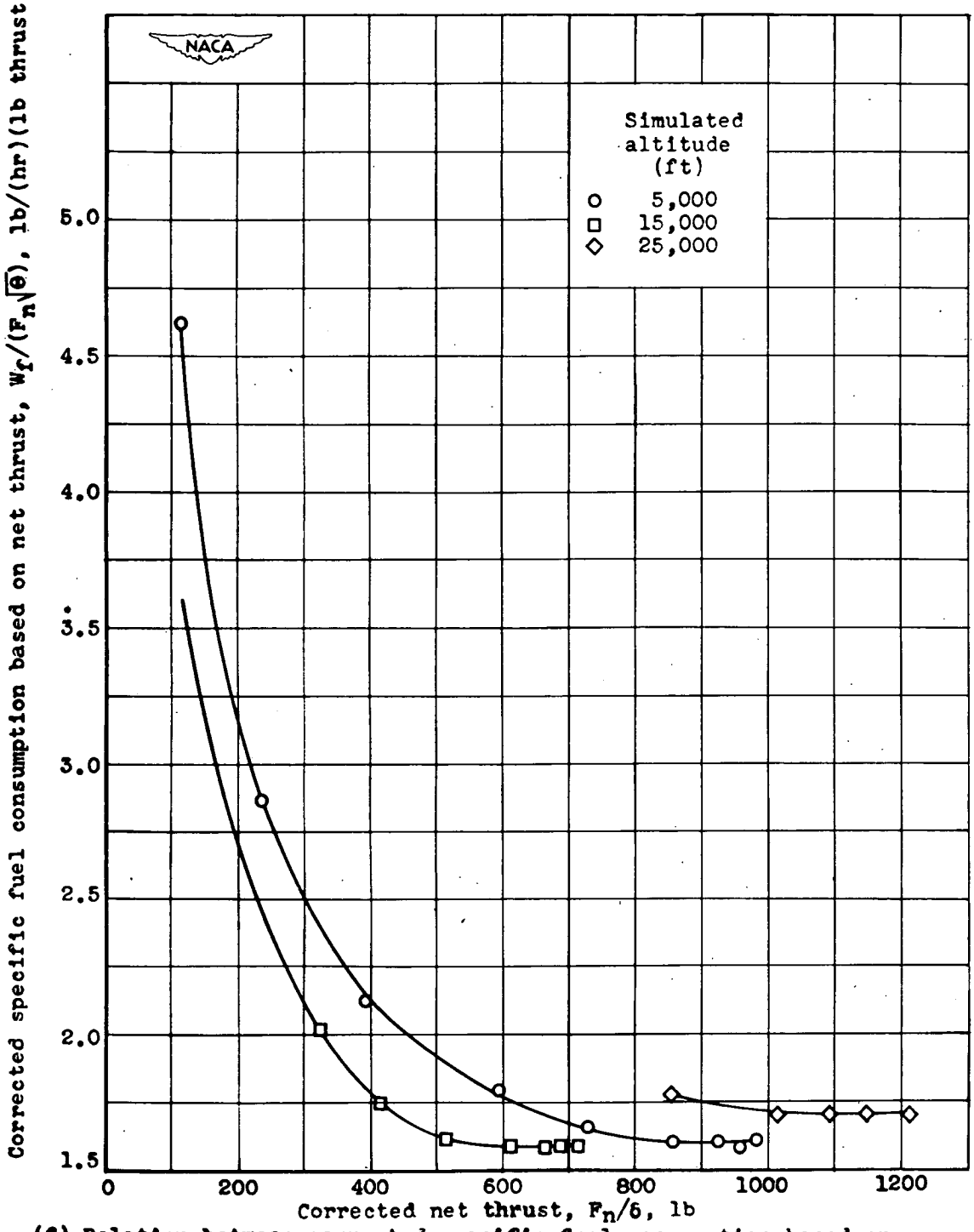

(f) Relation between corrected specific fuel consumption based on net thrust and corrected net thrust.

Figure 8.- Continued. Effect of altitude on generalized performance characteristics of 19B-8 turbojet engine. Free-stream ram-pressure ratio, 1.013. Tail-pipe-nozzle area, 135 square inches. Performance parameters corrected to NACA standard atmospheric conditions at sea level.

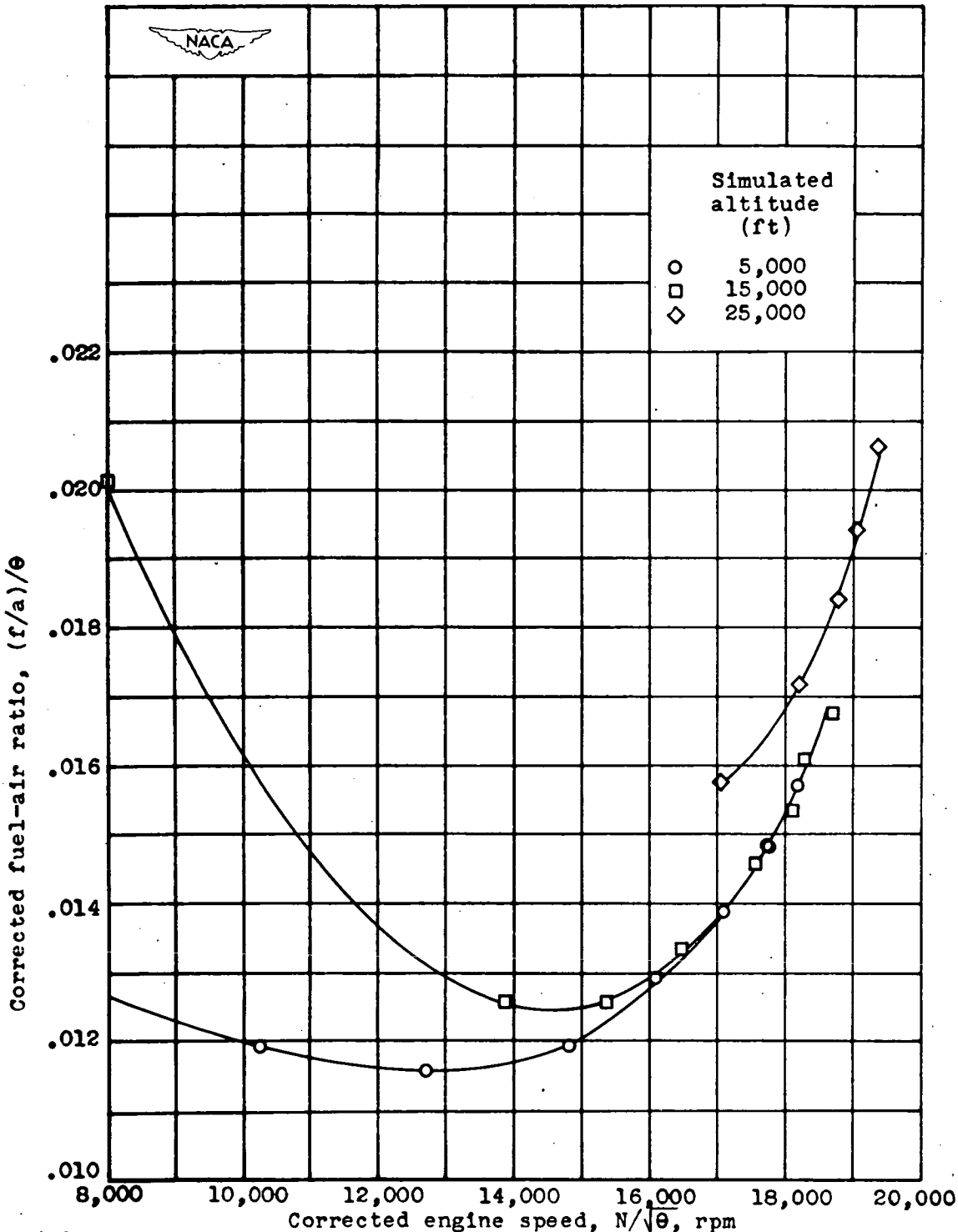

(g) Relation between corrected fuel-air ratio and corrected engine speed.

Figure 8.- Concluded. Effect of altitude on generalized performance characteristics of 19B-8 turbojet engine. Free-stream ram-pressure ratio, 1.013. Tail-pipe-nozzle area, 135 square inches. Performance parameters corrected to NACA standard atmospheric conditions at sea level.

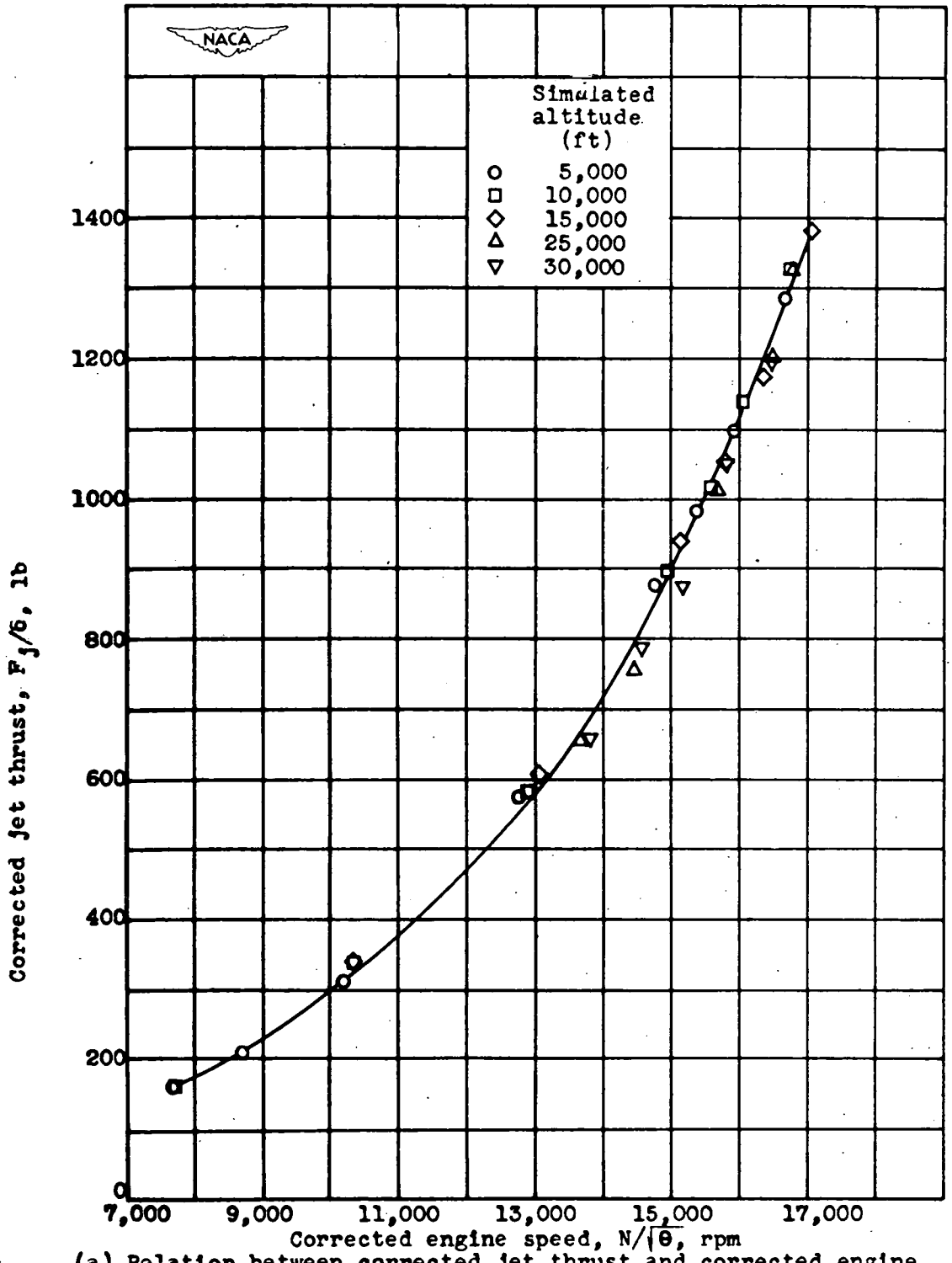

(a) Relation between corrected jet thrust and corrected engine speed.

Figure 9.- Effect of altitude on generalized performance characteristics of 19XB-1 turbojet engine. Static test conditions. Performance parameters corrected to NACA standard atmospheric conditions at sea level.

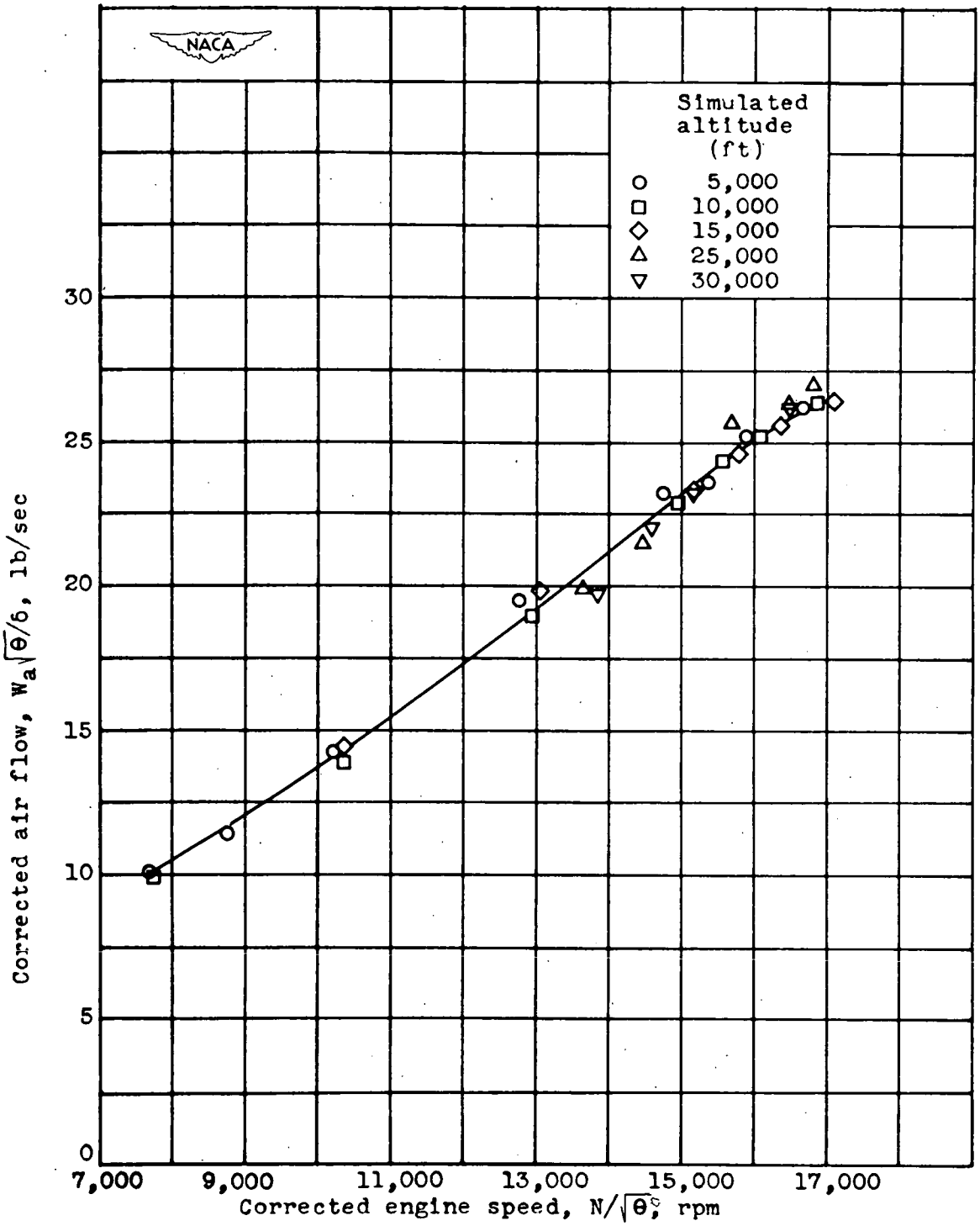

(b) Relation between corrected air flow and corrected engine speed.

Figure 9.- Continued. Effect of altitude on generalized performance characteristics of 19XB-1 turbojet engine. Static test conditions. Performance parameters corrected to NACA standard atmospheric conditions at sea level.

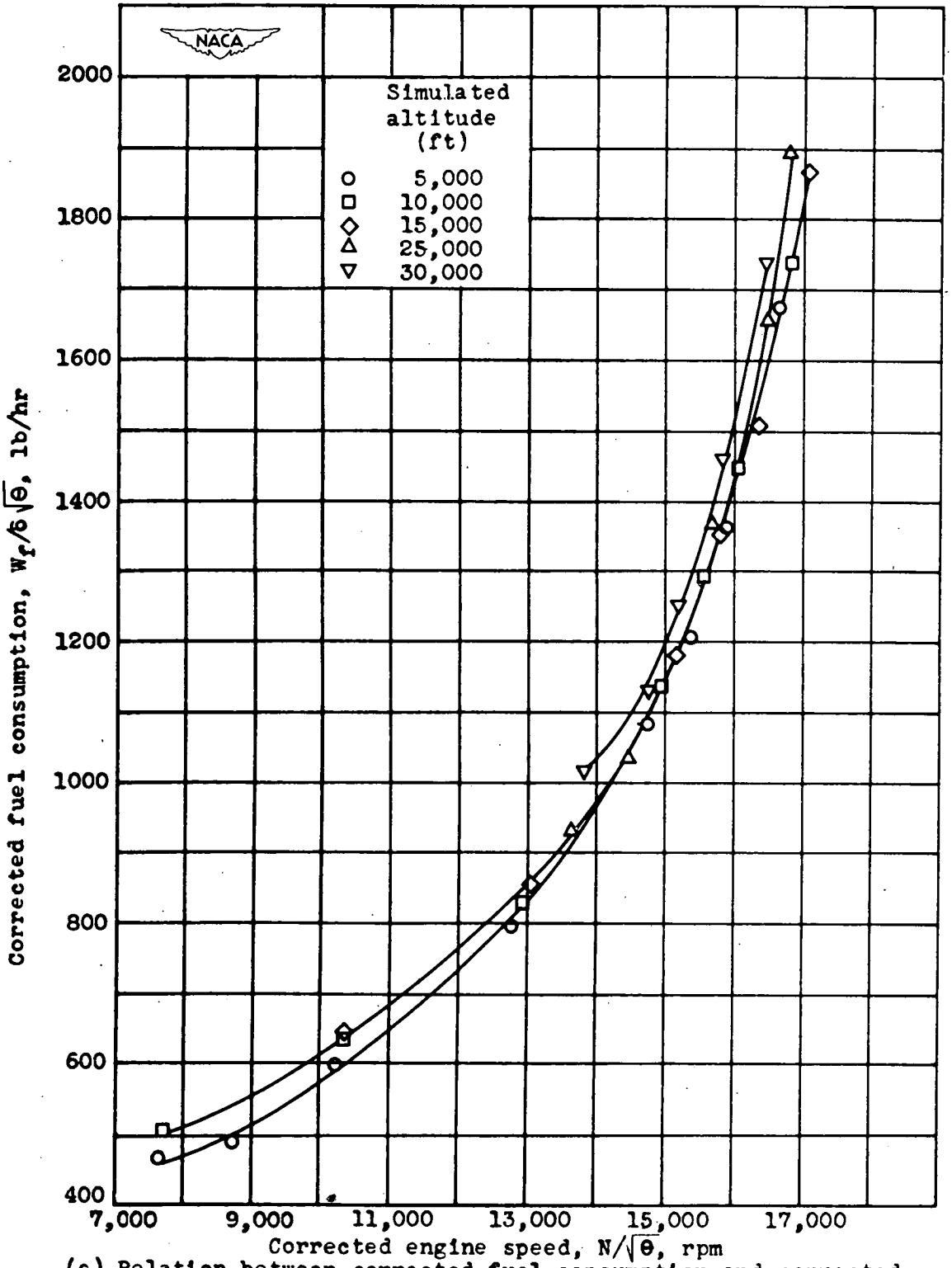

(c) Relation between corrected fuel consumption and corrected engine speed.

Figure 9.- Continued. Effect of altitude on generalized performance characteristics of 19XB-1 turbojet engine. Static test conditions. Performance parameters corrected to NACA standard atmospheric conditions at sea level.

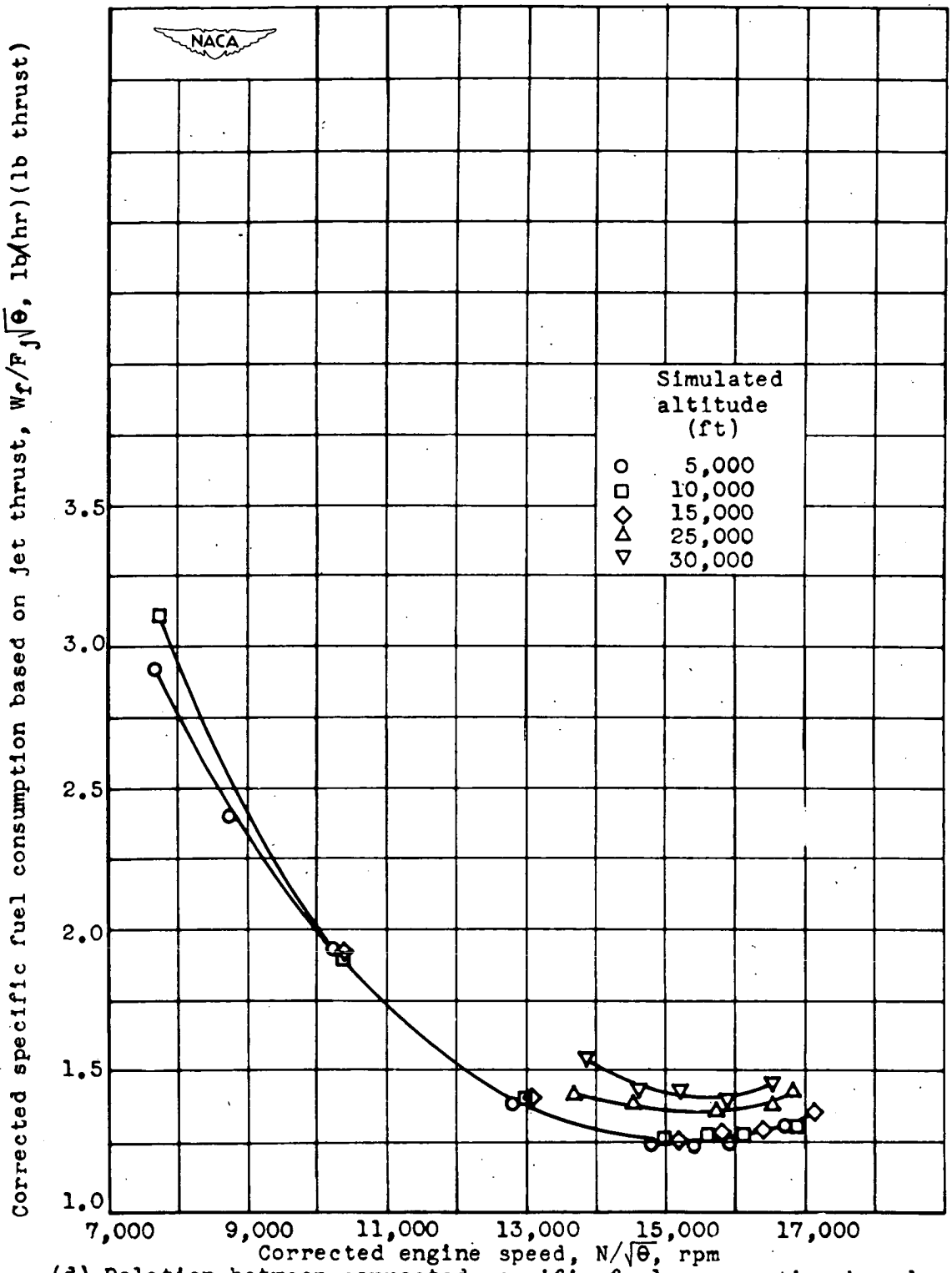

(d) Relation between corrected specific fuel consumption based on jet thrust and corrected engine speed.

Figure 9.- Continued. Effect of altitude on generalized performance characteristics of 19XB-1 turbojet engine. Static test conditions. Performance parameters corrected to NACA standard atmospheric conditions at sea level.

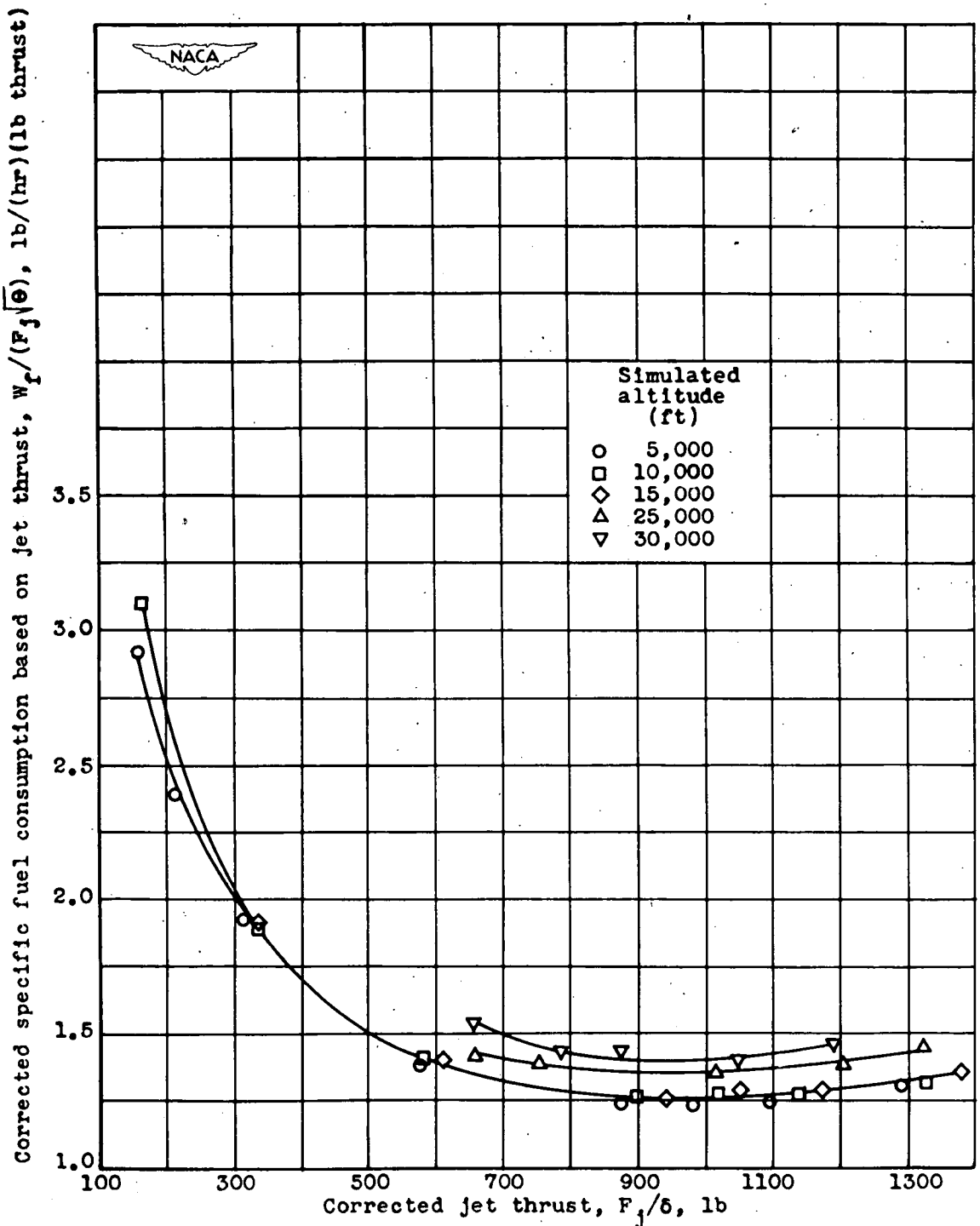

(e) Relation between corrected specific fuel consumption based on jet thrust and corrected jet thrust.

Figure 9.- Continued. Effect of altitude on generalized performance characteristics of 19XB-1 turbojet engine. Static test conditions. Performance parameters corrected to NACA standard atmospheric conditions at sea level.

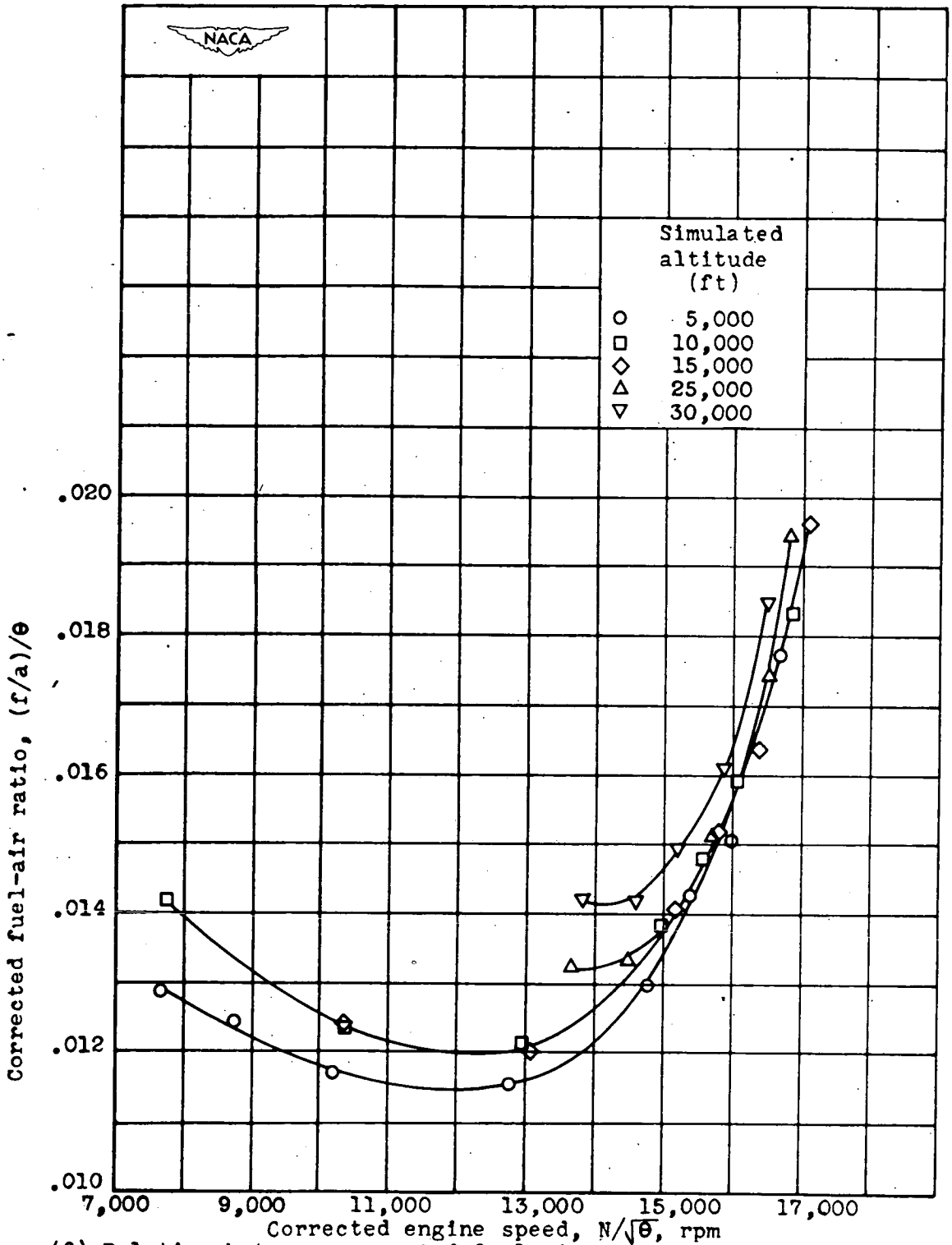

(f) Relation between corrected fuel-air ratio and corrected engine speed.

Figure 9.- Concluded. Effect of altitude on generalized performance characteristics of 19XB-1 turbojet engine. Static test conditions. Performance parameters corrected to NACA standard atmospheric conditions at sea level.

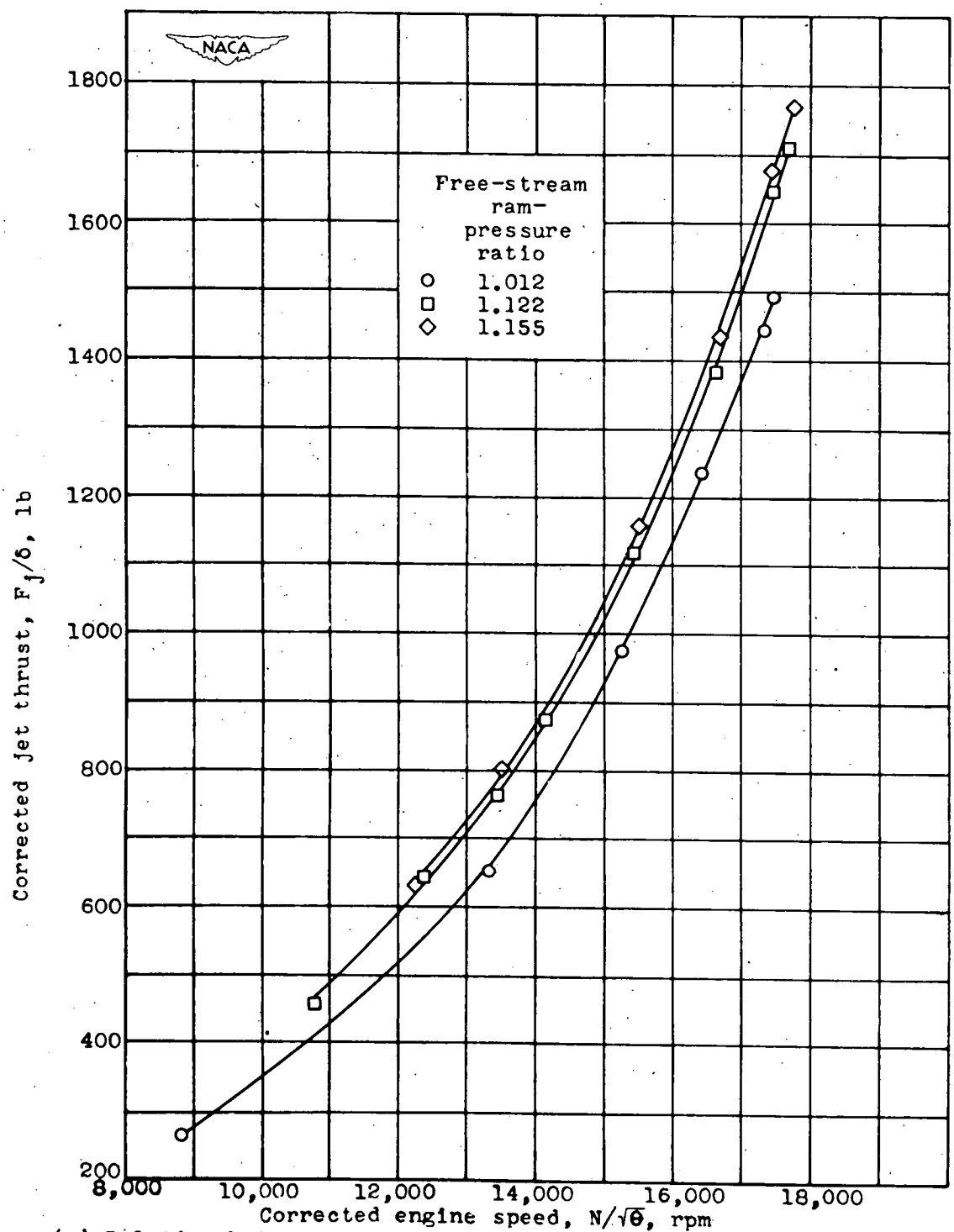

(a) Relation between corrected jet thrust and corrected engine speed.

Figure 10.- Effect of ram-pressure ratio on generalized performance characteristics of 19B-8 turbojet engine. Tailpipe-nozzle area, 106 square inches; simulated altitude, 15,000 feet. Performance parameters corrected to NACA standard atmospheric conditions at sea level.

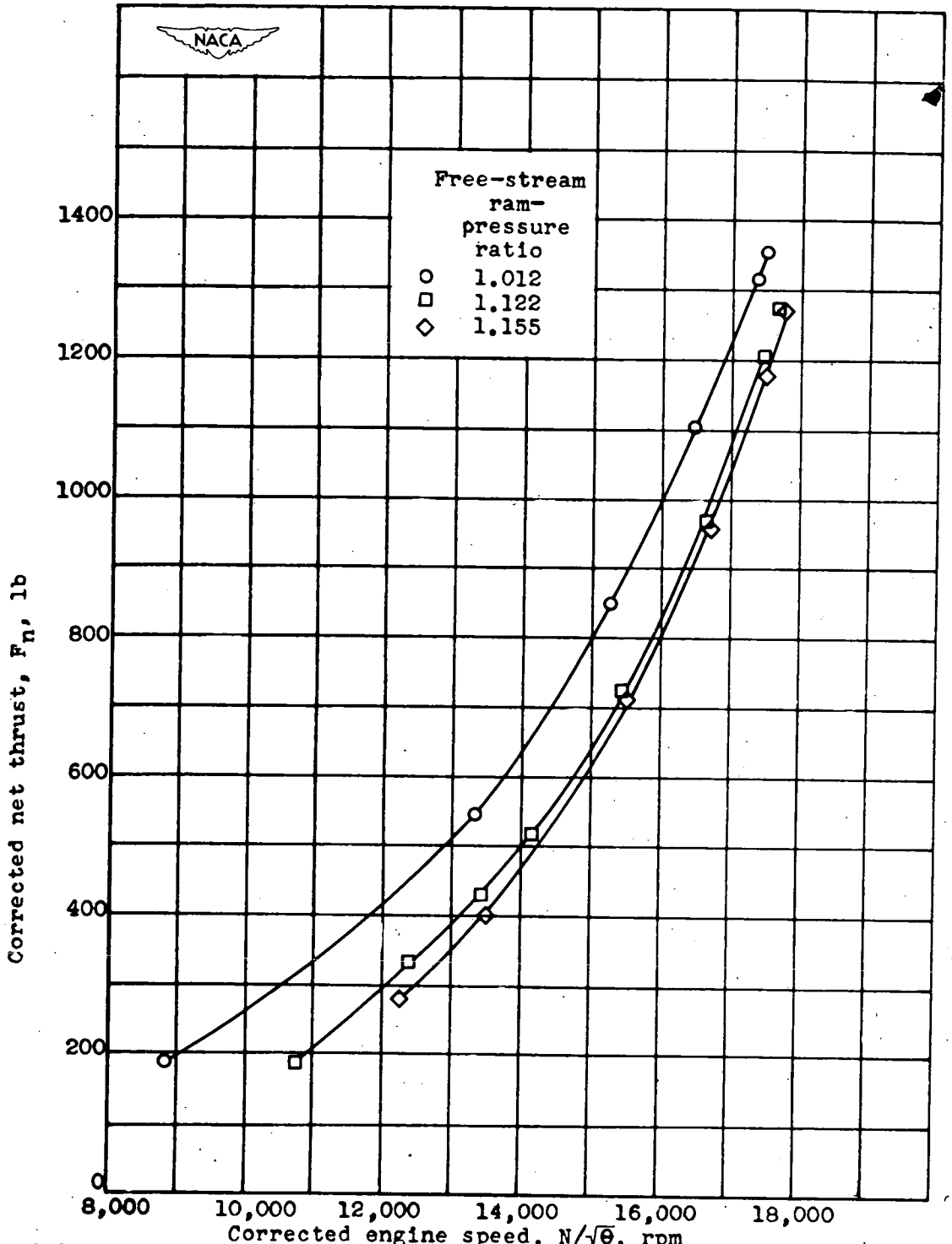

(b) Relation between corrected net thrust and corrected engine speed.

Figure 10.- Continued. Effect of ram-pressure ratio on generalized performance characteristics of 19B-8 turbojet engine. Tail-pipe-nozzle area, 106 square inches; simulated altitude, 15,000 feet. Performance parameters corrected to NACA standard atmospheric conditions at sea level.

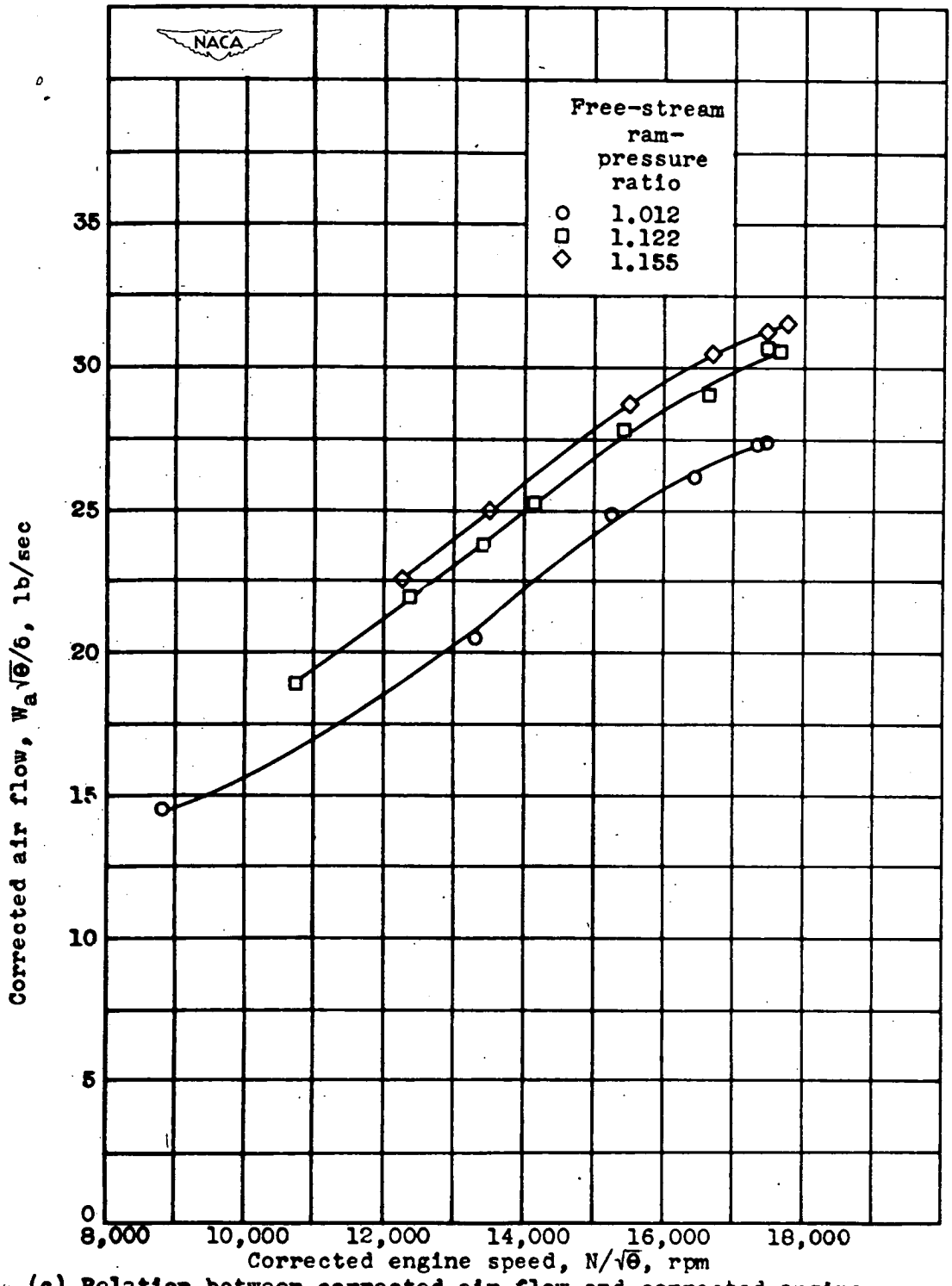

(c) Relation between corrected air flow and corrected engine speed.

Figure 10.- Continued. Effect of ram-pressure ratio on generalized performance characteristics of 19B-8 turbojet engine. Tail-pipe-nozzle area, 106 square inches; simulated altitude, 15,000 feet. Performance parameters corrected to NACA standard atmospheric conditions at sea level.

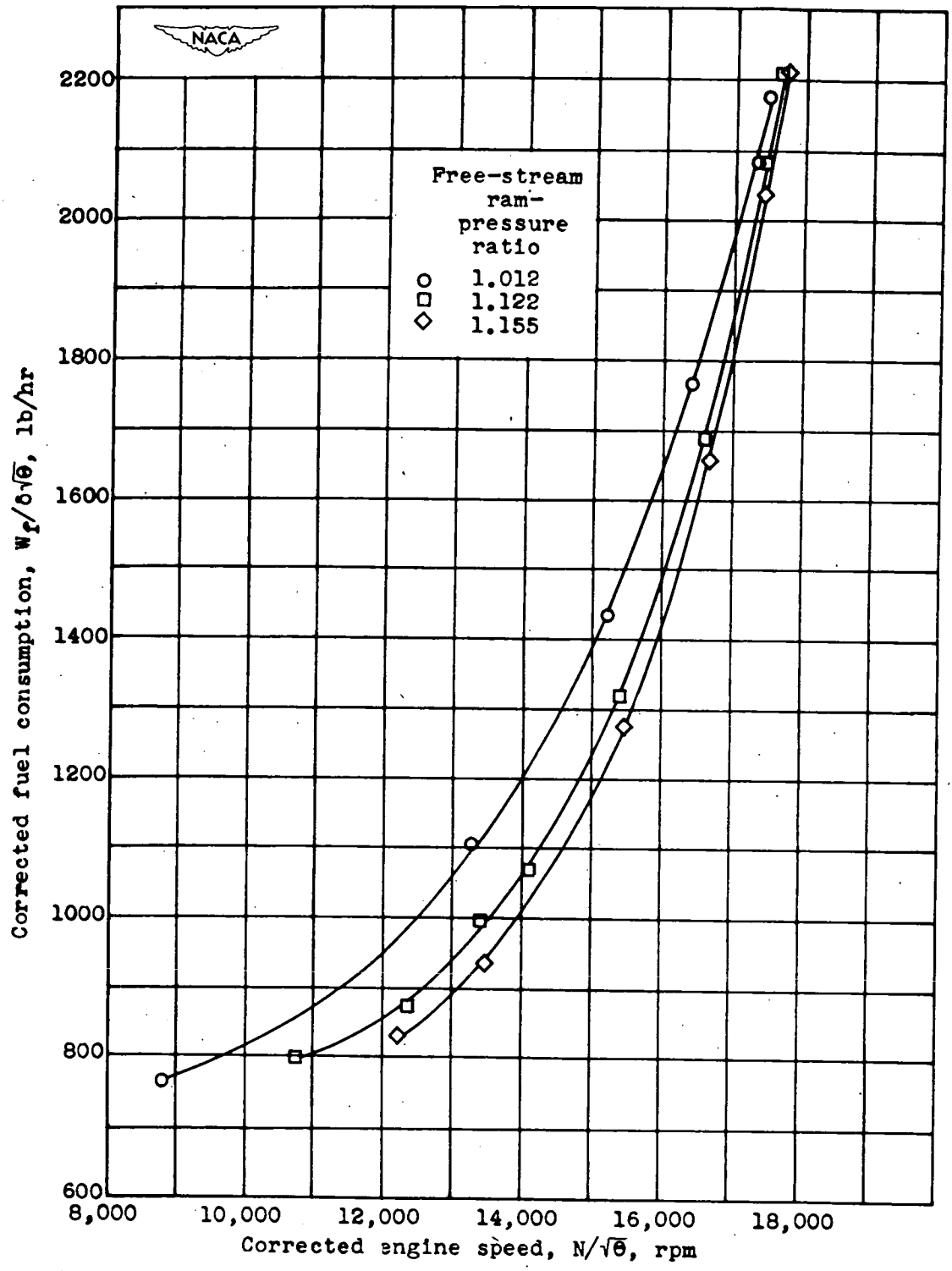

(d) Relation between corrected fuel consumption and corrected engine speed.

Figure 10.- Continued. Effect of ram-pressure ratio on generalized performance characteristics of 19B-8 turbojet engine. Tail-pipe-nozzle area, 106 square inches; simulated altitude, 15,000 feet. Performance parameters corrected to NACA standard atmospheric conditions at sea level.

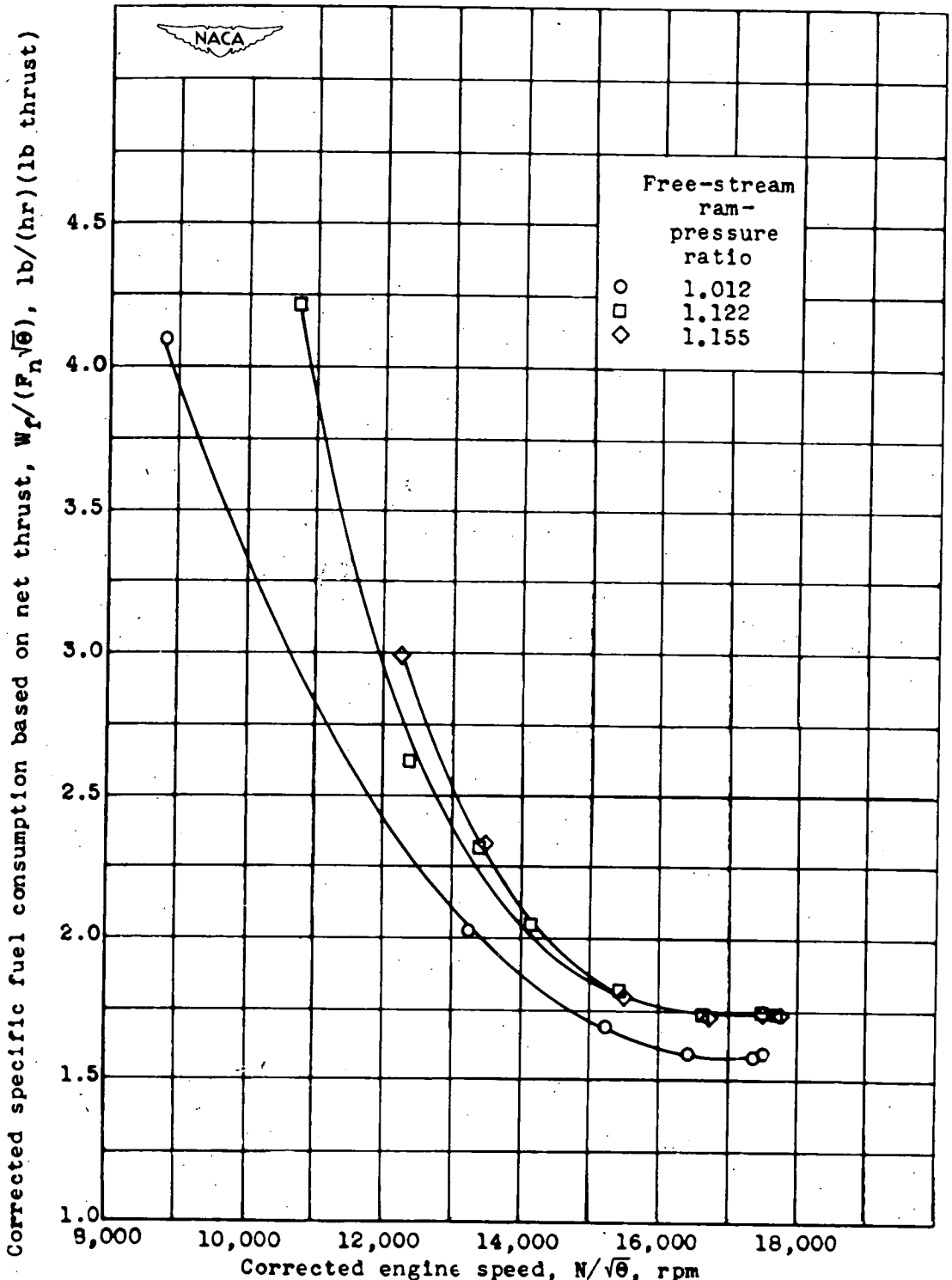

(e) Relation between corrected specific fuel consumption based on net thrust and corrected engine speed.

Figure 10.- Continued. Effect of ram-pressure ratio on generalized performance characteristics of 19B-8 turbojet engine. Tail-pipe-nozzle area, 106 square inches; simulated altitude, 15,000 feet. Performance parameters corrected to NACA standard atmospheric conditions at sea level.

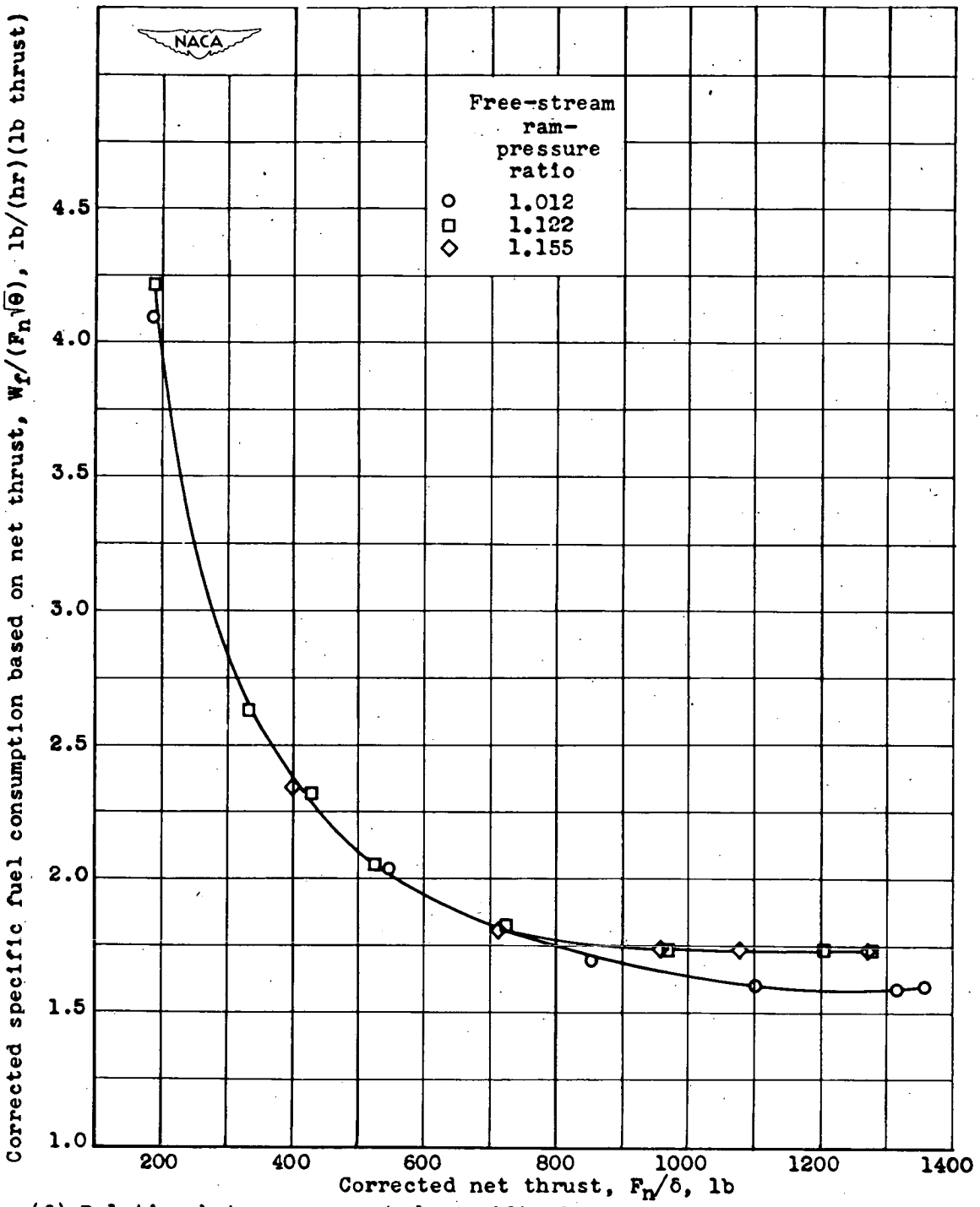

(f) Relation between corrected specific fuel consumption based on net thrust and corrected net thrust.

Figure 10.- Continued. Effect of ram-pressure ratio on generalized performance characteristics of 19B-8 turbojet engine. Tail-pipe-nozzle area, 106 square inches; simulated altitude, 15,000 feet. Performance parameters corrected to NACA standard atmospheric conditions at sea level.

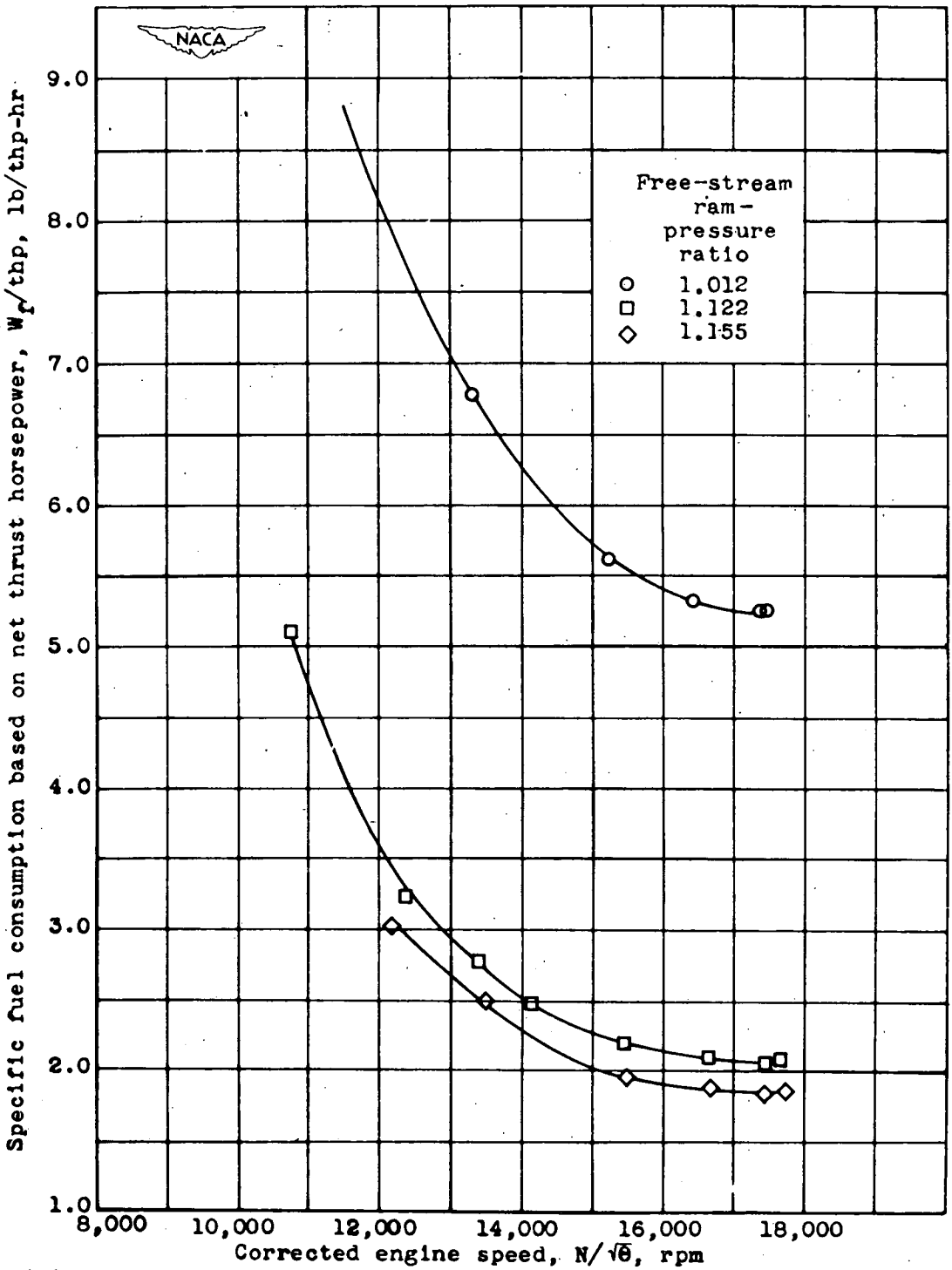

(g) Relation between specific fuel consumption based on net thrust horsepower and corrected engine speed.

Figure 10.- Continued. Effect of ram-pressure ratio on generalized performance characteristics of 19B-8 turbojet engine. Tail-pipe-nozzle area, 106 square inches; simulated altitude, 15,000 feet. Performance parameters corrected to NACA standard atmospheric conditions at sea level.

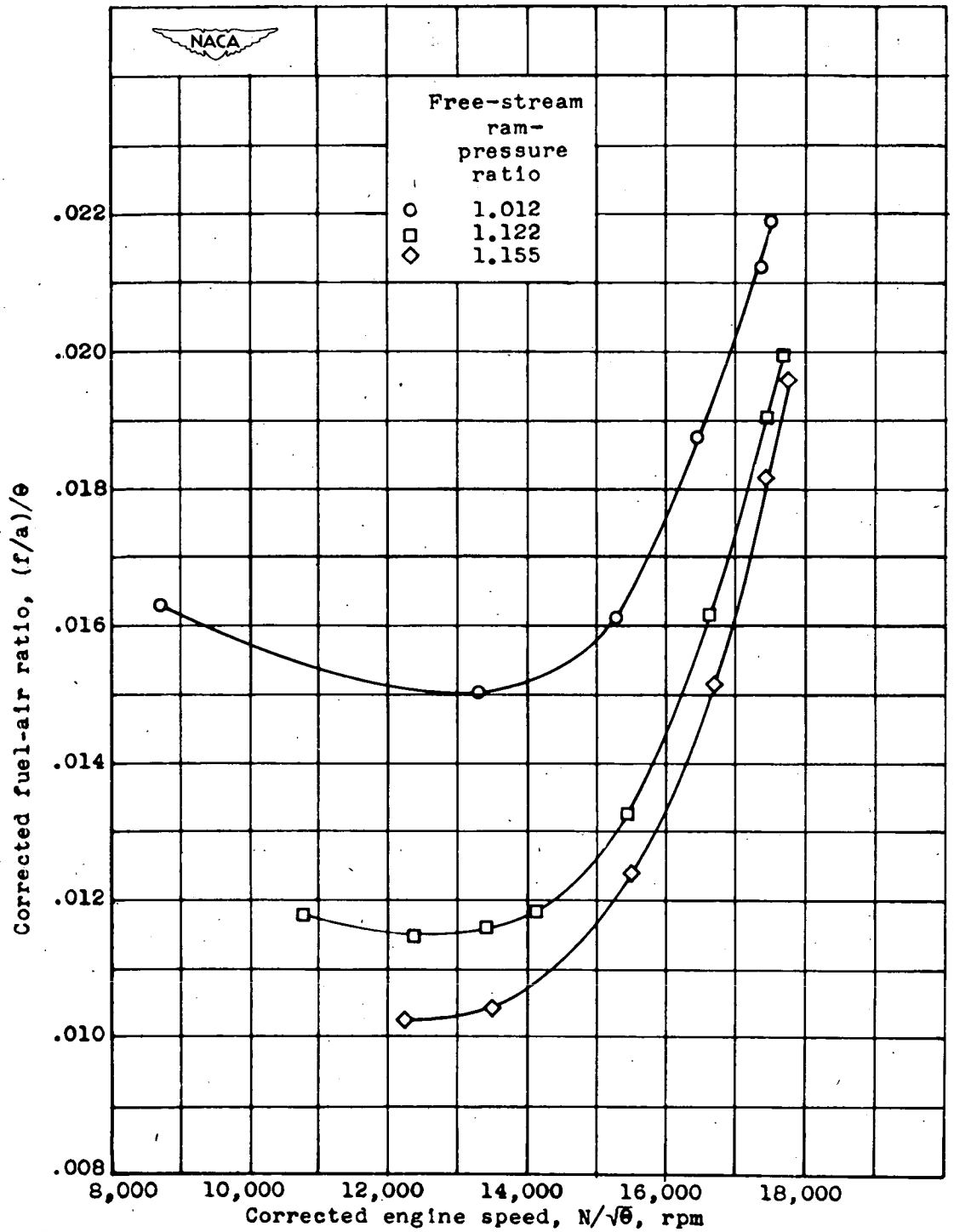

(h) Relation between corrected fuel-air ratio and corrected engine speed.

Figure 10.- Concluded. Effect of ram-pressure ratio on generalized performance characteristics of 19B-8 turbojet engine. Tail-pipe-nozzle area, 106 square inches; simulated altitude, 15,000 feet. Performance parameters corrected to NACA standard atmospheric conditions at sea level.

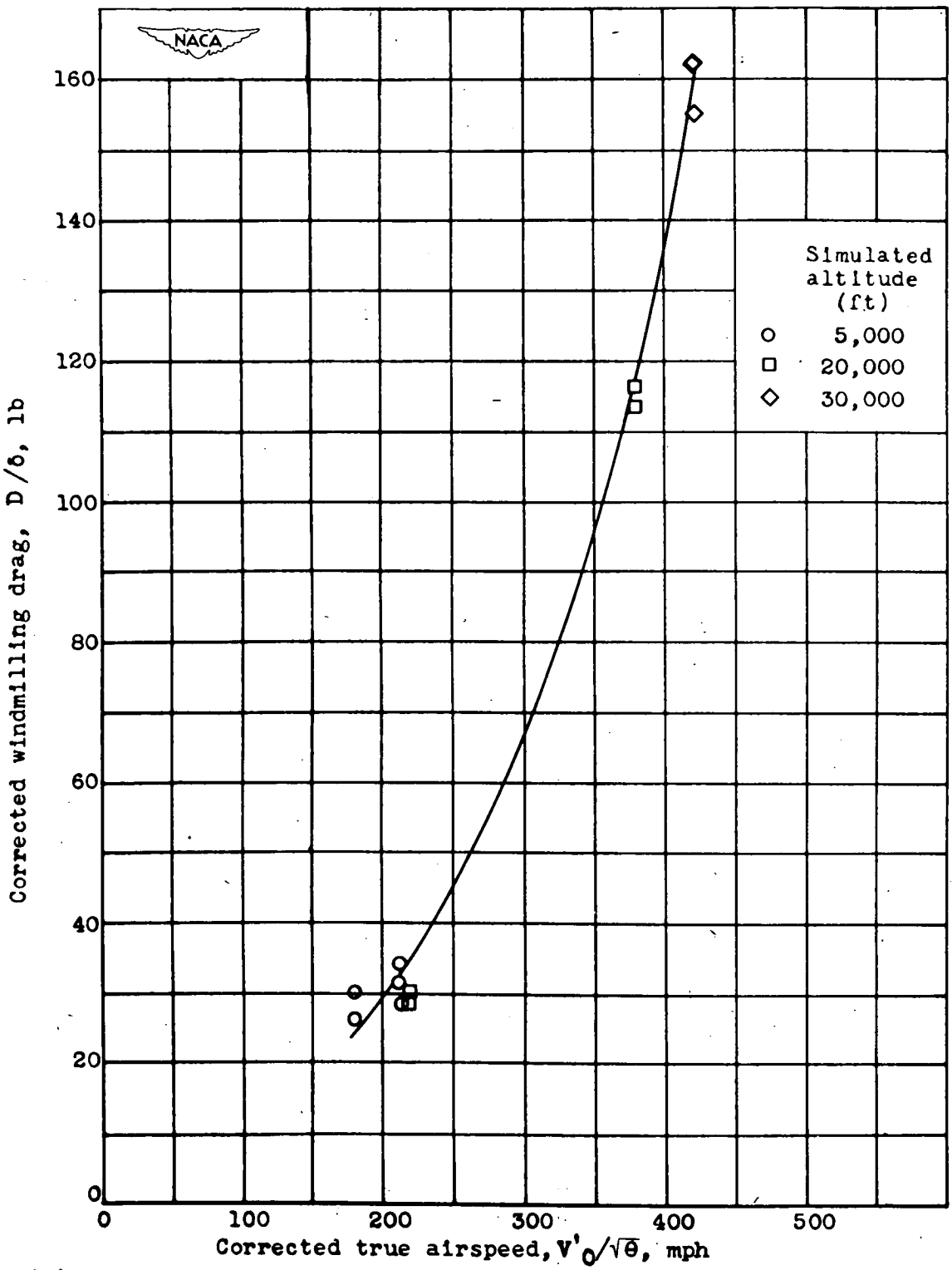

(a) Relation between corrected windmilling drag and corrected true airspeed. Windmilling drag and true airspeed corrected to NACA standard atmospheric conditions at sea level.

Figure 11.- Effect of altitude on windmilling drag characteristics of 19B-8 turbojet engine. Tail-pipe-nozzle area, 135 square inches.

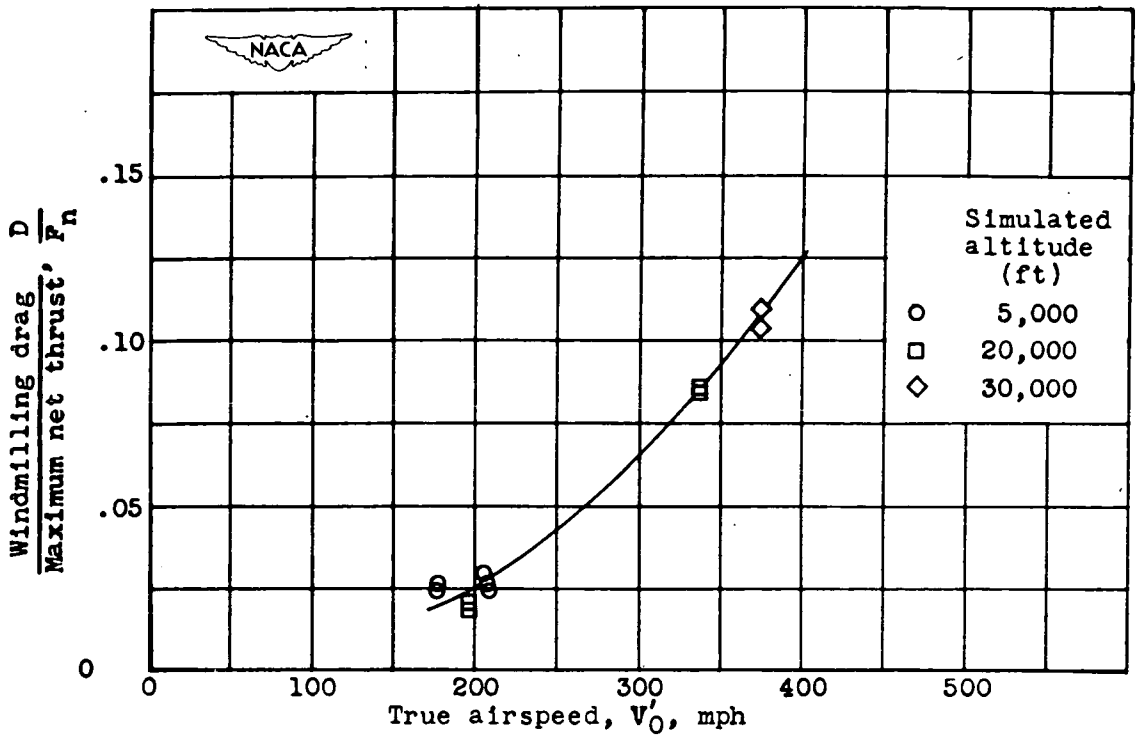

(b) Relation between true airspeed and ratio of windmilling drag to maximum net thrust.

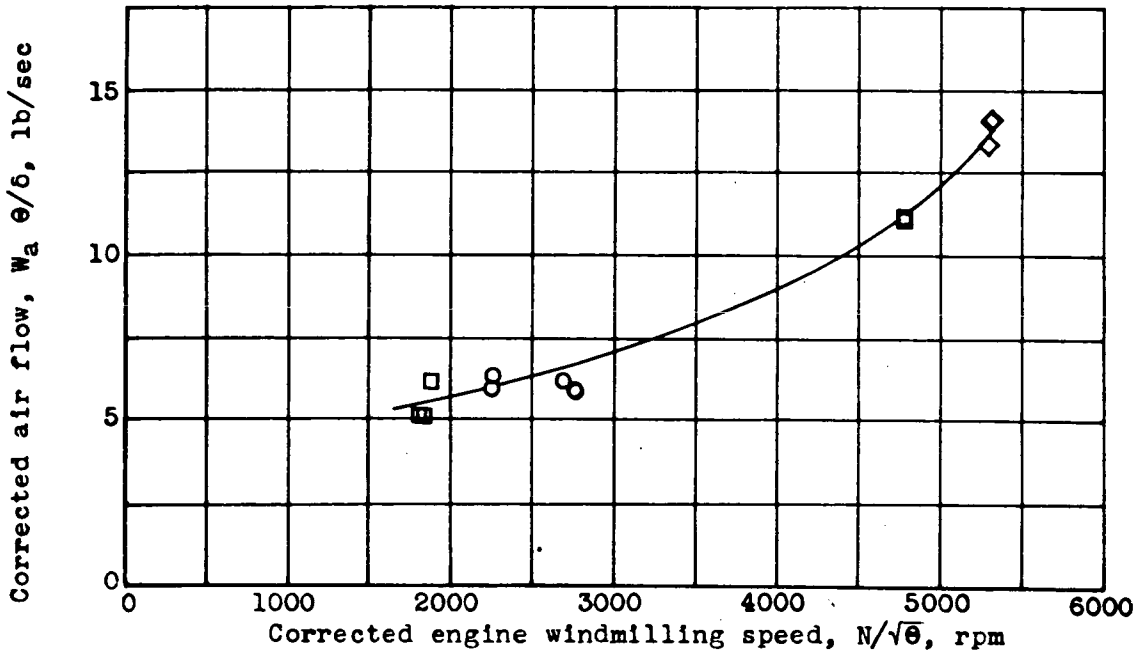

(c) Relation between corrected air flow and corrected engine windmilling speed. Air flow and engine windmilling speed corrected to NACA standard atmospheric conditions at sea level.

Figure 11.- Concluded. Effect of altitude on windmilling drag characteristics of 19B-8 turbojet engine. Tail-pipe-nozzle area, 135 square inches.